AD_____

Award Number: DAMD17-00-1-0409

TITLE: Elevated Levels of Somatic Mutation as a Biomarker of Environmental Effects Contributing to Breast Carcinogenesis

PRINCIPAL INVESTIGATOR: Stephen G. Grant, Ph.D.

CONTRACTING ORGANIZATION: University of Pittsburgh
Pittsburgh, PA 15260

REPORT DATE: July 2006

TYPE OF REPORT: Final

PREPARED FOR: U.S. Army Medical Research and Materiel Command
Fort Detrick, Maryland 21702-5012

REPORT DOCUMENTATION PAGE

Form Approved
OMB No. 0704-0188

1. REPORT DATE	2. REPORT TYPE	3. DATES COVERED
01-07-2006	Final	1 Jul 2000 – 30 Jun 2006

4. TITLE AND SUBTITLE

Elevated Levels of Somatic Mutation as a Biomarker of Environmental Effects Contributing to Breast Carcinogenesis

5a. CONTRACT NUMBER

5b. GRANT NUMBER
DAMD17-00-1-0409

5c. PROGRAM ELEMENT NUMBER

6. AUTHOR(S)

Stephen G. Grant, Ph.D.

5d. PROJECT NUMBER

5e. TASK NUMBER

5f. WORK UNIT NUMBER

7. PERFORMING ORGANIZATION NAME(S) AND ADDRESS(ES)

University of Pittsburgh
Pittsburgh, PA 15260

8. PERFORMING ORGANIZATION REPORT NUMBER

9. SPONSORING / MONITORING AGENCY NAME(S) AND ADDRESS(ES)
U.S. Army Medical Research and Materiel Command
Fort Detrick, Maryland 21702-5012

10. SPONSOR/MONITOR'S ACRONYM(S)

11. SPONSOR/MONITOR'S REPORT NUMBER(S)

12. DISTRIBUTION / AVAILABILITY STATEMENT
Approved for Public Release; Distribution Unlimited

13. SUPPLEMENTARY NOTES
Original contains colored plates: ALL DTIC reproductions will be in black and white.

14. ABSTRACT

Environmental exposures undoubtedly play a role in the development of breast cancer, but few individual agents have been unequivocally identified as risk factors. Rather than seek out individual agents, we hypothesize that the cumulative effect of environmental exposures on an individual can be quantified through a blood-based assay, and further, that such a "biomarker" might distinguish breast cancer patients from age-matched controls. These biomarker data can then be added to a risk assessment procedure for breast cancer, and ultimately, might help identify the types of exposure specifically associated with cancer in the breast. Moreover, we have shown that a major factor modulating somatic mutational burden is DNA repair capacity, and that this characteristic can also be used to identify individuals at increased risk for breast cancer. Changes in DNA repair capacity may also be amenable to manipulation, which might allow us to intervene in the process of breast carcinogenesis, and individually optimize breast cancer treatment.

15. SUBJECT TERMS
somatic mutation, GPA assay, environmental exposure, genotoxicity, DNA repair, gene expression

16. SECURITY CLASSIFICATION OF:				18. NUMBER OF PAGES	19a. NAME OF RESPONSIBLE PERSON
					USAMRMC
a. REPORT	b. ABSTRACT	c. THIS PAGE			19b. TELEPHONE NUMBER *(include area code)*
U	U	U	UU	78	

Table of Contents

Introduction

A number of important risk factors have been identified for breast cancer (1), and several sophisticated risk models developed that have found wide application; indeed, breast cancer risk assessment is the paradigm for the field of cancer etiology and ontology. It surprising, therefore, that despite these efforts, most breast tumors arise independent of these known risk factors. About 10% of incident breast cancer can be attributed to hereditary factors, including heterozygosity for the specific predisposing genes *BRCA1* and *BRCA2*. A further 15% of breast cancers can be accounted for by a complex mix of life history factors (including ages at menarche and menopause, number of term births, etc.), which have been widely interpreted as representing interindividual differences in endogenous hormone (estrogen) production. This leaves the great majority (~75%) of breast cancer unaccounted for. We have found that the most commonly used method of determining breast cancer risk, the Gail model (2), does a poor job of identifying individuals at risk due to the possibility of carrying a mutation in the *BRCA1* or *BRCA2* genes, such that "high risk" populations ascertained by this method under-represent the genetic component of breast cancer risk (3). Moreover, we have begun to dissect the Gail model, and high risk populations based on this model, into three groups: those who are at high risk due to non-specific family history, those that are at high risk due to life history factors that have been widely interpreted as representing lifetime exposure to endogenous hormones, especially estrogen, and those who are at high risk due to the previous detection of a suspicious, but not malignant, lesion (we have found that one reason that the Gail model does not apply well to African-Americans is their reluctance to undergo biopsy of lesions discovered by screening mammography). We believe that these different types of high-risk individuals may react differently to cancer causative agents, and, possibly chemopreventive agents, as well.

It is also assumed that environmental exposures are involved in breast carcinogenesis, and strong evidence for the effect of radiation has been presented. Total genotoxic exposure, especially the contributions of the countless chemicals in the environment, are impossible to calculate based on the individual agents themselves. Such exposure monitoring also does not integrate the individual response to genotoxic exposure that modulates its effect on processes such as carcinogenesis. We have proposed that direct monitoring of genetic effects at a surrogate locus in a easily available tissue can provide a biodosimter of environmental effects, and we have provided preliminary evidence that blood-based assays of somatic mutation can provide this data. Interindividual variability in DNA repair processes would be a major modulator of the biological response to environmental genotoxicants, and we have the unique ability to functionally measure this capacity not only in blood cells, but in the breast tissue itself.

Body

Risk factors for the development of breast cancer remain largely unknown, however, several clear elements have emerged: family history of breast cancer, metabolic factors related to hormone production, and exposure to X irradiation (1). Breast cancer incidence may also be influenced by the accumulation of two types of man-made chemicals in the environment; those that mimic hormonal effects, known as "xenoestrogens", and those that mimic the DNA-damaging effects of X irradiation, or "genotoxicants". We hypothesize that breast cancer incidence should be a product of both the total cumulative exposure to genotoxic agents, including but not limited to X-rays, as modified by differences in individual response to this exposure as mediated by host factors, such as metabolic detoxification (or activation) and DNA repair capacity.

Although there is bound to be some element of tissue specificity for both genotoxic exposure and susceptibility to DNA damage, except in certain cases, such as established "high risk" individuals, it is impractical to monitor somatic mutation in breast tissue itself. Blood, however, and its progenitor tissue bone marrow, are present throughout the body, and most xenobiotic exposures to the breast are likely to be transported to the breast tissue through the blood. The *GPA* assay is fast and inexpensive, utilizing flow

technology to quickly quantify rare mutational events. However, due to its genetic basis, it has previously only be applied to individuals heterozygous for the MN blood group, which make up approximately 50% of the population.

A second blood-based somatic mutation assay, based on the X-linked *HPRT* locus, is universally applicable, but requires cell culture and drug selection, making it more expensive and labor-intensive (4). Moreover, one class of *HPRT* mutants have been specifically identified as occurring via illegitimate V(D)J recombination (5), a mutagenic process that is characteristic of loss of double strand break DNA repair, such as in the cancer-prone syndrome ataxia telangiectasia (AT). The *BRCA1* and *BRCA2* breast cancer predisposition genes have also been implicated in this type of repair, so may also have a characteristic increase in these types of mutants (6). Illegitimate V(D)J recombination itself, however, should not occur in the breast epithelium, as it is not a cell-type associated with immune function.

Our hypothesis predicts that the somatic mutational burden of cancer patients should be higher than that of disease-free controls. This prediction was first applied to a mixed population of cancer patients, and these results, originally preliminary data for this proposal, have been published (7). These data include significant contributions from cancers (breast, prostate, testicular) with acknowledged "hormonal" factors, suggesting that a dependence on genotoxic exposures is not mutually exclusive with an association with endocrine factors.

We have now optimized the ability to use these data as indicators of cancer risk. By establishing a demarcation point of greater than 30 *GPA* allele loss mutations per million cells, we are able to demonstrate significant discrimination of the cancer population from the cancer-free population in a retrospective study (**Table 1**). This analysis appears to apply equally well to the subset of breast cancer patients, despite the "hormonal" nature of their disease. Indeed, with an adjustment in the demarcation point for the age of the patients, this approach also seems to apply to childhood cancers, such as sporadic retinoblastoma (**Table 2**).

		GPA Mutant Frequencies[1]		
Population	Total Assayed	< 30.0	> 30.0	OR[2] (95% CI[3])
adult controls	802	709	93	
all cancer patients	98	63	35	**4.24** (3.68-4.87)
breast cancer patients	47	29	18	**4.73** (3.75-5.98)

Table 1. Increased proportion of individuals with high *GPA* mutation frequencies in adult cancer patients vs. controls. [1]variant frequencies x 10^{-6}, [2]odds ratio, [3]confidence interval

		GPA Mutant Frequencies[1]		
Population	Total Assayed	< 15.0	> 15.0	OR[2] (95% CI[3])
pediatric controls	28	25	3	
retinoblastoma patients	52	33	19	**4.80** (1.39-16.56)

Table 2. Increased proportion of individuals with high *GPA* mutation frequencies in pediatric cancer patients vs. controls. [1]variant frequencies x 10^{-6}, [2]odds ratio, [3]confidence interval

We have recently demonstrated that we can detect "high" levels of somatic mutational burden, regardless of the *GPA* allelotype of the individual (8). This allows us to apply the *GPA* assay, regardless of genotype, for diagnosis of the cancer-prone diseases ataxia telangiectasia (9), Fanconi anemia (8), and, potentially, Bloom

syndrome (10,11). Moreover, the assay is similarly universally applicable in other scenarios where an increased somatic mutation is expected or can be used to discriminate individuals, such as in the response to genotoxic chemotherapy in breast cancer patients (12). Although mutants are not as well separated from wild-type cells in *GPA* homozygotes vs. heterozygotes, this problem is offset to some degree by the fact that the products of mutation of both alleles in *GPA* homozygotes have the same mutant phenotype, doubling the actual mutation frequency. Thus, we have demonstrated that we can reliably identify peaks of 50 or more mutant cells per million analyzed in *GPA* homozygotes, but, since this represents the mutation frequency at two alleles rather than one, the actual mutation frequency that we can detect is 25 per million. Note that this is below the level we have established as distinguishing breast cancer patients, and therefore, in the prospective context, individuals at risk of developing breast and other cancers. For this application, therefore, the *GPA* assay is universally applicable; although we will not always be able to assign a reliable quantitative mutation frequency to an individual, we will be able to determine that they are not "at risk". This is a very important step in terms of translating these results from the theoretical to a practical population screen for individuals who have sustained genotoxic insults that put them at risk of developing cancer.

In collaboration with Dr. Jean Latimer of the University of Pittsburgh Cancer Institute we have attempted to extend these observations to the molecular level. Dr. Latimer is an expert in nucleotide excision repair (NER), a type of DNA repair usually associated with DNA damage caused by exposure to ultraviolet light (pyrimidine dimers, among other species) (13). She has also developed a reliable means of culturing normal breast epithelium and tumor (20). We are in the process of revising a manuscript on this cell culture method that we had submitted to the journal *Nature Methods*; we are performing cytokeratin-14 staining on these cultures to demonstrate the presence of myoepithelial cells pursuant to revising the manuscript for reconsideration. We have used these techniques to begin to determine whether loss or deficiency of NER could play a role in the higher somatic mutation frequencies we have documented in sporadic breast cancer patients. These studies were based on three observations: 1) NER activity modifies bodily response to a major class of environmental mutagens, bulky adducting long-chain and polyaromatic hydrocarbons, so is likely to be involved in most cancers that have a component of environmental exposure in their etiology; 2) since it requires the products of 25 genes, the NER pathway offers a large target for environmental mutagenesis; and, 3) early studies suggested that breast cancer patients (21) were deficient in NER, and there has been recent recapitulation of these findings (22,23).

Since the NER pathway is so complex, it is difficult to assay individual components, although a cell-free protein reconstruction system has been established (24). There are basically three methods for practically measuring NER, and all require actively proliferating cells; the unscheduled DNA synthesis (UDS) assay, involving label incorporation during repair of damage caused by delivery of UV or a UV-mimetic chemical (25), is by far the most widely applied, having been used as a screen for genotoxic chemicals by the National Toxicology Program (26). Drs. Grant and Latimer had previously collaborated in a study using the *GPA* and UDS assays to characterize a newly diagnosed pediatric patients suffering from Rothmund-Thomson syndrome, a premature aging syndrome with elements of DNA repair deficiency (27). The UDS assay was therefore our assay of choice for functionally assessing the entire NER pathway.

Our first results in this system demonstrated several interesting characteristics of DNA repair in the breast epithelium: the NER capacity of these cells was only 25% of that measured in skin fibroblasts, there was a 9% coefficient of variation, establishing a considerable "range of normal", and NER capacity was not associated with either the age of the donor nor the proliferation of the cell sample (28). These results are significant, because another laboratory has established that the background frequency of somatic mutation, as measured with the HPRT assay, is 10-100-fold higher in epithelial cells than in other cell-types (29).

The UDS assay has been performed on peripheral blood lymphocytes (PBL) (25), and we recently published a large survey of normal individuals analyzed this way (N = 33) (25). Unfortunately, that study also established tissue-specific differences in NER capacity between fibroblasts, lymphocytes and epithelial cells, such that coordinate regulation of the three cell types cannot be assumed. A preliminary analysis of nine blood samples

from newly diagnosed breast cancer patients, however, suggests that 1) breast cancer is associated with NER deficiency, and 2) that blood-based assay of NER deficiency is feasible (**Figure 1**). Lymphocyte NER from the breast cancer patients were significantly lower ($P = 0.005$) than in unaffected controls, averaging only 0.23 ± 0.09 of the NER capacity of the mean of our control population.

Figure 1. NER capacity of PBLs from disease-free controls (N = 33) and newly diagnosed (pre-therapy) breast cancer patients. NER capacity was assessed with the UDS assay.

Our ability to establish explant cultures of breast epithelial tissue has allowed us to extend these observations to the tissue of interest. UDS analysis of 17 stage I breast tumors demonstrated that the breast tumors were significantly lower in NER capacity than the breast reduction samples, exhibiting an average of 47% normal activity ($P = 0.0002$). None of the breast tumor cultures exhibited an NER capacity equal to the average of the reduction mammoplasty samples, and half of the tumors had NER capacities lower than that of the lowest breast reduction. As shown in **Table 3**, if 70% of normal NER activity is used to distinguish these data the UDS assay is able to discriminate normal and tumor samples with a sensitivity of 88%, a specificity of 78% and a significant odds ratio (OR) of **27**.**0**. This result clearly establishes that deficiency of NER is associated with breast cancer incidence. These data have been submitted as a manuscript to the *Journal of the National Cancer Institute*. We are presently completing experiments requested by their reviewers to extend the functional analysis of NER to the molecular level using RNase protection, Western analysis and expression microarray.

Population	Total Assayed	NER Capacities[1] < 0.70	> 0.70	OR[2] (95% CI[3])
breast cancer patients (stage 1 tumor)	17	15	2	**27**.**0** (14.4-50.8)
breast cancer patients (stage 1 NTA[4])	13	8	5	**5**.**8** (2.4-14.0)
breast cancer patients (stages 1 + 2)	42	32	10	**11**.**5** (7.25-18.3)
disease-free controls	23	5	18	

Table 3. Increased proportion of tissue samples with low NER capacities in breast cancer patients vs. controls.
[1]relative to average of breast reduction samples, [2]odds ratio, [3]confidence interval, [4]non-tumor adjacent normal tissue

Using a pair of commercially available multiplexed sets of probes for RNAse protection of NER-associated genes (**Figure 2**), we have observed a consistent, concurrent, significant downregulation of eight genes in the NER pathway: *CSB* ($P < 0.001$), *XPA* ($P = 0.03$), *TFIIHp52* ($P = 0.018$), *TFIIHp44* ($P = 0.01$), *TFIIHp34* ($P = 0.008$), *Cdk7* ($P = 0.009$), *CycH* ($P = 0.024$), and *XPB* ($P = 0.019$) (**Figures 3** and **4**). Indeed, although they do

not reach significance due to low expression levels or variability, there is a trend for lower expression in tumor samples for all but one of the 20 NER genes analyzed (**Figure 5**). These data have so far been confirmed in ongoing analyses of these samples by microarray (**Figure 6**) and Western analysis (**Figure 7**). These data suggest that there is a mechanism of coordinate control over most or all of the NER genes. Promotor analysis reveals no obvious transcription factor commonalities among the whole set of NER genes, nor in the our subset of "candidate" genes, although smaller subgroups share very similar sets of promotor elements (**Figure 8**). Another possibility is that the NER genes are regulated epigenetically via DNA methylation in the promotor region. Analysis of the CG distributions of 25 NER genes reveals that 23 have "CpG islands" in their promotor regions (**Figure 9**). This proportion is significantly higher than the 60%% expected from the entire genome (30). We intend to continue our characterization of the NER deficiency we have found in the tissues of breast cancer patients and use these data to pursue funding to determine the mechanism of gene downregulation at the molecular level. These data have important implications with regard to the etiology of breast cancer, as well as the design of chemotherapeutic agents that might exploit the vulnerability of breast tumors to agents causing DNA damage that must be repaired by the NER pathway.

We have also been attempting to establish methods to analyze other types of DNA damage and repair in these breast epithelial and tumor samples. We have developed a method of

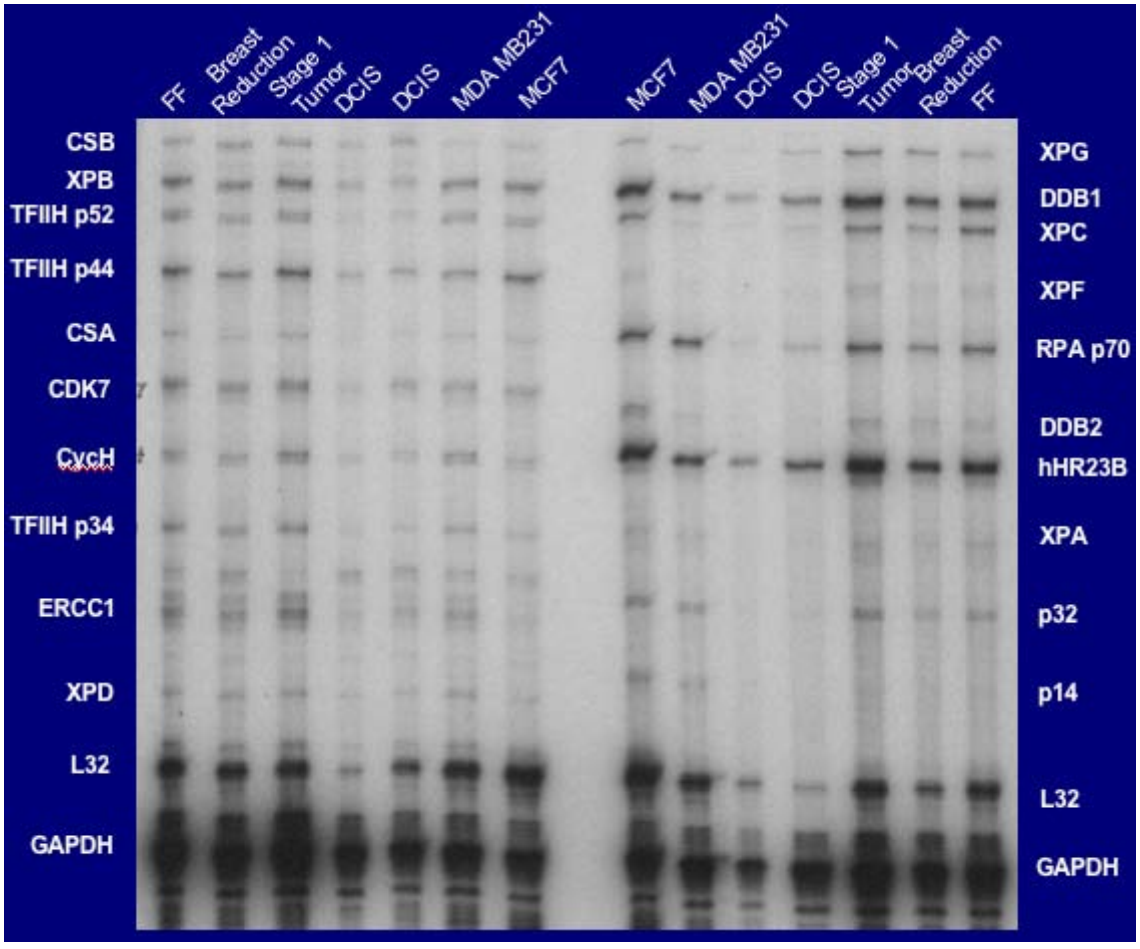

Figure 3. RNAse protection gels showing the probes to 20 NER-associated genes hybridized to RNA isolated from a number of different types of breast-derived tissues, tumors and cell lines.

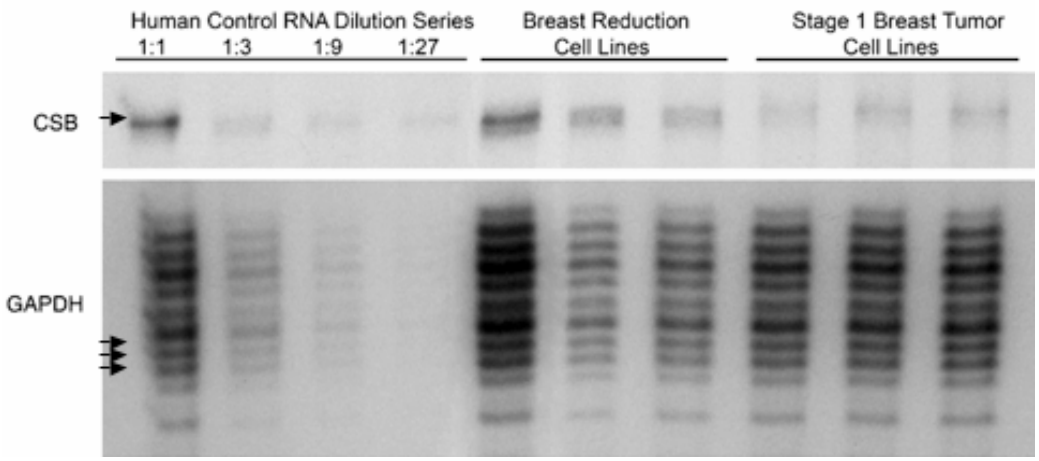

Figure 4. Representative RNAse protection gel showing hNER2 kit hybridized to a dilution series of human control RNA and 2 ug total RNA derived from 3 breast reduction cell lines, and 3 stage I tumor cell lines. Gene expression data are shown for the candidate NER gene *CSB* and the control housekeeping gene *GAPDH*. Bands used for quantitation are indicated by arrows

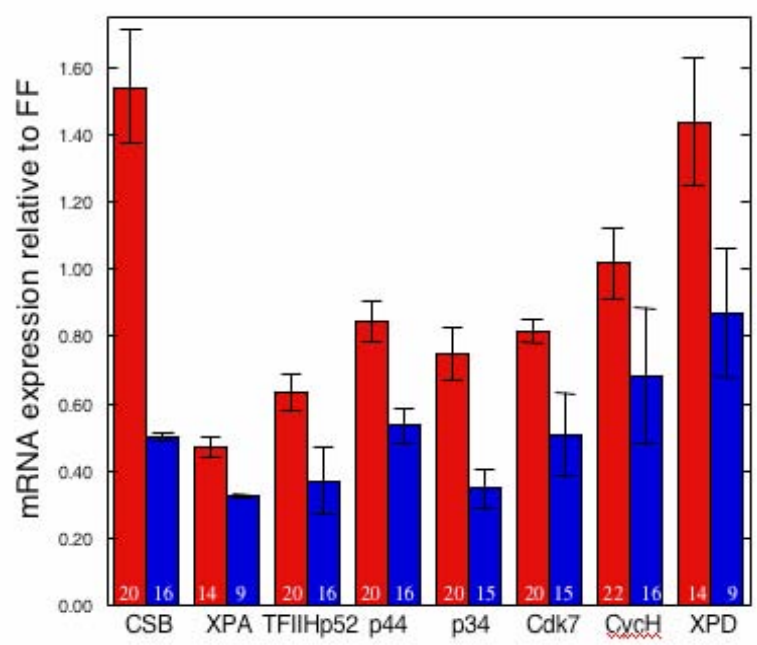

Figure 4. RNAse protection data showing the significant loss of mRNA expression in 8 candidate NER genes between breast reduction (normal) (red) and tumor cell lines (blue). Autoradiograms were normalized for loading using *GAPDH* and expressed relative to normal FF in each experiment. Total RNA was generated from 3 breast reduction cell lines were and 3 stage I tumor cell lines. Each bar represents the indicated number of independent analyses. Non-tumor adjacent cell lines showed similar results as the matching tumors.

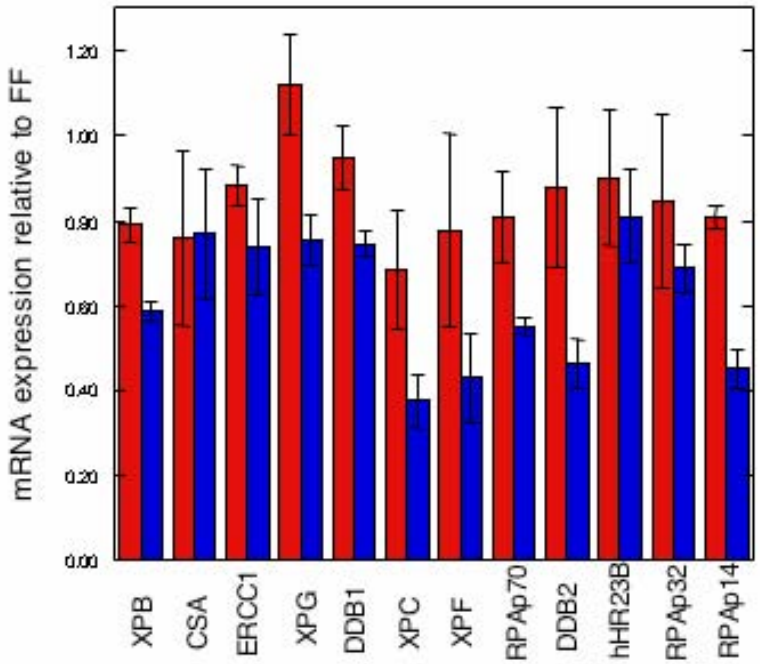

Figure 5. RNAse protection data showing the pattern of expression of the remaining 12 NER genes analyzed between breast reduction (normal) (red) and tumor cell lines (blue). Autoradiograms were normalized for loading using *GAPDH* and expressed relative to normal FF in each experiment. Total RNA was generated from 3 breast reduction cell lines were and 3 stage I tumor cell lines. Each bar represents at least 6 independent analyses. Non-tumor adjacent cell lines showed similar results as the matching tumors.

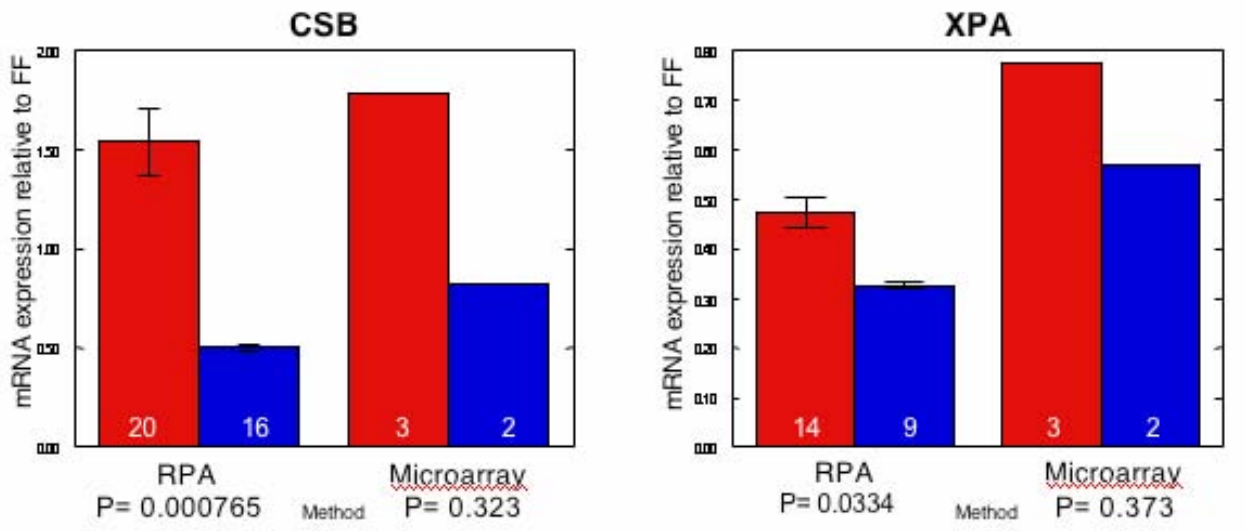

Figure 6. Gene expression microarray analysis of breast reduction (normal) (red) and stage I tumor (blue) samples show differences in NER gene expression consistent with the observed loss of functional activity in early stage tumors and decreases in gene expression as measured by RNAse protection. These differences, as measured by the microarray data, are not yet significant, however.

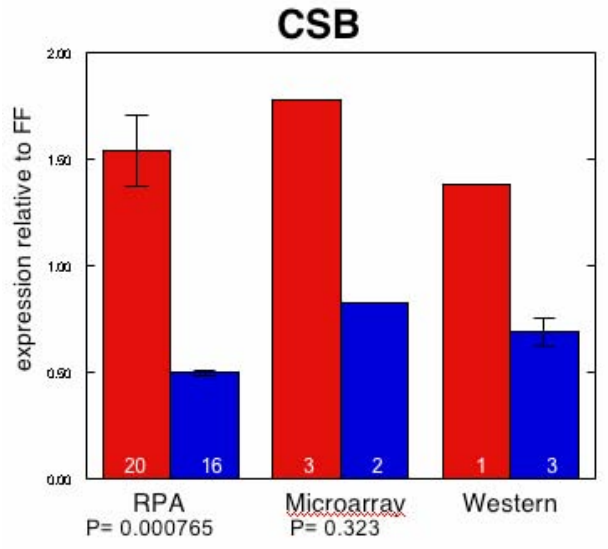

Figure 7. In certain candidate genes, functional deficiency of NER activity is accompanied by not only downregulation of the gene as measured by RNAse protection and gene expression microarray, but also by a relative deficicecy of the gene product as determined by Western analysis.

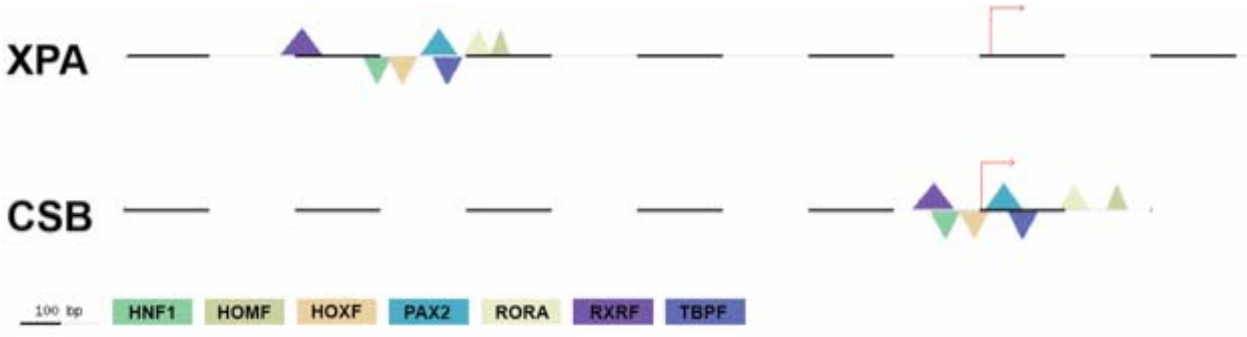

Figure 8. Seven transcription factor regulatory model linking the expression of the NER candidate genes *XPA* and *CSB*.

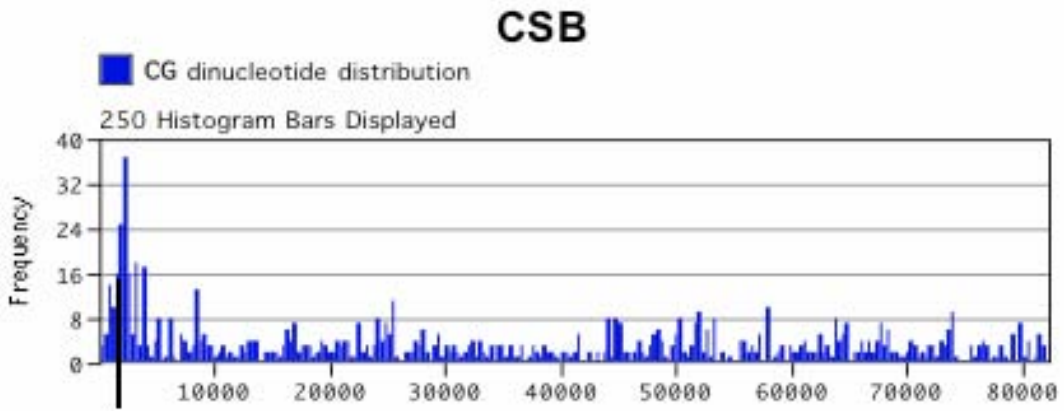

Figure 8. CG dinucleotide distribution of the *CSB* candidate gene showing the position of a "CpG island" in the 5' promotor region.

analyzing DNA double strand break damage and repair using pulsed field electrophoresis (31). This method is somewhat analogous to a large-scale comet assay, with the extent of DNA damage determined by the migration of DNA fragments out of the nucleus. Repair capacity can
then be measured by inducing DNA damage and allowing the cells time to repair the induced damage, as shown in **Figure 10**. We will also pursue funding to apply this assay to our breast tissue cell lines to determine whether a deficiency of DNA double strand break repair can be detected in breast cancer patients, as might be suggested by their susceptibility to ionizing radiation (1). This type of analysis may be particularly applicable to breast cancer patients who are carriers of the *BRCA1* or *BRCA2* genes, which have been implicated to play a role in this type of DNA repair (6).

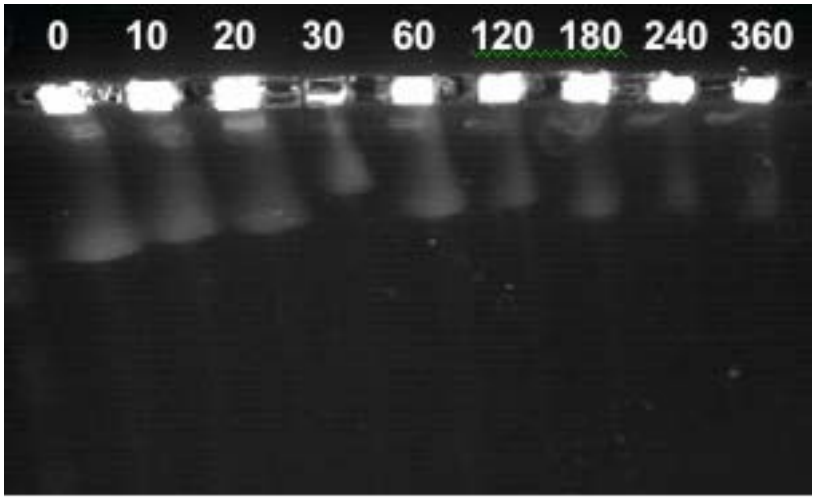

Figure 10. Repair of DSB damage in the Ishikawa endometrial cancer cell line following exposure to 60 Gy and repair for the indicated amount of time (minutes).

We have also extended our UDS results to include established breast cancer cell lines, stage 2 tumors and the histologically "normal" breast epithelium surrounding our stage 1 tumors. As shown in **Figure 11**, analysis of a number of established breast tissue-derived cell lines, including a putative "normal" line shows very high levels of NER. Thus, these lines are not representative of this characteristic of early stage breast cancer nor of the tissue-specific level of NER found in normal breast epithelium. A manuscript on these data has been written; since the cell line data are compared to the NER results from the stage 1 tumors, this paper awaits the acceptance of a manuscript containing those data.

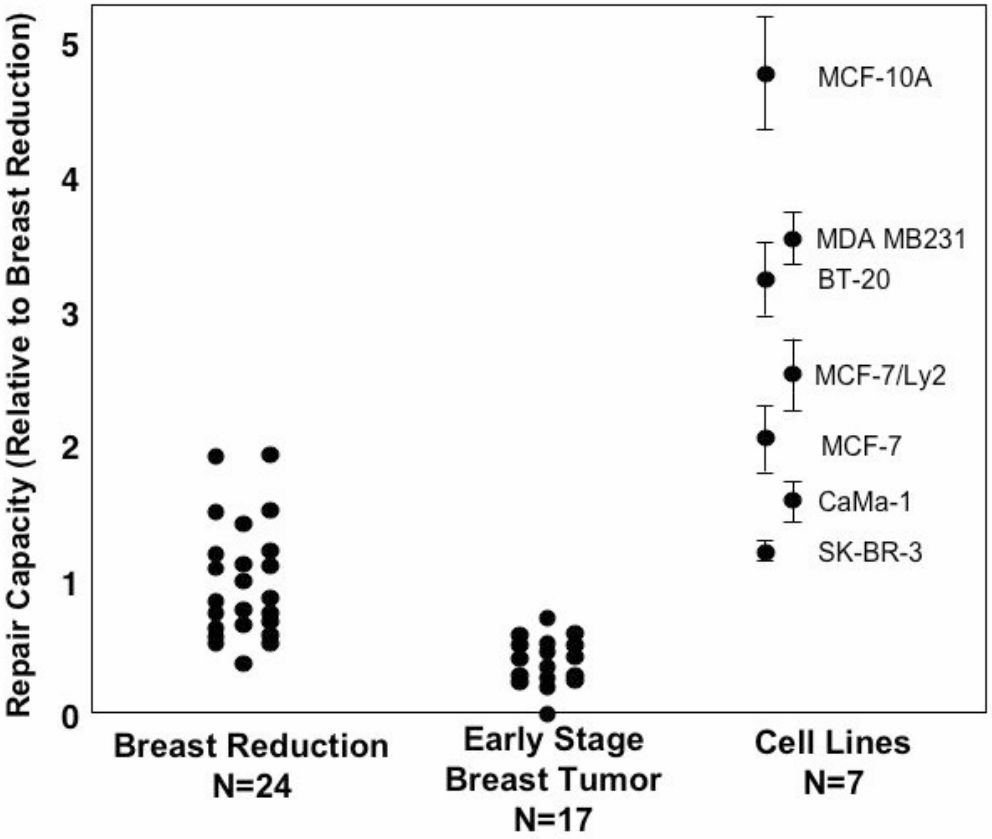

Figure 11. NER capacity of 6 established breast cancer cell lines and one putative "normal" line (MCF-10A) compared to data from normal breast epithelium (from breast reduction mammoplasty) and stage 1 breast tumors. Cell line data is based on a minimum of 3 independent analyses and is presented with error bars representing the SEM.

We have also generated UDS data on 13 samples of histologically normal, "non-tumor" adjacent breast epithelial samples from breat cancer patients (12 of which are matched to tumor samples). To our surprise, instead of exhibiting normal levels of NER (normal for breast epithelial tissue), we found that these samples were also significantly deficient in NER (32). These results also have important implications for the etiology and treatment of breast cancer, implying that the normal tissue around a tumor is actually pre-neoplastic, including exhibiting genomic instability. These data are consistent with the concept of "field carcinogenesis", which has been previously observed at the molecular level in breast cancer (33). Moreover, these data can also be used to distinguish cancer patients from controls (sensitivity 62%, specificity 78%) (**Table 3**), suggesting that UDS analysis of breast biopsy material may be clinically useful, even in the absence of abnormal histology. These data continue to be a significant improvement over the *GPA* assay results, and suggest that such NER measurements would be a better risk assessment tool for breast cancer, (although biopsy itself is a known risk factor [1]).

Finally, UDS results from 25 stage 2 breast tumors show that they share many characteristics of the stage 1 results. They exhibit a mean NER capacity of 0.69 ± 0.09 relative to the mean of the normal controls, significantly lower than the breast reduction controls ($P = 0.004$), but not significantly different from the NER capacity of the stage I samples ($P = 0.07$). If these data are added to the stage I results and similarly evaluated, the UDS assay with a cut-off of 70% normal activity can discriminate normal and tumor samples with a sensitivity of 76% and a significant OR of 11.5 (**Table 3**).

Key Research Accomplishments

- We have established that somatic mutational burden, as measured with *GPA* assay, is a potential predictor of breast cancer incidence.

- We have established that the application of the *GPA* assay for population screening of breast cancer risk is not limited by *GPA* genotype.

- We have established that breast cancer patients exhibit NER deficiency in blood lymphocytes, tumor tissue and normal epithelium from the affected breast, and that these measurements may also be potential predictors of breast cancer incidence.

- We have determine that there is concurrent downregulation of many of the genes in the NER pathway during breast carcinogenesis, and begun to investigate possible mechanisms, such as shared promotor elements and susceptibility to epigenetic effects.

- We have developed a method of analyzing DNA double strand break repair that can be applied to the samples generated in this study.

Reportable Outcomes

- One paper describes the application of the *GPA* assay to individuals not heterozygous for the *GPA* locus, providing the issue is to determine whether they have a "high" somatic mutational burden consistent with a genetic predisposition to cancer

Evdokimova, V.E., McLoughlin, R.K., Wenger, S.L., and Grant, S.G. (2005) Use of the glycophorin A bone marrow somatic mutation assay for rapid, unambiguous identification of Fanconi anemia homozygotes regardless of *GPA* genotype. *American Journal of Medical Genetics* **135A**: 59-65 (published online 04-08-05).

- Two papers involving our identification and analysis of high risk breast cancer patients:

Latimer, J.J., Rubinstein, W.S., Johnson, J.M., Kanbour-Shakir, A., Vogel, V.G., and Grant, S.G. (2005) Haploinsufficiency for *BRCA1* is associated with normal levels of DNA nucleotide excision repair in breast tissue and blood lymphocytes. *BMC Medical Genetics* **6**: 26 (published online 06-14-05).

Rubinstein, W.S., Latimer, J.J., Sumkin, J.H., Huerbin, M.B., Grant, S.G., and Vogel, V.G. (2006) Prospective screening study of 0.5 Tesla dedicated magnetic resonance imaging for the detection of breast cancer in young high risk women. *BMC Women's Health* (in press).

- One paper on the development of a new method to quantify double-stranded DNA damage and repair:

Joshi, N., and Grant, S.G. (2005) DNA double strand break damage and repair assessed by pulsed-field gel electrophoresis. *Methods In Molecular Biology* **291**: 121-129.

- Our initial studies on NER capacity in stage 1 breast tumor vs. normal epithelial tissue samples have been presented at six national, international or regional meetings, and they will form the basis of the Ph.D, thesis of M.D./Ph.D. student Jennifer M. Johnson):

Kelly, C.M., Johnson, J.M., Wenger, S.L., Vogel, V., Kelley, J., Johnson, R., Amortequi, A., Mock, L., Grant, S.G., and Latimer, J.J. (2003) Analysis of functional DNA repair in primary cultures of the non-tumor adjacent breast identifies two classes of breast cancer patient. Presented at the 2003 meeting of the *American Association for Cancer Research*, Washington, D.C. *Proceedings of the American Association for Cancer Research* **44**: 974-975.

Latimer, J.J., Johnson, J.M., Kelly, C.M., Mock, L., Vogel, V.G., Johnson, R., Kelley, J., Brufsky, A.M., Amortequi, A., Shestack, K., and Grant, S.G. (2004) Evidence for both hereditary deficiency and somatic loss of nucleotide excision repair in human breast cancer. Presented at the Sixth Annual *Midwest DNA Repair Symposium*, University of Kentucky, Lexington, Kentucky.

Latimer, J.J., Johnson, J.M., Kelly, C.M., Grant, S.G., Vogel, V.G., Brufsky, A.M., and Kelley, J. (2004) Human breast cancer tumors manifest both hereditary deficiency and somatic loss of DNA (nucleotide excision) repair. Presented at the 2004 meeting of the *Environmental Mutagen Society*, Pittsburgh, Pennsylvania. *Environmental and Molecular Mutagenesis* **44**: 211.

Latimer, J.J., Johnson, J.M., Kelly, C.M., Mehat, S.B., Grant, S.G., Vogel, V.G., and Kelley, J. (2004) Loss of expression of CSB and XPA in both hereditary deficiency and somatic loss of DNA (nucleotide excision) repair in human breast cancer. Presented at the American Society for Microbiology conference on *DNA Repair and Mutagenesis: From Molecular Structure to Biological Consequences*, Southampton, Bermuda.

Grant, S.G., Johnson, J.M., and Latimer, J.J. (2005) Genetic basis of DNA repair deficiency in sporadic breast cancer. Presented at *A Promise In Action—The Susan G. Komen Breast Cancer Foundation 2005 Mission Conference*, Washington, D.C.

Latimer, J.J., Johnson, J.M., Kelly, C.M., Beaudry-Rodgers, K., Vogel, V.G., Kelley, J., Johnson, R., Amortegui, A., Mock, L., and Grant, S.G. (2005) Genetic analysis of DNA nucleotide excision repair deficiency in novel non-tumor adjacent and tumor cell lines suggests a new paradigm of breast cancer etiology. Presented at the 2005 *Department of Defense Breast Cancer Research Program Era of Hope Meeting*, Philadelphia, Pennsylvania.

- Three manuscripts based on this work have been submitted and are now in revision:

Latimer, J.J., Kelly, C.M., Kelley, J., Johnson, R., Kanbour-Shakir, A., Vogel, V.G., and Grant, S.G. Intrinsic loss of nucleotide excision repair in breast cancer. *Journal of the National Cancer Institute*

Latimer, J.J., Giuliano, K., Kelly, C.M., Johnson, J.M., Focht, D., Amortegui, A., Grant, S.G., Vogel, V.G., and Beer Stolz, D. A novel paradigm for mammary tissue engineering using embryonic stem cell based medium. *Nature Methods*

Latimer, J.J., Rubinstein, W.S., Das, R.M., and Grant, S.G. Elevated levels of blood-based somatic mutation in a manifesting *BRCA1* mutation carrier. *Journal of Medical Genetics*

- Two manuscripts based on this work are in preparation, and close to submission:

Johnson, J.M., Beaudry-Rodgers, K., Piersall, L.D., Grant, S.G., and Latimer, J.J. Elevated DNA nucleotide excision repair capacity in breast cancer cell lines relative to primary breast tumor cultures.

Latimer, J.J., Dimsdale, J.M., Johnson, J.M., Kisin, E., Edwards, R., and Grant, S.G. Primary human ovarian epithelial cultures are functionally similarly to breast in DNA nucleotide excision repair capacity.

- We anticipate further manuscripts based on the completed gene expression data generated by RNAse protection, the ongoing gene expression microarray and Western analyses, the stage 2 tumor NER results and the NTA NER results.

Conclusions

We have determined that mutagenesis is an important element in breast cancer incidence and that factors that modulate this effect, such as environmental exposures and genetic susceptibility may be useful in performing individual estimations breast cancer risk. We have developed a method to integrate these factors into a single measure of "somatic mutational burden" using the blood-based *GPA* assay, and demonstrated that the application of the assay for this purpose is not limited to a subset of the population. We have determined that breast epithelial cells are relatively deficient in activity of the NER DNA repair pathway, and that early stage tumors and even histologically normal NTA from an affected breast are significantly reduced in NER capacity. We have shown how these data can also be used in a screening scenario to detect women at increased risk of breast cancer, and pointed out the implication of these results for the design of breast cancer treatment regimen. We are now characterizing this affect at the molecular level, including pursuing means of modulating NER during ccarcinogenesis and treatment, and are pursuing studies to extend these results to other factors that potentially modulate somatic mutation burden, such as DNA double strand break repair.

References

1. Gierach G, Vogel VG. (2004) Epidemiology of breast cancer. *In:* Advanced Therapy of Breast Disease, 2nd Edition (Singletary SE, Robb GL, Hortobagyi GN, eds). Decker, Hamilton, pp. 58-83.
2. Gail MH, Benichou J (1992) Assessing the risk of breast cancer in individuals. *In*: Cancer Prevention (DeVita VT Jr, Hellmann S, Rosenberg SA, eds), Lippincott, Philadelphia, pp. 1-15.
3. Rubinstein WS, Latimer JJ, Sumkin JH, Huerbin MB, Grant SG, Vogel VG. (2006) Prospective screening study of 0.5 Tesla dedicated magnetic resonance imaging for the detection of breast cancer in young, high risk women. BMC Women's Health (in press).
4. Grant SG, Jensen RH (1993) Use of hematopoietic cells and markers for the detection and quantitation of human *in vivo* somatic mutation. *In*: Immunobiology of Transfusion Medicine (Garratty G, ed), Marcel Dekker, New York, pp. 299-323.
5. Fuscoe JC, Zimmerman LJ, Harrington-Brock K, Burnette L, Moore MM, Nicklas JA, O'Neill JP, Albertini RJ (1992) V(D)J recombinase-mediated deletion of the *hprt* gene in T-lymphocytes from adult humans. Mutation Research 283: 13-20.
6. Futaki M, Liu JM (2001) Chromosomal breakage syndromes and the BRCA1 genome surveillance complex. Trends in Molecular Medicine 7: 560-655.

7. Grant SG (2001) Molecular epidemiology of human cancer: biomarkers of genotoxic exposure and susceptibility. Journal of Environmental Pathology, Toxicology and Oncology 20: 237-253.
8. Evdokimova VE, McLoughlin RK, Wenger SL, Grant SG (2005) Use of the glycophorin A bone marrow somatic mutation assay for rapid, unambiguous identification of Fanconi anemia homozygotes regardless of *GPA* genotype. American Journal of Medical Genetics 135A: 59-65 (published online 04-08-05).
9. Grant SG, Reeger W, Wenger SL (1998) Diagnosis of ataxia telangiectasia with the glycophorin A somatic mutation assay. Genetic Testing 1: 261-267.
10. Langlois RG, Bigbee WL, Jensen RH, German J (1989) Evidence for elevated *in vivo* mutations and somatic recombination in Bloom's syndrome. Proceedings of the National Academy of Science (USA) 86: 670-674.
11. Kyoizumi S, Nakamura N, Takebe H, Tatsumi K, German J, Akiyama M (1989) Frequency of variant erythrocytes at the glycophorin-A locus in two Bloom's syndrome patients. Mutation Research 214: 215-222.
12. Grant SG, Kelley JL, Vogel VG, Brufsky AM, Bigbee WL, Latimer JL (2005) Variability in bone marrow mutational response in breast cancer patients treated with genotoxic chemotherapy [Abstract]. Mutation Research 577(Supplement 1): e165.
13. Thompson LH. (1998) Nucleotide excision repair: its relation to human disease. *In:* DNA Damage and Repair, Volume 2: DNA Repair in Higher Eukaryotes (Nickoloff JA, Hoekstra MF, eds), Humana, Totowa (NJ), pp. 335-393.
20. Latimer JJ (2000) Epithelial cell cultures useful for in vitro testing. US patent 6074874.
21. Kovacs E, Stucki D, Weber W, Muller HJ. (1986) Impaired DNA-repair synthesis in lymphocytes of breast cancer patients. Eur J Cancer Clin Oncol 22: 863-869.
22. Xiong P, Bondy ML, Li D, Shen H, Wang LE, Singletary SE, Spitz MR, Wei Q. (2001) Sensitivity to benzo(a)pyrene diol-epoxide associated with risk of breast cancer in young women and modulation by glutathione S-transferase polymorphisms: a case-control study. Cancer Research 61: 8465-8469.
23. Kennedy DO, Agrawal M, Shen J, Terry MB, Zhang FF, Senie RT, Motykiewicz G, Santella RM. (2005) DNA repair capacity of lymphoblastoid cell lines from sisters discordant for breast cancer. Journal of the National Cancer Institute 97: 127-132.
24. Araujo SJ, Tirode F, Coin F, Pospiech H, Syvaoja JE, Stucki M, Hubscher U, Egly JM, Wood RD. (2000) Nucleotide excision repair of DNA with recombinant human proteins: definition of the minimal set of factors, active forms of TFIIH, and modulation by CAK. Genes and Development 14: 349-359.
25. Cleaver JE, Thomas GH. (1981) Measurement of unscheduled synthesis by autoradiography. *In*: DNA Repair: A Laboratory Manual of Research Procedures, Volume I, (Friedberg, E.C., and Hanawalt, P.C., eds), Marcel Dekker, New York, pp. 277-287.
26. Williams GM, Mori H, McQueen CA. (1989) Structure-activity relationships in the rat hepatocyte DNA-repair test for 300 chemicals. Mutation Research 221: 263-286.
27. Grant SG, Wenger SL, Latimer JJ, Thull D, Burke LW. (2000) Analysis of genomic instability using multiple assays in a patient with Rothmund-Thomson syndrome. Clinical Genetics 58: 209-215.
28. Latimer JJ, Nazir T, Flowers LC, Forlenza MJ, Beaudry-Rodgers K, Kelly CM, Conte JA, Shestak K, Kanbour-Shakir A, Grant SG. (2003) Unique tissue-specific level of DNA nucleotide excision repair in primary human mammary epithelial cultures. Experimental Cell Research 291: 111-121.
29. Martin GM, Ogburn CE, Colgin LM, Gown AM, Edland SD, Monnat RJ Jr. (1996) Somatic mutations are frequent and increase with age in human kidney epithelial cells. Human Molecular Genetics 5: 215-221.
30. Larsen F, Gundersen G, Lopez R, Prydz H. (1992) CpG islands as gene markers in the human genome. Genomics 13: 1095-1107.
31. Joshi N, Grant SG. (2005) DNA double strand break damage and repair assessed by pulsed-field gel electrophoresis. Methods In Molecular Biology 291: 121-129.
32. Kelly CM, Johnson JM, Wenger SL, Vogel V, Kelley J, Johnson R, Amortequi A, Mock L, Grant SG, Latimer JJ (2003) Analysis of functional DNA repair in primary cultures of the non-tumor adjacent breast

identifies two classes of breast cancer patient [Abstract]. Proceedings of the American Association for Cancer Research 44: 974-975.
33. Deng G, Lu Y, Zlotnikov G, Thor AD, Smith HS. (1996) Loss of heterozygosity in normal tissue adjacent to breast carcinomas. Science 274: 2057-2059.

Appendices

1. Evdokimova V, McLoughlin RK, Wenger SL and Grant SG. (2005) Use of the Glycophorin a somatic mutation assay for rapid, unambiguous identification of fanconi anemia homozygotes regardless of GPA Genotype. Am. Journal of Medical Genetics 125A:59-65.
2. Rubinstein WS, Latimer JJ, Sumkin JH, Huerbin M and Grant SG. Prospective screening study of 0.5 Tesla dedicated magnetic resonance imaging for the detection of breast cancer in young, high-risk women.
3. Latimer, J.J., Rubinstein, W.S., Johnson, J.M., Kanbour-Shakir, A., Vogel, V.G., and **Grant**, **S**.**G**. (2005) Haploinsufficiency for *BRCA1* is associated with normal levels of DNA nucleotide excision repair in breast tissue and blood lymphocytes. *BMC Medical Genetics* **6**: 26 (published online 06-14-05).
4. Joshi, N., and **Grant**, **S**.**G**. (2005) DNA double strand break damage and repair assessed by pulsed-field gel electrophoresis. *Methods In Molecular Biology* **291**: 121-129.

American Journal of Medical Genetics 135A:59–65 (2005)

Use of the Glycophorin A Somatic Mutation Assay for Rapid, Unambiguous Identification of Fanconi Anemia Homozygotes Regardless of *GPA* Genotype

Viktoria N. Evdokimova,[1] Reagan K. McLoughlin,[2] Sharon L. Wenger,[3] and Stephen G. Grant[1]*

[1]*Department of Environmental and Occupational Health, Graduate School of Public Health, University of Pittsburgh, Pittsburgh, Pennsylvania*
[2]*Department of Human Genetics, Graduate School of Public Health, University of Pittsburgh, Pittsburgh, Pennsylvania*
[3]*Department of Pathology, West Virginia University, Morgantown, West Virginia*

A 7-year-old girl was hospitalized with pancytopenia requiring blood transfusion. She and an older brother with suspicious symptoms were referred for laboratory testing to confirm a clinical diagnosis of Fanconi anemia (FA). Blood samples from these two children and one parent were examined with the *GPA* somatic mutation assay. The patient's total *GPA* somatic mutation frequency of 1.4×10^{-4} was determined despite the confounding effects of her recent transfusion, and was greater than 10-fold higher than that of a population of pediatric controls, consistent with the known FA phenotype. Her brother was not informative for the standard *GPA* assay, which requires heterozygosity for the MN blood group, but was analyzed with a modified assay that measured only allele loss mutation. His mutation frequency, 6.8×10^{-4} was also supportive of a diagnosis of FA. Both analyses also showed evidence of ongoing mutation through terminal erythroblast differentiation, a characteristic of patients with DNA repair syndromes which further confirmed the diagnoses. These conclusions were confirmed with traditional DEB-induced chromosome breakage studies. The quantitative and qualitative aspects of the *GPA* assay relevant for applying this test for FA diagnosis, and perhaps for carrier detection, are discussed.

KEY WORDS: **Fanconi anemia; FA; Fanconi anemia heterozygotes; GPA; somatic mutations; clinical diagnosis**

INTRODUCTION

Fanconi anemia (FA) is an autosomal recessive disorder with a monogenic mode of inheritance [Rogatko and Auerbach, 1988], caused by highly heterogeneous mutations in the genes of the FA complementation groups. FA affects all marrow elements, resulting in anemia, leucopenia, and thrombocytopenia, although there is significant clinical diversity [Auerbach et al., 1989]. Leukemia is a fatal complication and may occur in patients lacking full-blown features. FA also has a distinctive cellular phenotype: high frequencies of both spontaneous chromosome breakage and chromosome aberrations, usually rearrangements between non-homologous chromosomes [Schroeder et al., 1964; Bloom et al., 1966; Schroeder and German, 1974]. In addition, lymphocytes from FA patients show a G_2 phase arrest [Schindler et al., 1987] and FA cells have accelerated telomere erosion [Callen et al., 2002]. FA cells are hypersensitive to the cytotoxic and clastogenic effects of DNA cross-linking agents, such as the difunctional alkylating agent diepoxybutane (DEB) [Chaganti and Houldsworth, 1991].

The molecular diagnosis of FA is complicated by the heterogeneity of the mutation spectrum and the frequency of intragenic deletions. The accepted diagnostic laboratory test for identification of FA homozygotes remains the in vitro induction of chromosome breakage with DEB or mitomycin C [Auerbach et al., 1979, 1985, 1986; Rosendorff and Bernstein, 1988]. Although this analysis can be performed by most cytogenetics laboratories, it is labor-intensive, involving viable cell culture and some expertise to read the slides.

The flow cytometric glycophorin A (*GPA*) assay is based on detection and quantitation of somatic "allele loss" mutations at the glycophorin A locus (also called *GYPA*) on chromosome 4. This locus encodes a major red blood cell surface sialoglycoprotein existing in two common isoforms: M and N [Grant and Bigbee, 1993]. The *GPA* assay is potentially sensitive to a broad spectrum of mutational events, including point mutation, small insertions and/or deletions, chromosomal aneuploidy, epigenetic gene inactivation, homologous or non-homologous recombination [Grant et al., 1992a]. Previous studies have shown an association between *GPA* mutation level and elevated risk of cancer [Grant, 2001], particularly in the so-called "DNA repair" diseases ataxia telangiectasia (AT) [Bigbee et al., 1989; Hewitt and Mott, 1992], FA [Bigbee et al., 1991; Sala-Trepat et al., 1993], and Bloom syndrome [Langlois et al., 1987; Kyoizumi et al., 1989b], which show 10-, 50-, and 100-fold increases in *GPA* mutation frequencies, respectively [Grant et al., 1991]. We have recently shown that this increased *GPA* mutation frequency, in concert with a characteristic flow cytometric pattern, can be used in the laboratory diagnosis of AT [Grant et al., 1997].

The *GPA* assay is based on our ability to easily and unambiguously distinguish the two allelic gene products of the *GPA* locus in $GPA^{M/N}$ heterozygotes and therefore measure mutations with "single-hit" kinetics [Grant et al., 1992a]. This effectively limits the application of the assay to the ~50% of the population who are heterozygous, reasonable enough for screening studies, but unacceptable for clinical use. This study also demonstrates how the *GPA* assay may be applied

Grant sponsor: NIH; Grant number: HD33016; Grant sponsor: University of Pittsburgh (Competitive Medical Research grant).

*Correspondence to: Stephen G. Grant, Ph.D., Department of Environmental and Occupational Health, Graduate School of Public Health, University of Pittsburgh, 3343 Forbes Avenue, Pittsburgh, PA 15213. E-mail: sgg@pitt.edu

Received 14 January 2004; Accepted 21 January 2005

DOI 10.1002/ajmg.a.30687

in non-heterozygotes, providing that the expected mutation frequency is higher than background. We also demonstrate how the *GPA* assay can be applied even when a blood transfusion, a common treatment for anemic conditions, potentially confounds the analysis.

MATERIALS AND METHODS

Case History

A 7-year-old white female was hospitalized with nosebleed at which time pancytopenia was identified. She received a transfusion of packed red blood cells. Her height and weight were less than the 5th centile. She had a history of fatigue, pallor, poor growth, occasional infections and bruised easily. Her right kidney was somewhat smaller than the left, and malrotated. No other physical findings were noted.

The patient's 8.5-year-old brother had a medical history of hospitalization at 18 months of age for failure to thrive. His height and weight were less than the 5th centile. He had recurrent otitis media, hearing loss, pallor, and was easily fatigued.

A younger brother was apparently normal. The family reported a great maternal uncle who died at age 12, described as "tired." Blood samples from the patient and her older brother were sent for laboratory confirmation of clinical diagnosis or suspicion of FA, respectively. A sample from one of their parents was also submitted for analysis.

Cytogenetics

Peripheral blood samples from the patient, her older brother, and their parent were processed for routine cytogenetic analysis, including 72 hr incubation in RPMI 1640 medium and trypsin-Giemsa banding [Seabright, 1971]. Blood samples from normal controls were set up concurrently with each patient sample.

For FA testing, DEB was added 24 hr after the initiation of culture to give a final concentration of 0.01 μg/ml in one of two parallel cultures [Auerbach et al., 1981]. Cultures were incubated an additional 48 hr and harvested for metaphases using routine cytogenetic technique. Slides from cultures with and without DEB treatment were solid stained using Giemsa. One hundred cells were scored for chromosomal breakage and interchanges per culture. Laboratory reference for the range of breaks/cell for controls is 0.00–0.10 with or without DEB treatment. For FA patients, the range of spontaneous breakage per cell is 0.05–0.38 and the range of DEB-induced breakage per cell is 0.36–2.12. In our hands, chromosome breakage is 5.4-fold higher in these patients after DEB treatment, which is comparable to the approximately fivefold increase reported in the literature [Auerbach et al., 1981].

Somatic Mutation Assay

The "DB6" version of the *GPA* somatic mutation assay was performed as described [Grant, 2005]. Intact erythrocytes from the patient, two family members, and controls were "sphered" in hypotonic solution and fixed in formaldehyde/SDS buffer. Sphered cells were then labeled with two monoclonal antibodies, each specific to one allelic isoform of the glycophorin A protein via an extracellular epitope. A standard assay consisted of 5×10^6 cells analyzed by quantitative flow cytometric analysis of the conjugated fluorophors, at flow rates of 3,000–4,000 cells per second, using a rectangular gate in the forward scatter versus log side-scatter distribution to discriminate for intact cells and against antibody induced cell aggregates. Mutation frequencies were calculated as the number of events falling within this defined region of the histogram divided by the total number of analyzed cells. Analysis of samples with unusually high mutation frequencies were repeated, and the results given represent an average of these two assays. Concurrent control blood samples were also obtained from 11 healthy donors: 1 $GPA^{M/N}$ heterozygote and 10 $GPA^{M/M}$ homozygotes. The concurrently analyzed M/N control yielded a total mutation frequency of 8.0×10^{-6}, with equal representation of simple allele loss mutants and mutants with a phenotype consistent with allele loss and duplication [Grant et al., 1991]. These results are in excellent agreement with the historic mutation frequencies associated with this individual, who has been assayed 25 times in our laboratory, with mean total *GPA* mutation frequencies of $9.4 \pm 1.0 \times 10^{-6}$ cells analyzed, allele loss frequencies of $4.3 \pm 0.4 \times 10^{-6}$, and loss and duplication frequencies of $5.1 \pm 0.8 \times 10^{-6}$ ($P \approx 0.4$ for all three measurements). Historical control samples for this study were obtained from employees of the Lawrence Livermore National Laboratory and their families, from 1988 through 1991. Subsets of this data have been previously reported [Jensen et al., 1987, 1991]. Reference samples from confirmed FA patients and obligate heterozygotes were obtained from Dr. Arlene D. Auerbach of the International Fanconi Anemia Registry (IFAR) [Kutler et al., 2003].

Statistical Analysis

Analysis of individual results in the context of control populations was done with the *z*-test at $\propto = 0.05$ on ln transformed data. Comparisons between populations were performed with the *t*-test at the same level of significance on similarly transformed data.

RESULTS

Cytogenetics

The hospitalized patient had a normal female karyotype. She had 7 spontaneous gaps and breaks and one quadriradial out of 50 cells, and 75 breakage/interchange configurations among 100 cells following treatment with DEB. The latter included chromosomal gaps and breaks, a dicentric, triradials, quadriradials, acentric fragments and multiple interchange figures. Both of these values are well above the range of normal controls in our hands, and confirm a diagnosis of FA.

The older brother had a normal male karyotype and spontaneous gaps and breaks in 14 out of 100 cells. His DEB-induced culture contained 53 breakage/interchange configurations among 100 cells, which included gaps, breaks, a triradial, quadriradials, and acentric fragments. A bone marrow aspirate drawn at the time of testing was hypocellular. Once again, these results confirm the clinical diagnosis of FA.

The parent's spontaneous chromosome breakage level was 5/100 cells, which increased to 11/100 in the DEB-treated culture. The latter is slightly higher than the normal range of 1–10 induced breakage/interchange configurations per 100 cells, which may be related to his carrier status of the *FA* gene, but cannot be used reliably to diagnose heterozygotes [Cohen et al., 1982; Cervenka and Hirsch, 1983].

Somatic Mutation Analysis

Following routine cytogenetic and DEB tests, 500 μl aliquots of the whole blood samples from the patient, her brother, their parent, and healthy controls were serotyped for the M/N blood group and further processed for analysis with the *GPA* somatic mutation assay. The *GPA* assay enumerates variant cells potentially arising by a wide variety of molecular mechanisms associated with allelic "segregation" or loss of heterozygosity (LOH) [Worton and Grant, 1985; Grant et al., 1991]. These mutants can be further characterized by the level of expression of the remaining *GPA* allele into "N/Ø" variants, with a simple

allele loss phenotype, and "N/N" cells, which, in addition to the loss of the M allele, express the remaining N allele at twice the normal level. Previous studies have demonstrated an increased frequency of uninduced *GPA* mutation in FA patients corresponding to an average 30-fold increase in N/Ø variants and an 8-fold increase in N/N variants compared to unaffected controls [Bigbee et al., 1991; Sala-Trepat et al., 1993].

The patient had a heterozygous M/N phenotype, ideal for evaluation by the *GPA* assay. In practice, however, the flow histogram of her sample revealed a more complicated situation (Fig. 1). Major peaks of approximately equal size were evident in the areas of the histogram associated with both an M/M and an M/N genotype. It was hypothesized that one of the peaks consisted of cells from a transfusion of packed cells given 9 days prior to sample acquisition. Quantitation of the nucleic acid content of circulating red cells by staining with propidium iodide (PI) revealed that the cells comprising the M/M peak had a very low proportion of cells retaining nucleic acid, specifically mRNAs in reticulocytes, of 0.3% [Corver et al., 1994]. Cells in the M/N peak, and variant cells falling in the allele loss window had much higher reticulocyte proportions of 4.7%, suggesting that they were the patient's own cells, and that the vast majority of M/M cells were derived from the transfusion. The total *GPA* mutation frequency of the patient was 71.9×10^{-6} ($P = 0.0024$ versus normal pediatric controls), with an allele loss (N/Ø) frequency of 59.7×10^{-6} ($P < 0.0001$), and an allele loss and duplication (N/N) frequency of 12.2×10^{-6} ($P = 0.20$). This N/Ø frequency is already high enough to be considered an "outlier" [Bigbee et al., 1998] and is supportive of a diagnosis of FA [Bigbee et al., 1991; Sala-Trepat et al., 1993; Grant et al., 1997], but the analysis becomes even more definitive if these frequencies are adjusted for the number of transfused cells confounding the assay: total *GPA* mutation frequency = 143.5×10^{-6} ($P < 0.0001$), N/Ø frequency = 119.2×10^{-6} ($P < 0.0001$), N/N frequency = 24.3×10^{-6} ($P = 0.041$). The allele loss frequency from this patient is compared to those from the two previously reported, largely pediatric populations and a matched set of controls in Figure 2.

Although the uninduced N/Ø mutation frequency for this patient is elevated and therefore is consistent with a diagnosis of FA, this observation is not, in itself, conclusive (although in conjunction with the clinical findings reported above, it may be considered confirmative). Individuals with similarly elevated mutation frequencies have been observed in all populations surveyed with the *GPA* assay [Jensen et al., 1987; Akiyama et al., 1995; Radack et al., 1996]. We have found that the proportion of such outlier individuals is ~2% in newborns [Manchester et al., 1995], and increases with age [Bigbee et al., 1998]. In our previous application of the *GPA* assay to the diagnosis of AT [Grant et al., 1997], we pointed out several characteristics of the flow histogram that help in discriminating these patients from outlying controls, and some of these are also applicable to FA. First, we noted that the elevation in *GPA* mutation in AT was due exclusively to generation of allele loss type mutants; there was no evidence for an effect on the frequency of loss and duplication mutation in that disease. As mentioned earlier, it has been reported that, while an elevation in allele loss mutation is also a consistent observation in FA, there is also evidence for an elevation in loss and duplication mutants, although of lesser magnitude [Sala-Trepat et al., 1993]. In our hands, any elevation in the frequency of loss and duplication mutants is highly variable, and we do not consider it to be a reliable feature of the analysis [Grant et al., 2004]. In particular, it must be assured that additional events in the N/N window represent a true peak of variant cells with a loss and duplication phenotype, and are not simply spill over events from the large peak of N/Ø variants. In any case, an increased frequency of loss and duplication mutants may be considered as a possible but not mandatory feature of the FA phenotype. Our patient had a slightly elevated N/N mutation frequency when compared to those of the control population given in Figure 2 ($7.7 \pm 1.0 \times 10^{-6}$), but this does not weigh significantly in the diagnostic efficacy of her *GPA* analysis.

The next feature that typifies the *GPA* analysis of an AT or FA patient is the presence of a peak of cells corresponding to loss of the N allele rather than the M allele. Our preference for quantification of M allele loss in the form of the N/Ø and N/N variant classes is due to the technical parameters of the detection system rather than any inherent genetic difference in the M and N alleles. The N/Ø and N/N windows are set at less than 1% M allele-specific fluorescence, usually assuring unambiguous discrimination of wild type and mutant cells. The N-specific antibody used in the assay, however, cross-reacts with another, related sialoglycoprotein on the red cells surface, glycophorin B, which is expressed at about 1/3 the level of glycophorin A [Cartron and Rahuel, 1995]. Thus, loss of signal from a single copy of the *GPA* N allele reduces the total fluorescein fluorescence by less than an order of magnitude,

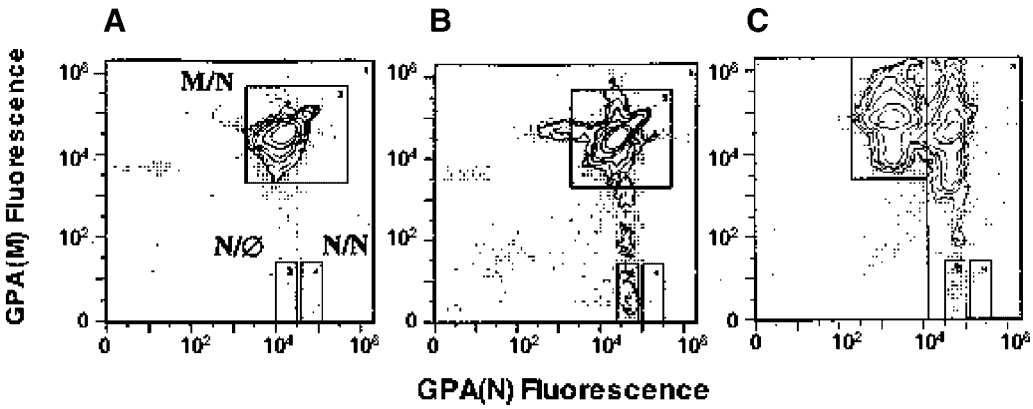

Fig. 1. Flow cytometric histograms of 10^6 erythrocytes from a normal control (**A**), a confirmed Fanconi anemia (FA) patient (**B**), and the current patient (**C**) analyzed with the *GPA* assay. The major peak in all three consists of heterozygous M/N cells with equal labeling with both fluorophors. Allele loss mutations appear in a window directly beneath the main peak with less than 1% GPA(M) fluorescence. Loss and duplication mutations appear in a equally sized window directly to the right of the allele loss window, indicative of a twofold increase in GPA(N) fluorescence (note log scale). Together, these two windows define total GPA mutation. A "ridge" of cells joining the main peak to the mutant window is evident in both the affected FA patient and the diagnostic sample. An "arm" of N-allele loss and loss and duplication mutants is also evident extending left from the main peak in the FA patient, but this area of the distribution is obscured in our patient sample by a large peak of M/M transfused cells.

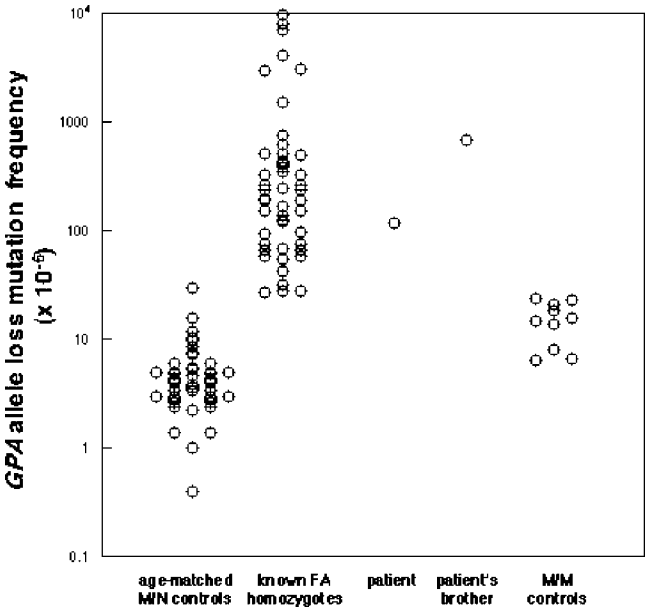

Fig. 2. Comparison of *GPA* allele loss mutation frequencies among FA patients, controls and diagnostic samples. Known FA patients and age-matched controls were derived from unpublished data and that of Sala-Trepat et al. [1993]. All are $GPA^{M/N}$ heterozygotes, as is the patient. M/M controls were obtained specifically for comparison with the patient's brother, but as adult samples, would be expected to have a slightly higher mutation frequency. These samples also reflect allele-loss from two alleles rather than one, and may have a higher background simply because they cannot be distinguished from the constitutive GPA phenotype as well by the antibodies used in the *GPA* assay.

rather than the 100-fold loss of phycoerythrin fluorescence associated with loss of an M allele. We, therefore, only quantify N allele-loss variants in cases such as this, where a large peak of mutants is expected (others regularly quantitate N allele-loss, however, in their unique version of the *GPA* assay [Kyoizumi et al., 1989a]). In any case, if FA is characterized by high frequencies of ongoing mutation, there should be approximately equal peaks of M allele loss and N allele loss mutants [Grant et al., 1997]. In this patient, however, the large peak of M/M cells attributable to transfusion obscures this area of the histogram. The fact that there were any PI-positive reticulocytes detectable in this peak, when the transfusion occurred over a week prior to sampling might suggest that there are actually a considerable number of mutant M/Ø and M/M variants generated by the patient contributing to this peak.

Finally, the most powerful qualitative feature of the flow histogram from an AT or FA patient is the presence of a "ridge" of cells joining the allele loss mutant peaks with the wild-type peaks [Grant et al., 1997]. This ridge does not appear in *GPA* analyses of normal individuals, even of outliers with unusually high mutation frequencies [Bigbee et al., 1998], nor does it appear in analyses of individuals with high mutation frequencies due to historic genotoxic exposures, such as survivors of the atomic bombing of Hiroshima [Langlois et al., 1987; Kyoizumi et al., 1989a]. We believe that this ridge is due to high frequencies of ongoing mutation occurring after the onset of *GPA* expression during erythroblast maturation, leading to a spectrum of partial mutant phenotypes. Besides patients with DNA repair syndromes, the only other situation where we have seen this phenomenon is in patients with an ongoing significant genotoxic exposure, such as cancer patients undergoing mutagenic chemotherapy [Bigbee et al., 1990; Grant et al., 2004]. This patient clearly shows evidence of such ongoing mutation (Fig. 2). Once again, we would expect a similar ridge linking the wild type peak to the N-allele loss peak, if it were not obscured by the transfused cells.

The patient's older brother displayed some suspicious clinical symptoms, so it was even more important to provide laboratory data on whether he might have FA. Unfortunately, his *GPA* phenotype was homozygous M/M. In such a case, it is completely impossible to observe allele loss plus duplication events, since it regenerates the original genotype. Simple allele loss, to produce an M/Ø phenotype, should occur, but it would only reduce the M-specific labeling by half, and these variants would occur in the "apron" of the main M/M peak. On the other hand, since there are two, indistinguishable M alleles in this individual, the frequency of M-allele loss variants should be twice as high as that observed in M/N heterozygotes. In running this sample, we hypothesized that if there was a large enough peak of M/Ø cells, suggesting that the brother was affected, it would be distinguishable as a separate peak immediately below the main M/M peak (Fig. 3).

Indeed, such a distinct peak was observed in the *GPA* flow histogram of this individual, yielding a frequency of allele-loss variants of 1360.6×10^{-6}. This is clearly an abnormally high "outlier" frequency when compared to our N/Ø variant frequencies from M/N heterozygotes, even when it is normalized to a single allele by dividing by the number, two, of M alleles that can be "lost" ($= 680.3 \times 10^{-6}$ [$P < 0.0001$]). There is also evidence for a ridge joining the mutant and wild-type peaks, an important qualitative feature of AT and FA *GPA* analyses. Since this analysis seemed to be useful, we similarly analyzed 10 samples from normal M/M individuals (Fig. 2; M/Ø variant frequency $= 31.9 \pm 4.8 \times 10^{-6}$), clearly establishing that the patient's brother had an unusually high frequency of allele loss mutation (>20-fold higher than controls, despite the fact that these are adult, not pediatric controls, and there is an established age effect in *GPA* somatic mutation [Jensen et al., 1987; Radack et al., 1996], even when performed with the assay that includes M/Ø variants in their analysis [Akiyama et al., 1995]). We therefore concluded that the results of the *GPA* analysis on this individual were supportive of a diagnosis of FA.

Based on these diagnoses, the children's parent must be an obligate heterozygote for FA. They had a rather low total *GPA* mutation frequency of 12.0×10^{-6} ($P = 0.43$ versus normal

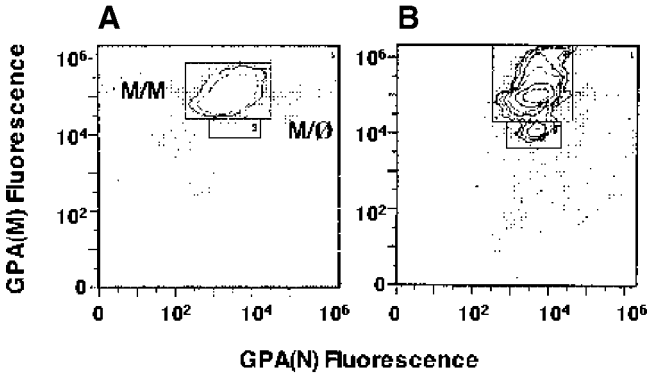

Fig. 3. Flow cytometric histograms of 10^6 erythrocytes from a normal $GPA^{M/M}$ control (**A**), and the current patient's brother (**B**) analyzed with the *GPA* assay. The major peak in both panels consists of homozygous M/M cells. This peak is only 1/3 closer to the Y-axis than the M/N peaks seen in Figure 1 because of cross-reaction of our GPA(N)-specific antibody with glycophorin B on the red cell surface. Allele loss phenotype M/Ø cells would fall directly beneath the main peak, with only half the GPA(M)-specific fluorescence of the main peak. At low, normal mutation frequencies, these cells (~10–20) are lost in the apron of the main peak. In the diagnostic sample, however, an unambiguous M/Ø is observed, as well as a ridge of cells with intermediate phenotypes extending to the main peak.

TABLE I. *GPA* Mutation Frequencies in Fanconi Anemia (FA) Heterozygote and Control Populations

	N	Total	*GPA* mutation frequencies[a] N/Ø	N/N
FA heterozygote	1	12.0	6.4	5.6
FA heterozygotes[b]	8	26.5 ± 4.0	13.5 ± 4.9	13.0 ± 1.2
Controls (aged 4–24)[b]	21	13.0 ± 1.4	6.2 ± 0.8	6.9 ± 0.7
Controls (aged 8–24)	61	13.5 ± 1.4	5.3 ± 0.4	8.2 ± 1.3
Controls (aged 25–55)	257	17.0 ± 0.6	7.2 ± 0.4	9.8 ± 0.5

[a] $\times 10^{-6}$.
[b] From Sala-Trepat et al. [1993].

adult controls), that was fairly equally divided between the allele loss (6.4×10^{-6} [$P = 0.34$]) and loss and duplication (5.6×10^{-6} [$P = 0.44$]) classes. Indeed, this total *GPA* mutation frequency is significantly lower ($P = 0.033$) than that of eight such obligate heterozygotes reported in Sala-Trepat et al. [1993] (Table I), who concluded that FA heterozygotes have slightly but significantly elevated *GPA* mutation frequencies. The low frequency in the patients' parent is primarily due to the loss and duplication class of variant ($P = 0.005$), since there is no significant difference in the frequency of allele loss variants ($P = 0.39$). If the comparison is extended to include a set of 28 obligate heterozygotes identified by the International Fanconi Anemia Registry (IFAR) at Rockefeller University, however, the present sample does not differ from this population in total *GPA* mutation frequency ($P = 0.18$), allele loss frequency ($P = 0.35$), or loss and duplication frequency ($P = 0.17$) (data not shown).

DISCUSSION

The data presented in this article confirm the reported elevated levels of somatic mutation at the autosomal *GPA* locus in FA patients and demonstrate how this result can be applied diagnostically. To date, we have performed a total of 152 analyses on putative FA patient samples and, by applying the diagnostic criteria outlined in the results, we have a perfect concordance with the DEB-induced chromosome breakage assay. This includes 145 samples from the IFAR (including 36 known FA patients) and 7 diagnostic cases, 3 positive, 4 negative. Thus, the *GPA* assay may be used either in conjunction with the DEB assay, or even instead of the DEB assay. The *GPA* assay requires much less blood than the DEB assay (essentially 100 μl, since phenotyping is no longer required), which is important in evaluating pediatric cases, requires no cell culturing, in vitro exposure or cytogenetic evaluation, and can be performed in a matter of hours. We have already shown that the *GPA* assay can be used to diagnose AT [Grant et al., 1997] and application to Bloom syndrome should be straightforward [Kyoizumi et al., 1989a; Langlois et al., 1989]. Thus, the assay has multiple clinical uses. Elevated *GPA* somatic mutation frequencies have also been observed in patients with Nijmegan breakage syndrome [Grant et al., 1992b], Cockayne syndrome [Lin et al., 1995], Werner syndrome [Kyoizumi et al., 1998; Moser et al., 2000], and possibly Rothmund–Thompson syndrome [Grant et al., 2000]. *GPA* mutation frequencies are also elevated in cancer patients [Okada et al., 1997; Grant, 2001]. Most significantly, we have shown that the *GPA* assay can be used to quantitatively biomonitor the effects of genotoxic chemotherapy [Bigbee et al., 1989; Grant et al., 2004], once again, regardless of *GPA* genotype, so that it may become a standard clinical technique.

We have previously published a set of guidelines for applying the *GPA* assay for the diagnosis of AT [Grant et al., 1997]. A similar set of criteria can be developed for FA. First, since allele loss mutation frequencies in FA patients are typically fivefold higher than the already elevated levels observed in AT [Grant et al., 1992a,b], similar quantitative criteria can be adopted for the two diseases, although the test should display a greater sensitivity for FA. AT patients have shown no evidence of increased frequencies of loss and duplication events, whereas there seems to be a variable increase in this class of mutants in FA. We suggest that this element of the analysis should be considered as supportive of the diagnosis if it is elevated, but neutral if it is not present. The best way to combine these criteria is to consider the total *GPA* mutation frequency as well as the N/Ø mutation frequency. Thus, a putative FA patient should have either an allele loss frequency equal to or greater than 30×10^{-6}, or a total *GPA* mutation frequency equal to or greater than 50×10^{-6}, or both. Applying these criteria to the combined FA datasets and younger (≤24-years-old) controls in Table I, the allele loss aspect of the test alone has a sensitivity of 92% and a specificity of 97% (four false negatives and one false positive). The contribution of the loss and duplication mutants is demonstrated by the improvement when the total *GPA* mutation frequency criterion is applied to this population: the test now has a sensitivity of 98% and a specificity of 100%. Indeed, the one remaining false negative has a combined mutation frequency of 49.4×10^{-6}, whereas the highest control has a frequency of 28.0×10^{-6}. If older adults and FA heterozygotes are added to the test population the sensitivity is unaffected, and the specificity is retained at a high level (98%), but there are now 10 false positives by either testing criteria. This illustrates the need to add qualitative assessment of the histogram to the testing procedure, especially if it is applied to adults. It is interesting to note that 3 and 4, respectively, of the false positives for allele loss and total *GPA* mutation frequency were FA heterozygotes.

The *GPA* assay was originally developed as a screening assay for human genotoxic exposures, and in this context it has been widely applied [Grant and Bigbee, 1993]. The genetic limitation that only $GPA^{M/N}$ heterozygotes are informative for the test has not been a major detriment to its application in exposure monitoring, since that is often a population-based procedure. For clinical application, however, having the test applicable to only half the test population has been an insurmountable problem. For example, in the populations presented in this article, a total of 192 samples received from IFAR (including known FA homozygotes, family members, and controls) were not assayed because of their homozygous *GPA* genotype. In addition, six diagnostic samples were not analyzed for the same reason. The present data suggest that all of these samples are now approachable from the standpoint of determining whether or not they are indicative of the FA phenotype. In this study, we report the diagnosis of a FA homozygote with an M/M GPA phenotype, because allele loss mutants, the major class affected by FA, are still detectable in such individuals (indeed, since they have two M alleles, their frequency is actually enhanced twofold over M/N heterozy-

gotes). Data from cancer patients, where the mutants are induced by genotoxic chemotherapy, suggest that similar results are possible from N/N homozygotes.

An additional 24 known FA homozygous samples from IFAR were not scored for *GPA* mutation due to recent transfusions. As this is a common treatment for the pancytopenia associated with FA (and, indeed, was the reason the current patient was referred for testing), any widespread diagnostic application of the *GPA* assay in putative FA patients depends on our ability to overcome this problem. We were fortunate in this case that the transfusion was comprised only of cells of M/M genotype, in a patient with a distinct M/N genotype. Thus, although the transfused red cells obscured any N-allele loss or loss and duplication variant cells, the presence of these cells did not affect the interpretation of the assay. Had the transfusion been of cells of mixed GPA phenotypes, e.g., from multiple donors, it is possible that the analysis would not have been informative. If the transfusion had been of N/N cells, these cells would have obscured the major peak of mutants used to establish the FA diagnosis, although, in this case, the N-allele loss peak (with an M/Ø phenotype) would not have been obscured. In some cases, with sufficient clinical support, this might be enough to confirm a diagnosis of FA. If the transfused cells had been of the same genotype as the patient, heterozygous M/N, these cells would have contributed greatly to the "normal" peak and only at background "normal" frequencies to the variants, effectively diluting the mutational signal used for diagnosis. Moreover, the effect of the transfused cells on the denominator of the calculation, total cells analyzed, cannot be compensated for, as was done for our patient, since the two cell populations would be indistinguishable. If the transfusion contributed approximately half of the red cell population, as was seen in the current patient, this dilution would reduce the sensitivity of the *GPA*-based diagnostic test to 84%, based on our current population. Thus, if the *GPA* analysis is to be performed on an M/N individual, it is best to either obtain the sample before any transfusions or to take this intent into account in the choice of transfused cells. Thus, for M/N heterozygous patients, M/M transfused cells are the least intrusive in the analysis. Similarly, for M/M and N/N patients, transfusions of cells with the opposite homozygous phenotype would be best.

The parents in this family are obligate heterozygotes for FA, but the *GPA* assay results from the parent who provided a blood sample were both quantitatively and qualitatively normal (although their DEB-induced chromosome breakage frequency was slightly high). The chromosome breakage assay has been proposed for use for carrier detection [Auerbach and Wolman, 1978; Auerbach et al., 1981], however, it is not considered either reliable or unequivocal in this context [Cohen et al., 1982; Cervenka and Hirsch, 1983]. Sala-Trepat et al. [1993] reported *GPA* mutation frequencies on eight obligate heterozygotes (Table I). The total *GPA* mutation frequency, as well as both the N/Ø and N/N frequencies of the FA heterozygotes were significantly higher than their concurrently analyzed normal controls ($P < 0.001$, 0.03, and <0.001, respectively), however, the value of this comparison was diminished by the difference in ages between the two populations (the oldest control was younger than the youngest heterozygote). If their data from FA heterozygotes is compared to a subset of our own healthy control database with the same age range, both total *GPA* mutation frequency ($P = 0.008$) and N/Ø frequency ($P = 0.01$) are significantly elevated (Table I). Although it is unusual to compare populations across laboratories like this, the validity of the result is supported by the lack of difference observed when comparing control populations of similar age range ($P = 0.85$, 0.25, and 0.55, for total mutation frequency, allele loss and loss and duplication, respectively). In addition, we found that FA heterozygotes were much more likely to appear as false positives in our diagnostic *GPA* analysis. Indeed, the odds ratios (ORs) for FA heterozygotes with mutation frequencies above the diagnostic criteria were 8.04 (95% confidence interval [CI] 3.42–18.9) for total *GPA* mutation, 5.00 (95% CI 0.91–27.2) for allele loss alone, and 6.17 (95% CI 4.00–9.53) when the two criteria are combined (comparable ORs for FA homozygotes under the same circumstances range from 476 to 3,450). These criteria detect only 14% of FA heterozygotes, however, and 2.6% of normals. The OR for FA heterozygote detection by total *GPA* mutation frequency peaks at 9.77 (95% CI 7.10–13.4) at a cut-off of 40.0×10^{-6}, which captures 26% of heterozygotes, and 3.4% of controls, but remains positive and significant down to a cut-off of 10.0×10^{-6}, which would capture all heterozygotes including our patient's parent, but has an unacceptable false positive rate of 70% of the normal population.

Thus, these data suggest that FA heterozygotes may indeed have a slightly increased mutation frequency, mainly characterized by simple allele loss, compared to controls, but that the magnitude of the difference is unlikely to allow for unequivocal identification of individual heterozygotes. These data do, however, support the concept that FA heterozygotes have a distinct phenotype that predisposes them to cancer [Heim et al., 1992; Djuzenova et al., 2001]. This was unambiguously established when it was discovered that *BRCA2*, a cancer-predisposing tumor suppressor gene in heterozygous mutation carriers, was identified as the *FANCD1* gene, causing FA in the homozygous inactive state [Howlett et al., 2002].

ACKNOWLEDGMENTS

We would like to thank Dr. Arlene Auerbach and the staff of IFAR for providing samples from known FA patients, their families, and controls. The technical expertise of Barbara A. Nisbet, Ann E. Gorvad, Britt L. Luccy, and Christina M. Cerceo is gratefully acknowledged.

REFERENCES

Akiyama M, Kyoizumi S, Hirai Y, Kusonoki Y, Iwamoto KS, Nakamura N. 1995. Mutation frequency in human blood cells increases with age. Mutat Res 338:141–149.

Auerbach AD, Wolman SR. 1978. Carcinogen-induced chromosome breakage in Fanconi's anemia heterozygous cells. Nature 271:69–71.

Auerbach AD, Warburton D, Bloom AD, Chaganti RSK. 1979. Prenatal detection of the Fanconi's anemia gene by cytogenetic methods. Am J Hum Genet 31:77–81.

Auerbach AD, Adler B, Chaganti RS. 1981. Prenatal and postnatal diagnosis and carrier detection of Fanconi anemia by a cytogenetic method. Pediatrics 67:128–135.

Auerbach AD, Sagi M, Adler B. 1985. Fanconi anemia: Prenatal diagnosis in 30 fetuses at risk. Pediatrics 76:794–800.

Auerbach AD, Min Z, Ghosh R, Pergament E, Verlinsky Y, Nicolas H, Boue J. 1986. Clastogen-induced chromosomal breakage as a marker for first trimester prenatal diagnosis of Fanconi anemia. Hum Genet 73:86–88.

Auerbach AD, Rogatko A, Schroeder-Kurth TM. 1989. International Fanconi Anemia Registry: Relation of clinical symptoms to diepoxybutane sensitivity. Blood 73:391–396.

Bigbee WL, Langlois RG, Swift M, Jensen RH. 1989. Evidence for an elevated frequency of in vivo somatic cell mutations in ataxia telangiectasia. Am J Hum Genet 44:402–408.

Bigbee WL, Wyrobek AW, Langlois RG, Jensen RH, Everson RB. 1990. The effect of chemotherapy on the in vivo frequency of glycophorin A 'null' variant erythrocytes. Mutat Res 240:165–175.

Bigbee WL, Jensen RH, Grant SG, Langlois RG, Olsen DA, Auerbach AD. 1991. Evidence for elevated in vivo somatic mutation at the glycophorin A locus in Fanconi anemia. Am J Hum Genet 49(Suppl):446.

Bigbee WL, Fuscoe JC, Grant SG, Jones IM, Gorvad AE, Harrington-Brock K, Strout CL, Thomas CB, Moore MM. 1998. Human in vivo somatic mutation measured at two loci: Individuals with stably elevated background erythrocyte glycophorin A (*gpa*) variant frequencies exhibit normal T-lymphocyte *hprt* mutant frequencies. Mutat Res 397:119–136.

Bloom GE, Warner S, Gerald PS, Diamond LK. 1966. Chromosome abnormalities in constitutional aplastic anemia. N Eng J Med 274:8–14.

Callen E, Samper E, Ramirez MJ, Creus A, Marcos R, Ortega JJ, Olive T, Badell I, Blasco MA, Surralles J. 2002. Breaks at telomeres and TRF2-independent end fusions in Fanconi anemia. Hum Mol Genet 11:439–444.

Cartron JP, Rahuel C. 1995. MNSs and major glycophorins of human erythrocytes. Transfus Clin Biol 2:251–258.

Cervenka J, Hirsch BA. 1983. Cytogenetic differentiation of Fanconi anemia, "idiopathic" aplastic anemia, and Fanconi anemia heterozygotes. Am J Med Genet 15:211–223.

Chaganti RSK, Houldsworth J. 1991. Fanconi anemia: A pleotropic mutation with multiple cellular and developmental abnormalities. Ann Genet 34:206–211.

Cohen MM, Simpson SJ, Honig GR, Maurer HS, Nicklas JW, Martin AO. 1982. The identification of Fanconi anemia genotypes by clastogenic stress. Am J Hum Genet 34:794–810.

Corver WE, Cornelisse CJ, Fleuren GJ. 1994. Simultaneous measurement of two cellular antigens and DNA using fluorescein-isothiocyanate, R-phycoerythrin, and propidium iodide on a standard FACScan. Cytometry 15:117–128.

Djuzenova CS, Rothfuss A, Oppitz U, Speit G, Schindler D, Hoehn H, Flentje M. 2001. Response to X-irradiation of Fanconi anemia homozygous and heterozygous cells assessed by the single-cell gel electrophoresis (comet) assay. Lab Invest 81:185–192.

Grant SG. 2001. Molecular epidemiology of human cancer: Biomarkers of genotoxic exposure and susceptibility. J Environ Pathol Toxicol Oncol 20:245–261.

Grant SG. 2005. The *GPA* in vivo somatic mutation assay. Meth Mol Biol 291:179–195.

Grant SG, Bigbee WL. 1993. In vivo somatic mutation and segregation at the human glycophorin A (*GPA*) locus: Phenotypic variation encompassing both gene-specific and chromosomal mechanisms. Mutat Res 288:163–172.

Grant SG, Bigbee WL, Langlois RG, Jensen RH. 1991. Allele loss at the human *GPA* locus: A model for recessive oncogenesis with potential clinical application. Clin Biotechnol 3:177–185.

Grant SG, Bigbee WL, Langlois RG, Jensen RH. 1992a. Methods for the detection of somatic mutational and segregational events: Relevance to the monitoring of survivors of childhood cancer. In: Green DM, D'Angio GJ, editors. Late effects of treatment for childhood cancer. New York: Wiley-Liss. p 133–150.

Grant SG, Langlois RG, Auerbach AD, Manchester DK, Monnat RJ, Jensen RH, Bigbee WL. 1992b. Analysis of human DNA metabolism/repair diseases with the in vivo glycophorin A somatic segregation assay: Application of an improved assay and extension to new syndromes. Environ Mol Mutagen 19(Suppl 20):20.

Grant SG, Reeger W, Wenger SL. 1997. Diagnosis of ataxia telangiectasia with the glycophorin A somatic mutation assay. Genet Testing 1:261–267.

Grant SG, Wenger SL, Latimer JJ, Thull D, Burke LW. 2000. Analysis of genomic instability using multiple assays in a patient with Rothmund–Thomson syndrome. Clin Genet 58:209–215.

Grant SG, Wenger SL, Rubinstein WS, Latimer JJ, Bigbee WL, Auerbach AD. 2004. Elevated levels of somatic mutation in homozygotes and heterozygotes for inactivating mutations in the genes of the FA/BRCA DNA repair pathway. Am J Hum Genet 75(Suppl):94.

Heim RA, Lench NJ, Swift M. 1992. Heterozygous manifestations in four autosomal recessive human cancer-prone syndromes: Ataxia telangiectasia, xeroderma pigmentosum, Fanconi anemia, and Bloom syndrome. Mutat Res 284:25–36.

Hewitt M, Mott MG. 1992. The assessment of in vivo somatic mutations in survivors of childhood malignancy. Br J Cancer 66:143–147.

Howlett NG, Taniguchi T, Olson S, Cox B, Waisfisz Q, De Die-Smulders C, Persky N, Grompe M, Joenje H, Pals G, Ikeda H, Fox EA, D'Andrea AD. 2002. Biallelic inactivation of *BRCA2* in Fanconi anemia. Science 297: 606–609.

Jensen RH, Bigbee WL, Langlois RG. 1987. In vivo somatic mutations in the glycophorin A locus of human erythroid cells. Banbury Rep 28:149–159.

Jensen RH, Grant SG, Langlois RG, Bigbee WL. 1991. Somatic cell genotoxicity at the glycophorin A locus in humans. Prog Clin Biol Res 372:329–339.

Kutler DI, Singh B, Satagopan J, Batish SD, Berwick M, Giampietro PF, Hanenberg H, Auerbach AD. 2003. A 20-year perspective on the International Fanconi Anemia Registry (IFAR). Blood 101:1249–1256.

Kyoizumi S, Nakamura N, Hakoda M, Awa AA, Bean MA, Jensen RH, Akiyama M. 1989a. Detection of somatic mutations at the glycophorin A locus in erythrocytes of atomic bomb survivors using a single beam flow sorter. Cancer Res 49:581–588.

Kyoizumi S, Nakamura N, Takebe H, Tatsumi K, German J, Akiyama M. 1989b. Frequency of variant erythrocytes at the glycophorin-A locus in two Bloom's syndrome patients. Mutat Res 214:215–222.

Kyoizumi S, Kusunoki Y, Seyama T, Hatamochi A, Goto M. 1998. In vivo somatic mutations in Werner's syndrome. Hum Genet 103:405–410.

Langlois RG, Bigbee WL, Kyoizumi S, Nakamura N, Bean MA, Akiyama M, Jensen RH. 1987. Evidence for increased somatic cell mutations at the glycophorin A locus in atomic bomb survivors. Science 236:445–448.

Langlois RG, Bigbee WL, Jensen RH, German J. 1989. Evidence for elevated in vivo mutations and somatic recombination in Bloom's syndrome. Proc Natl Acad Sci USA 86:670–674.

Lin YW, Kubota M, Hirota H, Furusho K, Tomiwa K, Ochi J, Kasahara Y, Sasaki H, Ohta S. 1995. Somatic cell mutation frequency at the HPRT, T-cell antigen receptor and glycophorin A loci in Cockayne syndrome. Mutat Res 337:49–55.

Manchester DK, Nicklas JA, O'Neill JP, Lippert MJ, Grant SG, Langlois RG, Moore DH III, Jensen RH, Albertini RJ, Bigbee WL. 1995. Sensitivity of somatic mutations in human umbilical cord blood to maternal environments. Environ Mol Mutagen 26:203–212.

Moser MJ, Bigbee WL, Grant SG, Emond MJ, Langlois RG, Jensen RH, Oshima J, Monnat RJ Jr. 2000. Genetic instability and hematologic disease risk in Werner syndrome patients and heterozygotes. Cancer Res 60:2492–2496.

Okada S, Ishii H, Nose H, Okusaka T, Kyogoku A, Yoshimori M, Wakabayashi K. 1997. Evidence for increased somatic cell mutations in patients with hepatocellular carcinoma. Carcinogenesis 18:445–449.

Radack K, Martin V, Wones R, Buncher R, Pinney S, Mandell K. 1996. Intercorrelations and sources of variability in three mutagenicity assays: A population-based study. Mutat Res 350:295–306.

Rogatko A, Auerbach AD. 1988. Segregation analysis with uncertain ascertainment: Application to Fanconi anemia. Am J Hum Genet 42:889–897.

Rosendorff J, Bernstein R. 1988. Fanconi's anemia—Chromosome breakage studies in homozygotes and heterozygotes. Cancer Genet Cytogenet 33: 175–183.

Sala-Trepat M, Boyse J, Richard P, Papadopoulo D, Moustacchi E. 1993. Frequencies of *HPRT*$^-$ lymphocytes and glycophorin A variants erythrocytes in Fanconi anemia patients and control donors. Mutat Res 289: 115–126.

Schindler D, Seyschab H, Poot M, Hoehn H, Schinzel A, Fryns JP, Tommerup N, Rabinovitch PS. 1987. Screening test for ataxia telangiectasia. Lancet II:1398–1399.

Schroeder TM, German J. 1974. Bloom's syndrome and Fanconi's anemia: Demonstration of two distinctive patterns of chromosome disruption and rearrangement. Humangenetik 25:299–306.

Schroeder TM, Anschutz F, Knopp A. 1964. Spontane chromosomenaberrationen bei familiaerer panmyelopathie. Humangenetik 1:194–196.

Seabright M. 1971. A rapid banding technique for human chromosomes. Lancet II:971–972.

Worton RG, Grant SG. 1985. Segregation-like events in Chinese hamster cells. In: Gottesman MM, editor. Molecular cell genetics. New York: Wiley. p 831–867.

Prospective screening study of 0.5 Tesla dedicated magnetic resonance imaging for the detection of breast cancer in young, high-risk women

Wendy S. Rubinstein[1,2§], Jean J. Latimer[3,4,5], Jules H. Sumkin[6], Michelle Huerbin[4,6], Stephen G. Grant[3,4,5,7], and Victor G. Vogel[7,8]

[1]Department of Medicine, Northwestern University Feinberg School of Medicine, Chicago, IL, U.S.A.

[2]Evanston Northwestern Healthcare Center for Medical Genetics, Evanston, IL, U.S.A.

[3]Department of Obstetrics, Gynecology and Reproductive Sciences, School of Medicine, University of Pittsburgh, Pittsburgh, PA, U.S.A.

[4]Research Institute, Magee-Womens Hospital, Pittsburgh, PA, U.S.A.

[5]University of Pittsburgh Cancer Institute, Pittsburgh, PA, U.S.A.

[6]Department of Radiology, Magee-Womens Hospital, Pittsburgh, PA, U.S.A.

[7]Department of Environmental and Occupational Health, Graduate School of Public Health, University of Pittsburgh, Pittsburgh, PA, U.S.A.

[8]Department of Medicine, School of Medicine, University of Pittsburgh, Pittsburgh, PA, U.S.A.

[§]Corresponding author

Email addresses:

WSR: wrubinstein@enh.org

JLL: latimerj@pitt.edu

JHS: jsumkin@mail.magee.edu

MH: mhuerbin@wpahs.org

SGG: sgg@pitt.edu

VGV: vvogel@mail.magee.edu

Abstract

Background

Evidence-based screening guidelines are needed for women under 40 with a family history of breast cancer, a *BRCA1* or *BRCA2* mutation, or other risk factors. An accurate assessment of breast cancer risk is required to balance the benefits and risks of surveillance, yet published studies have used narrow risk assessment schemata for enrollment. Breast density limits the sensitivity of film-screen mammography but is not thought to pose a limitation to MRI, however the utility of MRI surveillance has not been specifically examined before in women with dense breasts. Also, all MRI surveillance studies yet reported have used high strength magnets that may not be practical for dedicated imaging in many breast centers. Medium strength 0.5 Tesla MRI may provide an alternative economic option for surveillance.

Methods

We conducted a prospective, nonrandomized pilot study of 30 women age 25-49 years with dense breasts evaluating the addition of 0.5 Tesla MRI to conventional screening. All participants had a high quantitative breast cancer risk, defined as ≥3.5% over the next 5 years per the Gail or BRCAPRO models, and/or a known *BRCA1* or *BRCA2* germline mutation.

Results

The average age at enrollment was 41.4 years and the average 5-year risk was 4.8%. Twenty-two subjects had BIRADS category 1 or 2 breast MRIs (negative or probably benign), whereas no category 4 or 5 MRIs (possibly or probably malignant) were observed. Eight subjects had BIRADS 3 results, identifying lesions that were “probably benign”, yet prompting further

evaluation. One of these subjects was diagnosed with a stage T1aN0M0 invasive ductal carcinoma, and later determined to be a *BRCA1* mutation carrier.

Conclusions

Using medium-strength MRI we were able to detect 1 early breast tumor that was mammographically undetectable among 30 young high-risk women with dense breasts. These results support the concept that breast MRI can enhance surveillance for young high-risk women with dense breasts, and further suggest that a medium-strength instrument is sufficient for this application. For the first time, we demonstrate the use of quantitative breast cancer risk assessment via a combination of the Gail and BRCAPRO models for enrollment in a screening trial.

Background

The sensitivity of mammography has been observed to be lower in women < 50 years of age (63-86%), compared with women $\geq$ 50 years (89-94%) [1-3]. The U.S. Preventive Services Task Force meta-analysis found that the time required to obtain a risk reduction in breast cancer mortality rates is longer for younger women [4]. The lower sensitivity of mammography in young women has been ascribed to their higher prevalence of mammographically dense breasts and, perhaps, faster tumor growth rates [1,2].

About 25% of all women have dense breast tissue, and this physiology is more common in younger women [5-9]. Indeed, dense breast tissue has been found to be an independent risk factor for breast cancer [10,11]. Screening mammography may have limited utility in women with dense breast tissue for a variety of reasons, including: similar attenuation properties of

breast lesions with dense glandular tissue; more radiation scatter and therefore higher required dose; and difficulty obtaining adequate exposure without image degradation [12]. Among women in a screening study, the sensitivity of mammography varied from 80% in women with extremely fatty breasts to a mere 30% for those with extremely dense breasts, and the odds ratio of an interval tumor was 9.47 for the latter group [13].

Younger women have a lower prevalence of breast cancer, which must be balanced against the false-positive rate of screening mammography [4]. However, the risk of breast cancer in young women with specific risk factors may equal or exceed that of older women for whom screening is unequivocally recommended. About 6% of breast cancer cases in women < 50 years of age are due to germline mutations in the *BRCA1* or *BRCA2* breast and ovarian cancer susceptibility genes [14,15]. Carriers are at exceptionally high risk, with potential breast cancer onset as early as the third decade and cumulative risk to age 40 reaching up to 20% [16]. While prophylactic mastectomy is the most effective risk-reducing therapy, many carriers would opt for heightened surveillance instead, given a sufficient degree of confidence in the opportunity for early detection [17].

There is evidence that breast density in *BRCA1* mutation carriers is similar to that of women in the general population [18]. Thus, resultant technical limitations of screening mammography are likely to apply to this group of relatively young high-risk women [19]. Specifically, in a study comparing mammography among 34 *BRCA1* or *BRCA2* mutation carriers with breast cancer vs. disease-free controls, false-negative mammography correlated independently with *BRCA1*/2 mutation, the histological feature of prominent pushing margins, and high breast density [20].

Also relevant to the management of germline mutation carriers is the involvement of the BRCA1 and BRCA2 proteins in recombination repair of ionizing radiation-induced double-strand DNA breaks [21-23]. Possible carcinogenic consequences of low-dose irradiation for young mutation carriers undergoing earlier mammography screening must be considered [21].

An adjunct to screening mammography is particularly needed for young women at high risk of breast cancer whose imaging is limited by radiographically dense breasts. Contrast-enhanced magnetic resonance imaging (MRI) of the breast is a potential surveillance approach that is highly sensitive, is not limited by radiographic density, and poses no radiation risks. The sensitivity of contrast-enhanced breast MRI for breast cancer detection has been reported to be as high as 94%-100% [24-26]. Specificities are more variable, with values ranging from 37%-97% [25-28]. Recent larger prospective screening studies conducted in high-risk cohorts confirm high sensitivities and demonstrate, for the first time, high specificities, as well [29,30].

Methods

Study design

This study is a prospective, nonrandomized clinical trial designed to investigate the usefulness of a prototypical midfield strength Magnetic Resonance Imaging System in a screening setting using quantitative risk assessment for eligibility. The study looked at the addition of 0.5 Tesla MRI to a screening regimen for young women at high risk of breast cancer with dense breast tissue consisting of conventional screening modalities. The study was designed as a pilot study, with an enrollment over one year of thirty women. The data presented are a summary of this pilot study.

Patient selection and consent

Thirty women between the ages of 25 and 49, inclusively, without a personal history of invasive or non-invasive breast cancer were recruited for this study between 10/27/99 and 4/19/00 via the joint Comprehensive Breast and Cancer Genetics Programs of the University of Pittsburgh Cancer Institute and Magee-Womens Hospital of UPMC. Women were required to have a negative or benign mammographic and physical evaluation within three months of enrollment. All subjects had mammographically dense breast tissue described as "heterogeneously" or "extremely dense" according to the American College of Radiology **B**reast **I**maging **R**eporting and **D**ata **S**ystem (BIRADS) lexicon [31]. Categorization of increased breast density was first determined by report on prior conventional film-screen mammographic examination, performed within 3 months of enrollment. Mammogram films were obtained and reviewed by the lead radiologist (JHS) to verify the presence of increased breast density. The four standard American College of Radiology BIRADS breast composition patterns are: (1) almost entirely fat; (2) predominantly fat with scattered fibroglandular densities; (3) heterogeneously dense; and (4) extremely dense. Women with fatty breasts or scattered areas of density with no focal areas of concentration were not eligible for the study. Exclusion criteria included a contraindication to MRI, breast implants, mastectomy, or a history of allergic reaction to gadolinium. Quantitative risk analysis was performed on all women prior to enrollment using the Gail and BRCAPRO-based CancerGene models. Participants had a minimum 5-year breast cancer risk on either model of 3.5% and/or a known mutation in *BRCA1* or *BRCA2*.

This study was reviewed and approved by the Magee-Womens Hospital of UPMC Institutional Review Board (MWH-99-081). The study was explained to all participants and

informed consent was obtained. Genetic testing was performed following genetic counselling under protocol MWH-97-082.

Risk analysis

Absolute 5-year breast cancer risk was determined using the Gail and BRCAPRO models [32,33], both of which have been extensively validated [34,35]. The Gail model directly calculates absolute 5-year risk of breast cancer using the following risk factors: age, race, number of first-degree relatives with breast cancer (maximum of 2), age at menarche, age at first live birth, number of breast biopsies, and atypical hyperplasia. The BRCAPRO program is based on the Berry model [33] and utilizes Mendelian principles with Bayesian updating to calculate carrier probabilities for germline *BRCA1* and *BRCA2* mutations by capturing extensive family history information about female and male breast cancer, ovarian cancer, age at cancer diagnosis, current age or age of death for relatives with and without cancer, and ethnicity. Absolute 5-year risk of breast cancer was then determined as follows: (the probability of being a *BRCA1/2* mutation carrier based on BRCAPRO) x (the yearly incidence of breast cancer in a mutation carrier, specific to the decade of life [36]) x (5 years). These calculations were performed automatically using the CancerGene program [37], now freely available at http://www4.utsouthwestern.edu/breasthealth/cagene.

Family history and personal risk factors were obtained through personal interview to obtain the most complete and accurate history possible. This information was collected on case report forms and entered into the models on computer. If both models resulted in a 5 year risk of $\geq$3.5%, the higher value was used for this calculation. As per the CancerGene program, known *BRCA1* and *BRCA2* carriers reach the 3.5% 5 year risk threshold at ages 27 and 32 years, respectively.

All women had a negative or benign breast examination, including physical examination and mammography within 3 months prior to study enrollment. All enrolled participants received a screening MRI as described below.

Device information

This study utilized a contrast-enhanced magnetic resonance imaging system produced by Aurora Imaging Technology, Wilmington, MA. The system involves a 0.5 Tesla magnet with gadolinium as a contrast agent. The Aurora system is a dedicated system specifically designed for breast imaging.

The 0.5T MRI uses local volume transmit/receive coils and a gradient strength of 1 G/cm. The RF system consists of a wide band receiver operating at 21 MHz. There is 0.3 kwatts RF power. Images can be viewed at either a workstation or by film generated from an interface with a laser camera.

Magnetic resonance imaging

Patients were scanned in the prone position and placed into the magnet feet first. Images were acquired in the axial plane with both breasts imaged simultaneously. The field of view was variable from 8-46 cm transverse and 20 cm axial. Standard 2D and 3D gradient echo and spin echo sequences were used. The dynamic, contrast-enhanced series was 3D. The matrix was 256 x 256 x 64 (x, y, z). The first sequence was non-contrast: T1 – Weighted GE, TR = 14 ms and TE = 6.0 ms, giving 64 2.0 mm thick slices, with an in-plane resolution of 1.4 mm x 1.4 mm. After completion of the non-contrast scan, intravenous gadolinium was administered at a dose of 0.1 mmol/kg of body weight at approximately 1.0 cc/sec. Post-contrast axial imaging was performed immediately, followed by a second scan approximately 4 minutes later for delayed imaging. Total imaging time is approximately 4 minutes per sequence or 12 minutes for actual

imaging (this relatively long time was not inconsistent with protocols during the time of the study). Immediate and delayed subtraction views were generated by computerized subtraction of the pre-contrast image from both the immediate and delayed post-contrast images. This post-imaging subtraction was used as the method of fat suppression, i.e., no active fat suppression was used. Regions of interest (ROIs) were placed on enhancing lesions of concern and three point time dependent intensity curves were generated for each region.

Lesions were characterized using both morphologic and kinetic criteria similar to the manner described [38,39]. An MR BIRADS category was assigned ranging from 1 (negative), 2 (benign), 3 (probably benign) 4 (possibly malignant), to 5 (probably malignant). Morphology was described according to the lexicon developed by the MRI working group, which was available to us prior to the final publication date [40]. Criteria used to evaluate and rate MRI-detected lesions were those published by Schnall *et al.* [41] combined with kinetic information. Kinetics were described by visually comparing the immediate post contrast images to the delayed post contrast images. Lesions were scored as early enhancement and early washout, early enhancement and delayed washout, or delayed enhancement. In a manner similar to Hylton *et al.* [42], lesions were considered suspicious if they had either morphologic or kinetic features suspicious for malignancy (rapid wash-in and washout). In addition, lesions graded as BIRADS 3 by either morphologic or kinetic criteria were offered further evaluation using ultrasound. Ultrasound results confirmed the MRI findings, but otherwise added no new information.

Results

Thirty women were enrolled in the study. The average age at enrollment was 41.1 years. The average 5-year breast cancer risk at enrollment, using either the Gail model or a BRCAPRO-

based cancer risk model, was 4.8%. The Gail model was actually only used to establish eligibility in 7 cases, whereas the BRCAPRO-based model was used in majority of cases, 23.

MRI results classified according to BIRADS category are shown in Figure 1. No results were observed in BIRADS categories 4 or 5. Subjects with MRI results of BIRADS 1 or 2 received no additional breast evaluations. Subjects with BIRADS 3 results were evaluated as summarized in Table 1. Follow-up involved invasive procedures in 4 of these 8 subjects. Among the 8 patients with BIRADS 3 results, one, subject 006, was diagnosed with stage I invasive ductal carcinoma.

Imaging results for subject 006 are given in Figure 2 (for a full clinical description of this patient, as well as live-cell analysis of her breast tissue for indices of proliferation, differentiation and genomic instability, see [41]). Her mammogram is depicted in Figure 2A, showing heterogeneously dense breast tissue. The MR images for this patient are shown in Figures 2B and 2C. In the upper-outer left breast there was a small (approximately 1 cm), round, well-demarcated enhancing lesion, seen on both the initial delay after contrast injection and the delayed contrast enhanced subtraction images. This lesion appeared to accumulate contrast to a greater extent on the delayed subtract ion images with an additional lesion adjacent to the first. In the right breast just above the nipple level medial and close to the chest wall an additional lesion was seen in the pre-contrast image. This lesion was approximately 1.5 cm, smooth and round. Core biopsy of the left breast revealed infiltrating ductal carcinoma in 2 of 5 core fragments; high nuclear grade, with no lymphatic invasion seen. The core biopsy of the right breast demonstrated benign pathology, specifically, fibrosis with focal ductal epithelial hyperplasia. The patient chose to undergo left modified radical mastectomy with left axillary lymph node dissection and contralateral prophylactic total mastectomy because of her genetic

risk status. Final pathology in the left breast was consistent with the imaging and core biopsy in size and description. Tumor size was 8 mm in greatest dimension, nuclear grade III, ER/PR and Her2/neu negative, and the nodal status (0/4) was negative (stage TIaN0M0). This subject represented 3.3% of the sampled high risk population and 12.5% of the population with "probably benign" MRIs.

Interim follow-up was required for 8 of 30 (27%) subjects, but only 4 (13%) underwent an invasive procedure. Clinical follow up was available on all 29 disease-free subjects at least one year beyond the performance of the study MRI, which is the standard length of follow up to exclude occult cancer, and no subjects developed breast carcinoma. Thus, the patients in BIRADS categories 2 and 3 likely did not harbor occult disease.

Discussion

Without data on cancer-specific mortality reduction, the decision to employ breast MRI surveillance rests heavily on other parameters, including test performance characteristics, cost, and methods of maximizing benefit vs. risk. Recent prospective studies have provided firmer data indicating that high sensitivity can be achieved with breast MRI without greatly sacrificing specificity. While reduction in cancer-specific mortality is the gold standard for surveillance tools, there is a pressing need to supplement mammography in high-risk women, particularly for *BRCA1* and *BRCA2* mutation carriers who are diagnosed with a high rate of interval tumors, roughly 50% [44]. Breast MRI results in a lower rate of interval tumors while circumventing the limitations of surveillance for women with dense breasts. However, for whom should breast MRI surveillance be employed and what are acceptable costs?

Medium vs. high field strength MRI

Despite the promise of breast MRI, there are still some issues that must be resolved prior to its use as a standard adjunct method of breast cancer surveillance. There is not yet a standard method in place for such imaging, and no consensus on how to best interpret lesions detected by MRI, and whether or when to biopsy lesions detected by MRI alone [see ref. 31]. Additionally, the high cost of breast MRI is severely limiting. Not only is there a large cost associated with the purchase of a high field strength magnet, but also there are additional costs for housing and maintaining the unit. The use of medium field strength magnets has been criticized for their low signal-to-noise ratio (SNR) per sampling time. However, the use of a medium field strength magnet, such as a 0.5 Tesla, would come at significant cost savings of up to 1/3 that of a higher field strength MRI system. Our study provides preliminary evidence that a medium field strength breast MRI system can be effectively used for high-risk surveillance.

There is evidence that the use of a medium field strength breast MRI system is comparable to a 1.5 T system. In a study published by Kuhl *et al*. [45], MRI was performed on a midfield system without loss of sensitivity as compared to a high field system. The study looked at 42 patients imaged on both a 0.5 T and 1.5 T MRI, finding that the image quality was comparable, and, with certain compensations, the 0.5 T system was more sensitive than the larger 1.5 T MRI. In a second study, Kuhl *et al*. [46] imaged 40 patients with nodular lesions using both 0.5 T and 1.5 T field strength units to determine if the two systems were comparable in selecting benign vs. malignant lesions. Malignant lesions and fibroadenomas demonstrated a similar enhancement uptake pattern on both systems. A rapid wash-out of contrast was seen only in malignant lesions, which appeared 10 times more frequently using the 0.5 T system as compared with 1.5 T MRI.

The appearance of T1-weighted gradient echo images generated from a contrast study depends on the SNR, the contrast-to-noise ratio (CNR) and the contrast agent used. The SNR is a function of the magnetic field strength, magnet shim, flip angle, voxel size, receiver gain, RF coil and image processing parameters. Magnetic field strength directly affects the SNR and the spin relaxation properties of the tissue. The SNR is linear with field strength—everything else being equal, 1.5 T magnets produce images with three times the SNR of images from 0.5 T magnets. In addition, the T1 of a given tissue/sample type is larger at higher field strengths. This implies that at a higher field strength, the spin relaxation of a given tissue/sample may be changed more that the same tissue/sample at a lower strength and thus may increase the difference observed in pre- and post-contrast images.

The CNR is a measure of the average intensity of an object compared to the average intensity of the noise floor for a given object and pulse sequence. The CNR is a function of the relation of the pulse sequence timing parameters (e.g., TE, TR) to the spin relaxation properties (e.g., T1, T2) of the object. Because the contrast agent changes the spin relaxation properties, it changes the CNR of the image. Above a minimum SNR threshold, the ability to detect a lesion using MRI is a function of the change in CNR of pre- and post-contrast images and the voxel size acquired. If the configuration of a 1.5T MRI scanner and a 0.5T MRI scanner is such that both are above the minimum level of SNR, have comparable CNR changes after adding a contrast agent, and have identical voxel sizes and scan durations, the ability to detect lesions is similar.

Our study demonstrates that medium field strength MRI can detect tumors that have been missed by conventional screening mammography. There are, however, certainly limitations to this initial study, including its small size; up to 3 months time differential between screening

mammogram and MRI; and lack of longitudinal follow up. No conclusions can be drawn regarding the overall sensitivity or specificity of screening with the 0.5 T MRI.

Screening guidelines for young high-risk women

There has been a dearth of evidence-based screening guidelines for women age < 40 with a family history of breast cancer, a *BRCA1* or *BRCA2* mutation, or other risk factors, largely because of the lack of randomized, controlled trials to inform the development of such guidelines [47-49].

As evidence accumulates regarding the efficacy of bilateral prophylactic mastectomy, data regarding the efficacy of screening is paramount so that women can make informed choices. In a large screening study of 251 mutation carriers, a high rate of interval tumors found on breast self-examination led to the suggestion that more frequent (i.e. semi-annual) mammography should be considered, particularly in younger women [50]. However, among women age 40-69, the estimated cumulative risk of a false positive result after 10 mammograms is 49% [51], resulting in additional visits, diagnostic tests, invasive procedures, morbidity, cost, and anxiety. Furthermore, there is evidence that false-positive rates are higher in younger women [52-54]. Ultimately, the sequelae of screening can spur the decision to undergo prophylactic surgery, giving one pause about recommending more frequent screening.

The variations in sensitivity and specificity for breast MRI exist for several reasons, including technical factors [55], interpretation criteria [28,30,38], patient selection, concomitant use of conventional imaging, and the level of pathologic verification of the abnormalities detected. The large disparity in specificities results from a variety of technical factors. For instance, the lowest reported specificity was calculated without the use of morphologic features

or quantification of enhancement, and certain high-risk lesions, such as atypical ductal hyperplasia, were considered as false positives [24].

All high-risk MRI screening studies reported thus far have used high field-strength magnets. Stoutjesdijk *et al*. [56] found that for the indeterminate BIRADS score of 3, the sensitivity of breast MRI was 100% with a specificity of 93% (95% confidence interval = 90%-96%) and the positive predictive value was 43%. Warner *et al*. [57] reported a sensitivity of 100% and noted that all four false negative mammograms had a BIRADS score of 1. In this study, increased breast density appeared to contribute to the poor sensitivity of mammography. An update of this study reporting findings on 236 Canadian women aged 25 to 65 years with *BRCA1* or *BRCA2* mutations found a specificity of 95.4% based on biopsy of BIRADS level 4 and 5 lesions, but did not take into account non-biopsy interventions engendered by level 3 lesions [30]. Moreover, high-risk women may be particularly susceptible to the emotional turmoil triggered by a diagnostic workup for breast cancer, considering their high-risk family histories.

The largest breast MRI surveillance study reported to date, based on 1909 eligible women including 358 germ-line mutation carriers, found a specificity of 89.8% for workup of level 3, 4, and 5 lesions [29]. However, this study did not examine possible differences in test performance among women at varying levels of risk, nor was breast density taken into account. While a lower limit of 15% lifetime risk constituted study eligibility, it remains unclear whether this risk level merits high-risk surveillance, particularly in women with average mammographic breast density. Our ongoing studies of surveillance screening with medium field strength MRI have shown that the false-positive rate is three-fold lower than that of mammography [58].

Conclusions

Toward quantitative balancing of risks and benefits in surveillance

We contend that the benefits of breast cancer surveillance cannot be satisfactorily balanced against the risks of screening without an accurate assessment of absolute breast cancer risk. We report for the first time the use of quantitative breast cancer risk assessment via application of both the established Gail model and a new, purely genetic, model based on the estimation of BRCA gene carrier risk via the BRCAPRO and CancerGene programs for use in enrollment in a breast cancer screening pilot study. Kriege *et al*. [29] used the Claus model [59] for risk stratification, but this model has not been as extensively validated as either the Gail or BRCAPRO models. In particular, omission of family history of ovarian cancer in the Gail and Claus models is one factor that can lead to underprediction of breast cancer risk; this constitutes a serious limitation to using either model alone [60]. At our current level of understanding, the Gail model identifies at least three types of women at high risk for breast cancer: those with a genetic risk associated with family history, those with a risk based on lifestyle factors associated with hormonal effects, and those who have presented with suspicious breast pathologies, regardless of the basis of their risk. Genetic analysis of the subjects who developed breast cancer in the NSABP P-1 Breast Cancer Prevention Trial indicates that the Gail model inefficiently identifies *BRCA1* and *BRCA2* gene carriers, since only 6.6% (19/288) of that high risk population carried such mutations [61]. Supplementation of the Gail model with the BRCAPRO-based model allows for a much more efficient ascertainment of women at high risk for breast cancer specifically due to the possibility that they carry a mutant *BRCA1* or *BRCA2* gene, based on our accumulated knowledge of the genetic syndromes associated with these gene mutations. Since 23 of our 30 subjects were enrolled due on their CancerGene-based cancer risk

rather than their risk based on the Gail model, this group represents a rather unique "high risk" population, perhaps with more in common with studies in *BRCA1/2* carriers such as that of Warner *et al*. [62] than previous populations enrolled through the exclusive use of the Gail or Claus models. Others have begun to enroll "high risk" subjects based on their BRCAPRO-based carrier status [63], but we are the first to add CancerGene to provide a quantitative cancer risk component that can be applied uniformly to patients regardless of the basis of their risk.

We have advanced the rationale for quantitative risk assessment in chemoprevention trials, with the advantages of improved power using a smaller study population, shorter study duration and lower cost [64]. The same rationale applies to surveillance trials. In addition, subjects at higher risk of breast cancer have a greater ratio of benefit vs. risk than average-risk women since, if the surveillance modality is efficacious, they have a greater opportunity for early detection. For trials that seek to measure specificity, breast cancer events are not crucial to determining the required sample size, yet for ethical reasons, subjects who stand to benefit the most ought to be preferentially studied. Ours is the first study to concentrate on high-risk women with mammographically dense breast tissue; the poorer sensitivity of mammography in this group should contribute to an especially high ratio of benefit vs. risk.

Another consideration is that some subjects with *BRCA1* or *BRCA2* mutations may be reluctant to enroll in a trial restricted to mutation carriers, since their genetic status would be known by virtue of their participation. Enrollment according to quantitative risk can allow women who are not yet prepared for genetic testing to participate in a high-risk surveillance trial. Furthermore, the concomitant use of the Gail and BRCAPRO-based models allows for the identification of a broader array of high-risk women [65]. The report of the Working Groups on Breast MRI advises that "a careful analysis of the woman's actual risk for breast cancer" be done

when considering the appropriateness of screening MRI [66]. They urge the development of partnerships with high-risk clinics and/or clinicians with significant experience with high-risk women. Ultimately, since the conduct of randomized, controlled trials in high-risk women faces numerous challenges, medical decision making models may be useful for balancing the benefits and risks using such parameters as age, quantitative breast cancer risk, and breast density.

Competing interests

The authors declare that they have no competing interests.

Authors' contributions

WSR designed the study, recruited and consented the patients, obtained funding, and drafted the manuscript. JJL and SGG contributed to the study evaluation and drafted the manuscript. JHS was responsible for the performance and interpretation of the mammography and MRI. MH was the research coordinator and helped design the study. VGV participated in the study design and data interpretation. All authors read and approved the final manuscript.

Acknowledgements

This study was supported by a grant from the Jewish Healthcare Foundation of Pittsburgh and in part by NIH grant CA 71894 and grants from the Ruth Estrin Goldberg Foundation and the Pennsylvania Department of Health. We greatly appreciate the contributions of genetic counselors Laura J. Rittmeyer, Suzanne M. O'Neill, Ph.D., June A. Peters, and Mona P. Stadler in the identification of subjects for this study and their clinical care.

References

1. Burhenne HJ, Burhenne LW, Goldberg F, Hislop TG, Worth AJ, Rebbeck PM, Kan L: **Interval breast cancers in the Screening Mammography Program of British Columbia: analysis and classification.** *Am J Roentgenol* 1994, **162:** 1067-1071 discussion **162:**1072-1075.
2. Kerlikowske K, Grady D, Barclay J, Sickles EA, Ernster V: **Likelihood ratios for modern screening mammography. Risk of breast cancer based on age and mammographic interpretation.** *JAMA* 1996, **276:**39-43.
3. Robertson CL: **A private breast imaging practice: medical audit of 25,788 screening and 1,077 diagnostic examinations.** *Radiology* 1993, **187:**75-79.
4. Humphrey LL, Helfand M, Chan BK, Woolf SH: **Breast cancer screening: a summary of the evidence for the U.S. Preventive Services Task Force.** *Ann Intern Med* 2002, **137:**347-360.
5. Wolfe JN: **Breast parenchymal patterns and their changes with age.** *Radiology* 1976, **121:**545-552.
6. Brisson J, Sadowsky NL, Twaddle JA, Morrison AS, Cole P, Merletti F: **The relation of mammographic features of the breast to breast cancer risk factors.** *Am J Epidemiol* 1982, **115:**438-443.
7. Gram IT, Funkhouser E, Tabar L: **Reproductive and menstrual factors in relation to mammographic parenchymal patterns among perimenopausal women.** *Br J Cancer* 1995, **71:**647-650.
8. Oza AM, Boyd NF: **Mammographic parenchymal patterns: a marker of breast cancer risk.** *Epidemiol Rev* 1993, **15:**196-208.

9. Tabar L, Dean PB: **Mammographic parenchymal patterns. Risk indicator for breast cancer?** *JAMA* 1982, **247:**185-189.

10. Byng JW, Yaffe MJ, Jong RA, Shumak RS, Lockwood GA, Tritchler DL, Boyd NF: **Analysis of mammographic density and breast cancer risk from digitized mammograms.** *Radiographics* 1998, **18:**1587-1598.

11. Harvey JA, Bovbjerg VE: **Quantitative assessment of mammographic breast density: relationship with breast cancer risk.** *Radiology* 2004, **230**:29-41.

12. Jackson VP, Hendrick RE, Feig SA, Kopans DB: **Imaging of the radiographically dense breast.** *Radiology* 1993, **188:**297-301.

13. Mandelson MT, Oestreicher N, Porter PL, White D, Finder CA, Taplin SH, White E: **Breast density as a predictor of mammographic detection: comparison of interval- and screen-detected cancers.** *J Natl Cancer Inst* 2000, **92:**1081-1087.

14. Peto J, Mack TM: **High constant incidence in twins and other relatives of women with breast cancer.** *Nat Genet* 2000, **25:**411-414.

15. Anglian Breast Cancer Study Group: **Prevalence and penetrance of *BRCA1* and *BRCA2* mutations in a population-based series of breast cancer cases.** *Br J Cancer* 2000, **83:**1301-1308.

16. Easton DF, Narod SA, Ford D, Steel M: **The genetic epidemiology of *BRCA1*. Breast Cancer Linkage Consortium.** *Lancet* 1994, **344:** 761.

17. Lynch HT, Lynch JF, Rubinstein WS: **Prophylactic mastectomy: obstacles and benefits.** *J Natl Cancer Inst* 2001, **93:**1586-1587.

18. Helvie MA, Roubidoux MA, Weber BL, Merajver SD: **Mammography of breast carcinoma in women who have mutations of the breast cancer gene *BRCA1*: initial experience.** *Am J Roentgenol* 1997, **168:**1599-1602.
19. Huo Z, Giger ML, Olopade OI, Wolverton DE, Weber BL, Metz CE, Zhong W, Cummings SA: **Computerized Analysis of Digitized Mammograms of BRCA1 and BRCA2 Gene Mutation Carriers.** *Radiology* 2002, **225**:519-526.
20. Tilanus-Linthorst M, Verhoog L, Obdeijn IM, Bartels K, Menke-Pluymers M, Eggermont A, Klijn J, Meijers-Heijboer H, van der Kwast T, Brekelmans C: **A *BRCA1/2* mutation, high breast density and prominent pushing margins of a tumor independently contribute to a frequent false-negative mammography.** *Int J Cancer* 2002, **102:**91-95.
21. Deng CX, Brodie SG: **Roles of *BRCA1* and its interacting proteins.** *BioEssays* 2000, **22:**728-737.
22. Jasin M: **Homologous repair of DNA damage and tumorigenesis: the BRCA connection.** *Oncogene* 2002, **21:**8981-8993.
23. Rosen EM, Fan S, Pestell RG, Goldberg ID: ***BRCA1* gene in breast cancer.** *J Cell Physiol* 2003, **196:**19-41.
24. Harms SE, Flamig DP, Hesley KL, Meiches MD, Jensen RA, Evans WP, Savino DA, Wells RV: **MR imaging of the breast with rotating delivery of excitation off resonance: clinical experience with pathologic correlation.** *Radiology* 1993, **187:**493-501.
25. Orel SG, Schnall MD, LiVolsi VA, Troupin RH: **Suspicious breast lesions: MR imaging with radiologic-pathologic correlation.** *Radiology* 1994, **190:**485-493.

26. Davis PL, McCarty KS, Jr: **Sensitivity of enhanced MRI for the detection of breast cancer: new, multicentric, residual, and recurrent.** *Eur Radiol* 1997, **7 Suppl 5**:289-298.

27. Harms SE: **MRI in breast cancer diagnosis and treatment.** *Curr Probl Diagn Radiol* 1996, **25:**193-215.

28. Heywang SH, Wolf A, Pruss E, Hilbertz T, Eiermann W, Permanetter W: **MR imaging of the breast with Gd-DTPA: use and limitations.** *Radiology* 1989, **171:**95-103.

29. Kriege M, Brekelmans CT, Boetes C, Besnard PE, Zonderland HM, Obdeijn IM, Manoliu RA, Kok T, Peterse H, Tilanus-Linthorst MM, Muller SH, Meijer S, Oosterwijk JC, Beex LV, Tollenaar RA, de Koning HJ, Rutgers EJ, Klijn JG, Magnetic Resonance Imaging Screening Study Group: **Efficacy of MRI and mammography for breast-cancer screening in women with a familial or genetic predisposition.** *N Engl J Med* 2004, **351:**427-437.

30. Warner E, Plewes DB, Hill KA, Causer PA, Zubovits JT, Jong RA, Cutrara MR, DeBoer G, Yaffe MJ, Messner SJ, Meschino WS, Piron CA, Narod SA: **Surveillance of *BRCA1* and *BRCA2* mutation carriers with magnetic resonance imaging, ultrasound, mammography, and clinical breast examination.** *JAMA* 2004, **292:**317-325.

31. American College of Radiology (ACR): *BI-RADS (Breast Imaging Reporting and Data System) Atlas*. Reston, VA: American College of Radiology; 2003.

32. Gail MH, Brinton LA, Byar DP, Corle DK, Green SB, Schairer C, Mulvihill JJ: **Projecting individualized probabilities of developing breast cancer for white females who are being examined annually.** *J Natl Cancer Inst* 1989, **81:**1879-1886.

33. Parmigiani G, Berry D, Aguilar O: **Determining carrier probabilities for breast cancer-susceptibility genes *BRCA1* and *BRCA2*.** *Am J Hum Genet* 1998, **62:**145-158.

34. Costantino JP, Gail MH, Pee D, Anderson S, Redmond CK, Benichou J, Wieand HS: **Validation studies for models projecting the risk of invasive and total breast cancer incidence.** *J Natl Cancer Inst* 1999, **91:**1541-1548.

35. Berry DA, Iversen ES, Jr, Gudbjartsson DF, Hiller EH, Garber JE, Peshkin BN, Lerman C, Watson P, Lynch HT, Hilsenbeck SG, Rubinstein WS, Hughes KS, Parmigiani G: **BRCAPRO validation, sensitivity of genetic testing of *BRCA1*/*BRCA2*, and prevalence of other breast cancer susceptibility genes.** *J Clin Oncol* 2002, **20:**2701-2712.

36. Ford D, Easton DF, Stratton M, Narod S, Goldgar D, Devilee P, Bishop DT, Weber B, Lenoir G, Chang-Claude J, Sobol H, Teare MD, Struewing J, Arason A, Scherneck S, Peto J, Rebbeck TR, Tonin P, Neuhausen S, Barkardottir R, Eyfjord J, Lynch H, Ponder BAJ, Gayther SA, Birch JM, Lindblom A, Stoppa-Lyonnet D, Bignon Y, Borg A, Hamann U, Haites N, Scott RJ, Maugard CM, Vasen H, Seitz S, Cannon-Albright LA, Schofield A, Zelada-Hedman M, and the Breast Cancer Linkage Consortium: **Genetic heterogeneity and penetrance analysis of the BRCA1 and BRCA2 genes in breast cancer families.** *Am J Hum Genet* 1998, **62:**676-689.

37..Euhus DM: **Understanding mathematical models for breast cancer risk assessment and counseling.** *Breast J* 2001, **7:**224-232.

38. Kuhl CK, Mielcareck P, Klaschik S, Leutner C, Wardelmann E, Gieseke J, Schild HH: **Dynamic breast MR imaging: are signal intensity time course data useful for differential diagnosis of enhancing lesions?** *Radiology* 1999, **211:**101-110.

39. Hylton NM: **Vascularity assessment of breast lesions with gadolinium-enhanced MR imaging.** *Magn Reson Imag Clin N Am* 1999, **9:**411-420.

40. Ikeda DM, Hylton NM, Kinkel K, Hochman MG, Kuhl CK, Kaiser WA, Weinreb JC, Smazal SF, Degani H, Viehweg P, Barclay J, Schnall MD: **Development, standardization, and testing of a lexicon for reporting contrast-enhanced breast magnetic resonance imaging studies.** *J Magn Reson Imag* 2001, **13:**889-895.

41. Schnall MD, Ikeda, DM. **Lesion Diagnosis Working Group Report.** *J Magn Reson Imag* 1999; **10**:982-990.

42. Hylton N. **Dedicated Breast MRI Systems Working Group Report.** *J Magn Reson Imag* 1999; **10**:1006-1009.

43. Latimer JJ, Rubinstein WS, Johnson, JM, Kanbour-Shakir A, Grant SG: **Haploinsufficiency for *BRCA1* is associated with normal levels of DNA nucleotide excision repair in breast tissue and blood lymphocytes.** *BMC Med Genet* 2005, **6**:26.

44. Robson ME, Offit K: **Breast MRI for women with hereditary cancer risk.** *JAMA* 2004, **292:**1368-1370.

45. Kuhl CK, Kreft BP, Hauswirth A, Elevelt A, Steudel A, Reiser M, Schild HH: **MR mammography at 0.5 tesla. I. Comparison of image quality and sensitivity of MR mammography at 0.5 and 1.5 T.** *Rofo Fortschr Geb Rontgenstr Neuen Bildgeb Verfahr* 1995, **162:**381-389 erratum **163:**96.

46. Kuhl CK, Kreft BP, Hauswirth A, Gieseke J, Elevelt A, Reiser M, Schild HH: **MR mammography at 0.5 tesla. II. The capacity to differentiate malignant and benign lesions in MR mammography at 0.5 and 1.5 T.** *Rofo Fortschr Geb Rontgenstr Neuen Bildgeb Verfahr* 1995, **162:**482-491.

47. Smith RA, Saslow D, Sawyer KA, Burke W, Costanza ME, Evans WP 3rd, Foster RS Jr, Hendrick E, Eyre HJ, Sener S; American Cancer Society High-Risk Work Group; American Cancer Society Screening Older Women Work Group; American Cancer Society Mammography Work Group; American Cancer Society Physical Examination Work Group; American Cancer Society New Technologies Work Group; American Cancer Society Breast Cancer Advisory Group: **American Cancer Society guidelines for breast cancer screening: update 2003.** *CA Cancer J Clin* 2003, **53:**141-169.
48. Burke W, Daly M, Garber J, Botkin J, Kahn MJ, Lynch P, McTiernan A, Offit K, Perlman J, Petersen G, Thomson E, Varricchio C: **Recommendations for follow-up care of individuals with an inherited predisposition to cancer. II. BRCA1 and BRCA2. Cancer Genetics Studies Consortium.** *JAMA* 1997, **277:**997-1003.
49. **Genetic/Familial High-Risk Assessment: Breast and Ovarian, Practice Guideline in Oncology version 1.2004, National Comprehensive Cancer Network** [http://www.nccn.org].
50. Scheuer L, Kauff N, Robson M, Kelly B, Barakat R, Satagopan J, Ellis N: **Outcome of preventive surgery and screening for breast and ovarian cancer in BRCA mutation carriers.** *J Clin Oncol* 2002, **20:**1260-1268.
51. Elmore JG, Barton MB, Moceri VM, Polk S, Arena PJ, Fletcher SW: **Ten-year risk of false positive screening mammograms and clinical breast examinations.** *N Engl J Med* 1998, **338:**1089-1096.
52. Harris R, Leininger L: **Clinical strategies for breast cancer screening: weighing and using the evidence.** *Ann Intern Med* 1995, **122:**539-547.

53. Harris R: **Variation of benefits and harms of breast cancer screening with age.** *J Natl Cancer Inst Monogr* **1997:**139-143.

54. Kerlikowske K, Grady D, Barclay J, Sickles EA, Ernster V: **Effect of age, breast density, and family history on the sensitivity of first screening mammography.** *JAMA* 1996, **276:**33-38.

55. Kaiser WA, Zeitler E: **MR imaging of the breast: fast imaging sequences with and without Gd-DTPA. Preliminary observations.** *Radiology* 1989, **170:**681-686.

56. Stoutjesdijk MJ, Boetes C, Jager GJ, Beex L, Bult P, Hendriks JH, Laheij RJ, Massuger L, van Die LE, Wobbes T, Barentsz JO: **Magnetic resonance imaging and mammography in women with a hereditary risk of breast cancer.** *J Natl Cancer Inst* 2001, **93:**1095-1102.

57. Warner E, Plewes DB, Shumak RS, Catzavelos GC, Di Prospero LS, Yaffe MJ, Goel V, Ramsay E, Chart PL, Cole DE, Taylor GA, Cutrara M: **Comparison of breast magnetic resonance imaging, mammography, and ultrasound for surveillance of women at high risk for hereditary breast cancer.** *J Clin Oncol* 2001, **19:**3524-3531.

58. Sumkin JH, Ganott MA, Hakim CM, Hardesty LA, Poller WR, Rubinstein WS: **MRI, ultrasound, and digital mammography for breast cancer screening in women at high risk [abstract].** American Roentgen Ray Society annual meeting, New Orleans, May 15-20, 2005.

59. Claus EB, Risch N, Thompson WD: **Genetic analysis of breast cancer in the cancer and steroid hormone study.** *Am J Hum Genet* 1991, **48:**232-242.

60. Tyrer J. Duffy SW, Cuzick J: **A breast cancer prediction model incorporating familial and personal risk factors.** *Stat Med* 2004, **23:**1111-1130.

61. King M-C, Wieand S, Hale K, Lee M, Walsh T, Owens K, Tait J, Ford L, Dunn BK, Costantino J, Wickerham L, Wolmark N, Fisher B: **Tamoxifen and breast cancer incidence among women with inherited mutations in *BRCA1* and *BRCA2*: National Surgical Adjuvant Breast and Bowel Project (NSABP-P1) Breast Cancer Prevention Trial.** *JAMA* 2001, **286:**2251-2256.

62. Warner E, Plewes DB, Hill KA, Causer PA, Zubovits JT, Jong RA, Cutrara MR, DeBoer G, Yaffe MJ, Messner SJ, Meschino WS, Piron CA, Narod SA: **Surveillance of *BRCA1* and *BRCA2* mutation carriers with magnetic resonance imaging, ultrasound, mammography, and clinical breast examination.** *JAMA* 2004, **292:**1317-1325.

63. Kriege M, Brekelmans CT, Boetes C, Besnard PE, Zonderland HM, Obdeijn IM, Manoliu RA, Kok T, Peterse H, Tilanus-Linthorst MM, Muller SH, Meijer S, Oosterwijk JC, Beex LV, Tollenaar RA, de Koning HJ, Rutgers EJ, Klijn JG and the Magnetic Resonance Imaging Screening Study Group: Efficacy of MRI and mammography for breast-cancer screening in women with a familial or genetic predisposition. *N Engl J Med* 2004, **351:**427-437.

64. Vogel VG: **High-risk populations as targets for breast cancer prevention trials.** *Prev Med* 1991, **20:**86-100.

65. Rubinstein WS, O'Neill SM, Peters JA, Rittmeyer LJ, Stadler MP: **Mathematical modeling for breast cancer risk assessment. State of the art and role in medicine.** *Oncology* 2002, **16:**1082-1094 discussion **16:**1094, **16:**1097-1099.

66. Lehman CD, Schnall MD, Kuhl CK, Harms SE: **Report of the Working Groups on Breast MRI: report of the High-Risk Screening Group.** *Breast J* 2004, **16 Suppl 2**:S9-S12.

Figures

Figure 1 - MRI results by BIRADS category

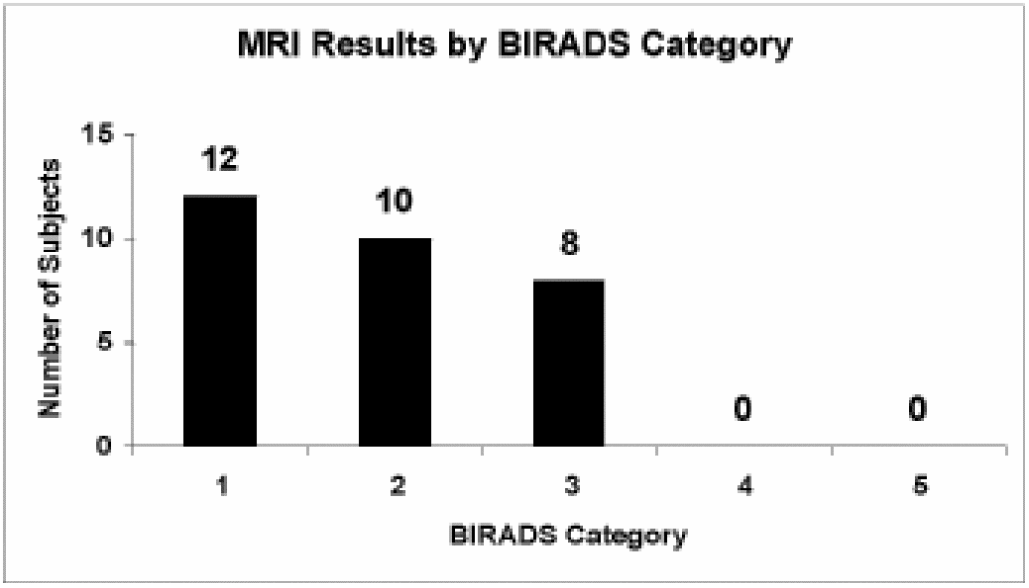

Figure 2 - Imaging of subject 006

A) Subject 006 pre-MRI mammogram demonstrating heterogeneously dense breast tissue. There is no evidence of a cancerous lesion. B) Pre-contrast MR image showing an approximately 1.5 cm, smooth, round, lesion in the right breast just above the nipple level medial and close to the chest wall (arrowhead). Core biopsy of this lesion demonstrated benign pathology, specifically, fibrosis with focal ductal epithelial hyperplasia [43]. C) Post-contrast MR images showing a small (approximately 1 cm), round, well-delineated enhancing mass (arrow) in the left breast at the 1:00 position. This mass was seen on both the initial delay after contrast injection (left) and the delayed contrast enhanced subtraction images (right). Core biopsy of this lesion indicated infiltrating ductal carcinoma, which was confirmed after removal via modified radical mastectomy [43].

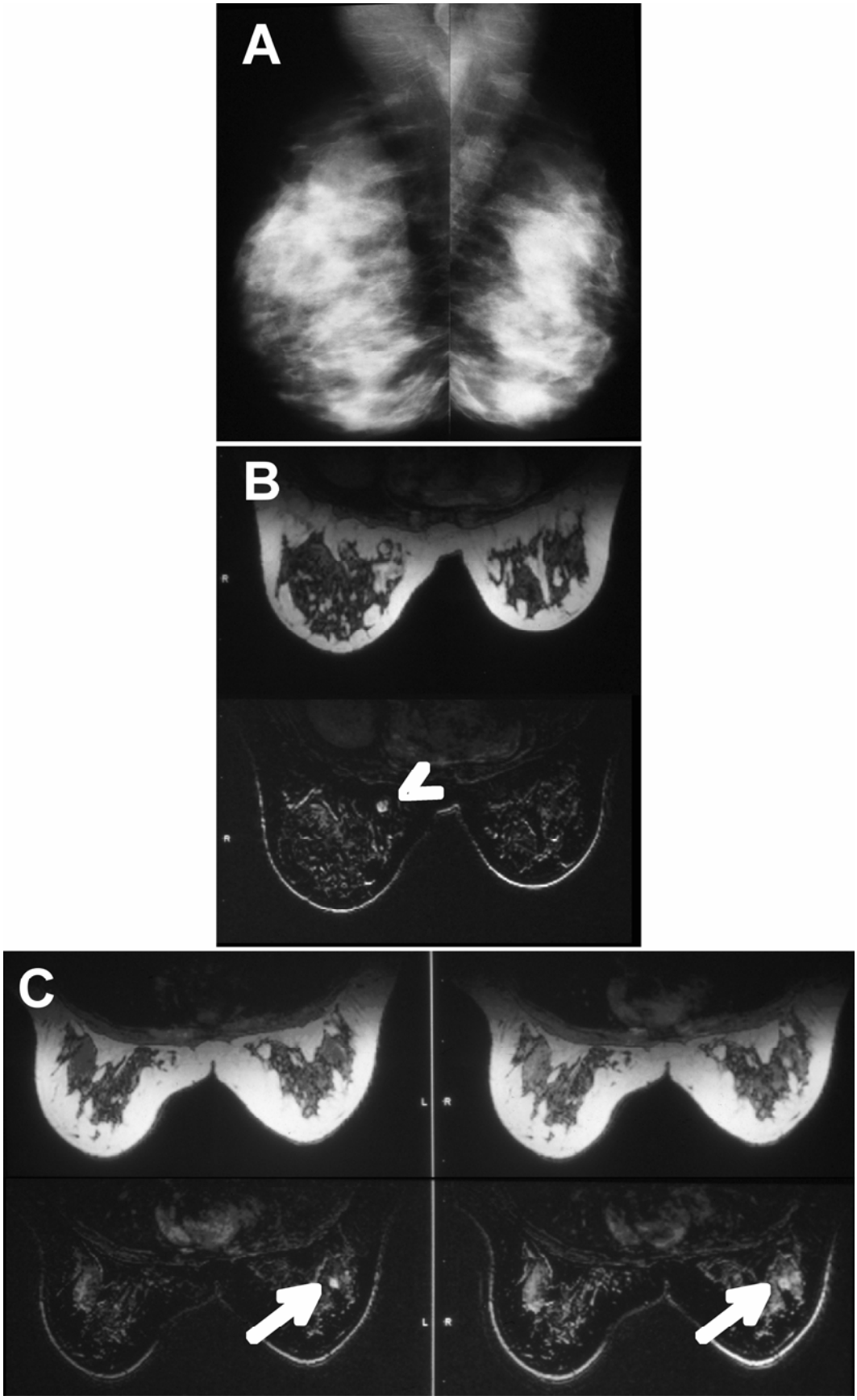
A
B
C

…

Tables

Table 1 - Post-MRI evaluation procedures for the BIRADS category 3 results

Procedure Type	Invasive	Non-Invasive
Short-Term (6 month) Clinical Follow-Up		1
Ultrasound with Normal Results		3
Ultrasound with Cyst Aspiration	1	
Ultrasound with Fine Needle Aspiration	1	
Ultrasound with Core Biopsy	2	
Total Patients:	**4**	**4**

BMC Medical Genetics

BioMed Central

Case report

Haploinsufficiency for *BRCA1* is associated with normal levels of DNA nucleotide excision repair in breast tissue and blood lymphocytes

Jean J Latimer*[1,2,3], Wendy S Rubinstein[4,5], Jennifer M Johnson[2], Amal Kanbour-Shakir[6], Victor G Vogel[7] and Stephen G Grant[1,2,3,8]

Address: [1]Department of Obstetrics, Gynecology and Reproductive Sciences, School of Medicine, University of Pittsburgh, Pittsburgh, PA, USA, [2]Biochemistry and Molecular Genetics Program, School of Medicine, University of Pittsburgh, Pittsburgh, PA, USA, [3]Research Institute, Magee-Womens Hospital, Pittsburgh, PA, USA, [4]Department of Medicine, Northwestern University Feinberg School of Medicine, Chicago, IL, USA, [5]Evanston Northwestern Healthcare Center for Medical Genetics, Evanston, IL, USA, [6]Department of Pathology, School of Medicine, University of Pittsburgh, Pittsburgh, PA, USA, [7]Department of Medicine, School of Medicine, University of Pittsburgh, Pittsburgh, PA, USA and [8]Department of Environmental and Occupational Health, Graduate School of Public Health, University of Pittsburgh, Pittsburgh, PA, USA

Email: Jean J Latimer* - latimerj@pitt.edu; Wendy S Rubinstein - wrubinstein@enh.org; Jennifer M Johnson - jmjst39@pitt.edu; Amal Kanbour-Shakir - akanbourshakir@mail.magee.edu; Victor G Vogel - vvogel@mail.magee.edu; Stephen G Grant - sgg@pitt.edu

* Corresponding author

Published: 14 June 2005

BMC Medical Genetics 2005, **6**:26 doi:10.1186/1471-2350-6-26

Received: 03 February 2005
Accepted: 14 June 2005

This article is available from: http://www.biomedcentral.com/1471-2350/6/26

Abstract

Background: Screening mammography has had a positive impact on breast cancer mortality but cannot detect all breast tumors. In a small study, we confirmed that low power magnetic resonance imaging (MRI) could identify mammographically undetectable tumors by applying it to a high risk population. Tumors detected by this new technology could have unique etiologies and/or presentations, and may represent an increasing proportion of clinical practice as new screening methods are validated and applied. A very important aspect of this etiology is genomic instability, which is associated with the loss of activity of the breast cancer-predisposing genes *BRCA1* and *BRCA2*. In sporadic breast cancer, however, there is evidence for the involvement of a different pathway of DNA repair, nucleotide excision repair (NER), which remediates lesions that cause a distortion of the DNA helix, including DNA cross-links.

Case presentation: We describe a breast cancer patient with a mammographically undetectable stage I tumor identified in our MRI screening study. She was originally considered to be at high risk due to the familial occurrence of breast and other types of cancer, and after diagnosis was confirmed as a carrier of a Q1200X mutation in the *BRCA1* gene. In vitro analysis of her normal breast tissue showed no differences in growth rate or differentiation potential from disease-free controls. Analysis of cultured blood lymphocyte and breast epithelial cell samples with the unscheduled DNA synthesis (UDS) assay revealed no deficiency in NER.

Conclusion: As new breast cancer screening methods become available and cost effective, patients such as this one will constitute an increasing proportion of the incident population, so it is important to determine whether they differ from current patients in any clinically important ways. Despite her status as a *BRCA1* mutation carrier, and her mammographically dense breast tissue, we did not find increased cell proliferation or deficient differentiation potential in breast epithelial cells from this patient which might have contributed to her cancer susceptibility. Although NER

deficiency has been demonstrated repeatedly in blood samples from sporadic breast cancer patients, analysis of blood cultured lymphocytes and breast epithelial cells for this patient proves definitively that heterozygosity for inactivation of *BRCA1* does not intrinsically confer this type of genetic instability. These data suggest that the mechanism of genomic instability driving the carcinogenic process may be fundamentally different in hereditary and sporadic breast cancer, resulting in different genotoxic susceptibilities, oncogene mutations, and a different molecular pathogenesis.

Background

A reduction in breast cancer mortality has been observed in recent years that has been partially attributed to the widespread adoption of screening mammography [1]. Traditional screening mammography, however, fails to detect 15% of incident cancers [2]. New, complementary imaging techniques are therefore under development that may increase the accuracy of primary screening. We performed a small study to validate the use of low power magnetic resonance imaging (MRI) to prospectively detect breast alterations and malignancy and to determine the feasibility of applying this technique to a high-risk population [3]. We present here a subject from that study whose early stage tumor was not detectable by mammography.

This patient was enrolled in the screening study due to her family history of breast and other neoplasias. After tumor diagnosis, she was determined to be heterozygous for a putative inactivating mutation in the *BRCA1* gene. In addition, she had dense breast tissue, an impediment to mammography that is in itself a risk factor for breast cancer [4]. Breast development and lactational differentiation also appear to individually modify breast cancer risk, with early term pregnancy conferring a persistent protective effect [5]. Exposure to ionizing radiation, while a lifetime risk factor for breast cancer, appears to be more dangerous when it occurs during alveolar differentiation of the breast at adolescence [6]. Using a novel tissue engineering system [7], we therefore examined the growth and differentiation of normal breast epithelial samples from this patient via live-cell imaging.

The *BRCA1* hereditary breast cancer gene has been shown to be involved in DNA double strand break repair [8,9]. DNA repair defects have also been identified in the peripheral blood cells of sporadic breast cancer patients [10-13], but, in this case, it seems to involve a different pathway of DNA repair, nucleotide excision repair (NER) [14-16]. We have extended this observation of NER deficiency to the tumor itself, as well as the adjoining non-diseased normal breast tissue [17]. NER is a complex pathway of DNA repair [18] normally associated with removal of pyrimidine-pyrimidine intrastrand crosslinks ("dimers") caused by exposure to UV light. NER deficiency is the basis of hereditary xeroderma pigmentosum (XP) [19], a disease with a 1200-fold increase in incidence of skin cancer [20]. The signal for activation of the NER pathway is actually very general; any lesion causing a distortion in the DNA helix, including crosslinks caused by oxidative radicals, certain types of mismatches (purine-purine or pyrimidine-pyrimidine) and so called "bulky" adducts caused by phase I metabolism of polyaromatic hydrocarbons [21]. It has recently been shown that *BRCA1* expression can enhance NER activity, although this analysis was not performed in breast cells [22,23]. We therefore applied the functional unscheduled DNA synthesis (UDS) assay for NER capacity to multiple samples of normal tissue from this patient, to determine whether haploinsufficiency for *BRCA1* was a mechanism of NER deficiency. We have developed a method to reliably culture non-diseased breast tissue (with a success rate of 100%) and breast tumors (with a success rate of 85%) [7,17].

Case presentation

We describe a breast cancer patient whose tumor was detected by MRI. She was enrolled into a pilot screening study of low power MRI due to her familial risk. She had mammographically dense breasts and her tumor was undetectable mammographically.

Patient description

The patient was a 35.7 year old woman who presented with a very strong family history of breast cancer as depicted in Figure 1, and negative physical and mammographic examination. She had extremely dense breast tissue bilaterally by mammography as well as fibrocystic breast tissue by physical examination. She had no previous personal history of breast biopsy or abnormal mammograms.

Risk profile

The 5 year breast cancer risk for this patient as calculated by the BRCAPRO model was 5.7%, and her probability of being a *BRCA1* or *BRCA2* carrier was 0.47. The Gail model risk assessment was calculated using the following information: Race-Caucasian; Age-35; Age at first menses-12; Age at first live birth-nulliparous; Number of first-degree relatives with breast cancer-2; Number of previous breast

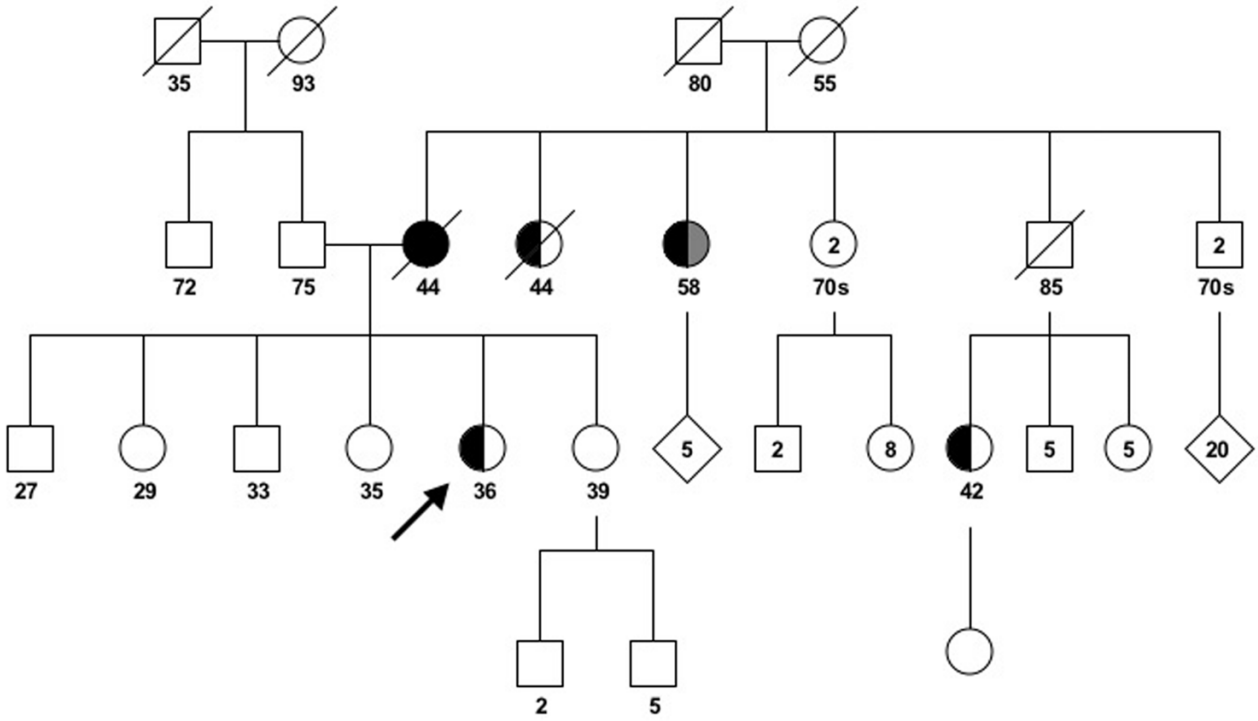

Figure 1

Pedigree of the patient (indicated by arrow). She, one maternal aunt and one maternal cousin had breast cancer diagnosed at 36, 44 and 41 years old, respectively, as indicated by the half-filled symbols, and her aunt died of the disease. Her cousin underwent lumpectomy followed by chemotherapy, radiotherapy and is presently on tamoxifen. Her mother had breast cancer in both breasts, diagnosed at ages 41 and 42, as indicated by the completely filled symbol. She underwent bilateral mastectomy and hysterectomy followed by chemotherapy and radiotherapy and died of the disease at age 44. A second maternal aunt was diagnosed with colon cancer at age 52 (light half-filled symbol) and breast cancer at age 55 (dark half-filled symbol). Based on this pattern of familial cancer the patient was considered to be at high risk of developing breast cancer and was entered into the low power MRI screening validation and feasibility study. Following her diagnosis, she was confirmed as carrying a Q1200X mutation in the *BRCA1* gene.

biopsies-0. The calculated 5 year Gail risk was 1.0% and her lifetime risk was 31.3%.

Genetic testing

Following genetic counseling, the patient elected to undergo DNA sequencing of the *BRCA1* and *BRCA2* genes, which revealed a Q1200X truncation mutation in one of her *BRCA1* alleles. The C to T mutation at codon 1200 in exon 11 results in the change of the amino acid glutamine to a stop codon with resulting protein truncation and loss of function. Exon 11 is the largest exon in *BRCA1* and has the highest frequency of reported mutations. The Q1200X mutation has been independently observed several times [24].

Imaging

The bilateral screening mammogram was compared to previous films from another hospital. The breast tissue was described as heterogeneously dense, thus lowering the sensitivity. There were no masses, significant calcifications or other findings and the mammogram was interpreted as negative bilaterally. A one-year follow-up was recommended.

The patient was then MRI scanned as previously described [3], with pre- and post-gadolinium enhancement images evaluating both breasts simultaneously in the axial plane. In the upper-outer left breast there was a small (approximately 1 cm), round, well-demarcated enhancing lesion.

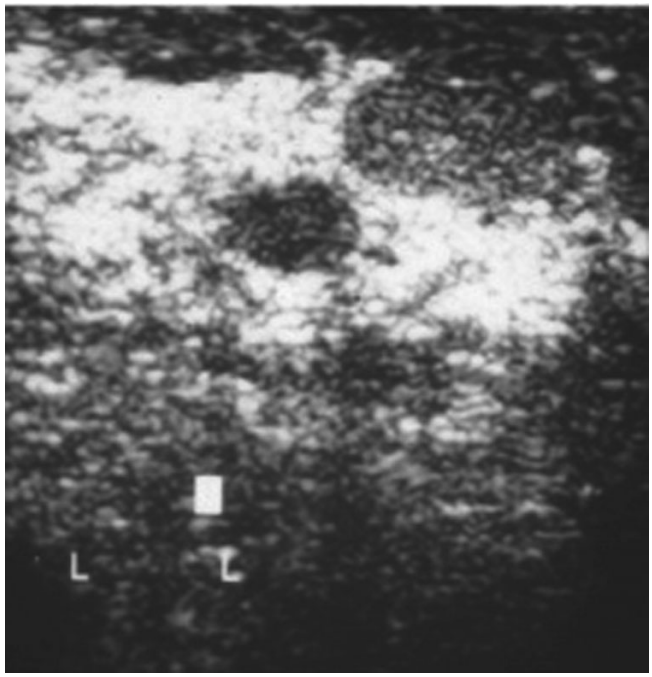

Figure 2
Ultrasound of the MRI-detected lesion. Following MRI, the patient was scheduled for ultrasound to identify the questionable lesions seen on MRI for possible core biopsy. Under ultrasound the lesion of concern was identified and biopsied at the 1:00 location in the left breast. Additionally, one lesion seen by MRI in the right breast at the 4:00 location was identified and biopsied.

This lesion was seen on both the initial delay after contrast injection and the delayed contrast enhanced subtraction images. The lesion appeared to accumulate contrast to a greater extent on the delayed subtraction images with an additional lesion adjacent to the first. In the medial aspect of the mid right breast, there were several small punctate areas of enhancement on both the immediate and delayed subtraction views. Also in the right breast just above the nipple level medial and close to the chest wall an additional enhancing lesion was seen. This lesion was approximately 1.5 cm, round, well-demarcated and continued to accumulate contrast on the delayed subtraction images. This lesion appeared to have a small non-enhancing septation.

Core biopsies

Under ultrasound, the lesion of concern in the left breast was identified and biopsied, as well as one lesion in the right breast (Figure 2). The core biopsy of the left breast revealed infiltrating ductal carcinoma in 2 of 5 core fragments; high nuclear grade, with no lymphatic invasion seen. The core biopsy of the right breast demonstrated benign pathology, specifically, fibrosis with focal ductal epithelial hyperplasia.

Final pathology, treatment plan and outcome

Although a surgical candidate for lumpectomy and radiation, the patient chose to undergo left modified radical mastectomy with left axillary lymph node dissection and contralateral prophylactic total mastectomy because of her genetic risk status. The pathology in the left breast was consistent with the imaging and core biopsy in size and description. Tumor size was 8 mm in greatest dimension, nuclear grade III, ER/PR and Her2/neu negative, and the nodal status (0/4) was negative (stage TIaN0M0). The patient underwent 4 cycles of chemotherapy and has been reportedly healthy since. Because of the positive *BRCA1* mutation results, she subsequently underwent prophylactic bilateral salpingo-oophorectomy.

Live-cell analysis of tissue explant cultures

A number of life history factors have been associated with breast cancer incidence that are widely interpreted as representing lifetime exposure of the breast tissue to estrogen-induced mitogenesis [25]. An alternative interpretation, based on epithelial cell differentiation, suggests that lactational differentiation, such as occurs during term pregnancy, confers resistance to carcinogenesis [26,27]. We have developed a novel human mammary epithelial (HME) tissue engineering system wherein many aspects of organotypic differentiation are reiterated in vitro [28]. In this system, breast epithelial cells initially retain cell-to-cell contact while they proliferate, then undergo an architectural reorganization, first to form three-dimensional mammospheres, and later vast networks of branching ductal and lobular structures. Tumor and some pre-neoplastic samples fail to form such architecture. Normal tissue from this patient, who is both a *BRCA1* mutation carrier and has dense breasts, was evaluated to determine whether either of these factors affected de novo differentiation in this system. Four discrete pieces of fresh tissue were provided for live-cell analysis from each of the patient's ipsilateral and contralateral breasts. In the case of the ipsilateral breast, this tissue was provided at increasing distance from the tumor margin in 1 cm increments. All of these normal samples attached and grew in our culture system and were examined for cell-to-cell interactions and morphology over a period of one month. In the context of breast reduction explant cultures from 22 patients with no breast disease, these patient samples manifested typical mixtures of fibroblastic and epithelial cells. After several days in culture without passaging, the epithelial cells began to self-organize, initially forming three-dimensional mammospheres (Figure 3A), and, after 2 weeks in culture, more complex pre-ductal linear columns of epithelial cells (Figure 3B). The tissue

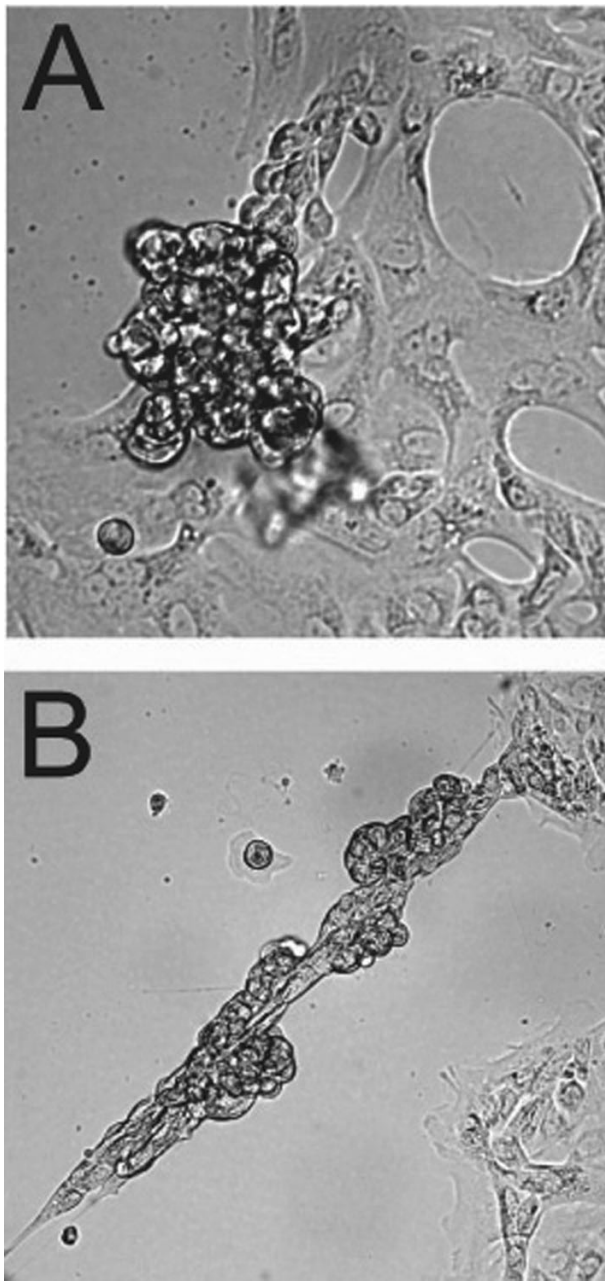

Figure 3
Micrographs of the non-diseased primary human mammary epithelial cultures (HMEC) from the *BRCA1* mutation carrier. A) Contralateral breast – A cluster of epithelial cells called a mammosphere is shown on the left center of the image sitting on a field of fibroblasts. B) Ipsilateral breast – The original fresh tissue block from which this culture was derived was located 4 cm from the infiltrating ductal carcinoma. The structure shown is a cluster of rounded epithelial cells manifesting a column configuration called "pre-ductal linearization". Both images were captured under Differential Interference Contrast (DIC) optics on a Zeiss Axiovert 100 microscope at a total of 140x magnification.

explants from both breasts showed similar patterns of behavior (Figure 3). Tissue cultured from a contemporaneous disease-free control and the contralateral breast of a sporadic breast cancer patient showed similar morphology and architecture (data not shown).

Cell growth kinetics

It has been suggested that the association between breast density and risk of breast cancer is due to increased cell proliferation [29]. One measure of cell growth and viability is the S-phase index (SPI) or the percentage of cells incorporating radiolabeled thymidine over a specific incubation period (in our case, 2 hours). In a previous study with 22 normal breast reduction epithelium [BRE] cultures we observed a wide range of proliferation rates, with SPI ranging from a low of 0.2% to a high of 46.0% (mean of 18.3 ± 2.6%) [30]. The contemporaneous control sample from a disease-free breast reduction patient had an SPI of 30.9%, at the higher end of this normal range. The ipsilateral and contralateral tissue samples from the hereditary breast cancer patient exhibited SPI of 26.6% and 26.2%, respectively, placing them at slightly over the 70th percentile for growth rate. The contralateral sample from the sporadic breast cancer patient had an SPI of 17.0%, placing it slightly under the 50th percentile. Thus, all of these breast cancer patient samples appeared to grow well in our system, with SPI well within the range of our normal samples. The similarity of the SPI values from the two samples from the *BRCA1* mutation carrier does not appear to be accidental; the chances of selecting two samples from the normal population with values as close or closer is very small (P = 0.026).

Functional analysis of NER capacity

Peripheral blood lymphocytes and normal breast epithelial tissue from the hereditary cancer patient were then cultured for performance of the functional UDS assay, which requires living cells for radiolabel incorporation during DNA repair synthesis following UV exposure. This assay is diagnostic for the inherited cancer-prone disease XP, where it is usually performed in lymphocytes or skin fibroblasts. Our novel HME tissue engineering system allows us to apply the assay to breast epithelial cells, and we have previously demonstrated tissue-specificity in the NER capacity of these cells in normal samples from patients undergoing breast reduction mammoplasty [30]. Patient data is therefore expressed relative to the average of our breast reduction controls.

Analysis of cultured blood lymphocytes from the patient established that they had normal NER capacity (99.6% of the average of our 33 normal samples) (Figure 4). This is well above the cut-off established in our sporadic breast cancer population, < 70% average normal activity, which when applied to our cases and controls yielded a

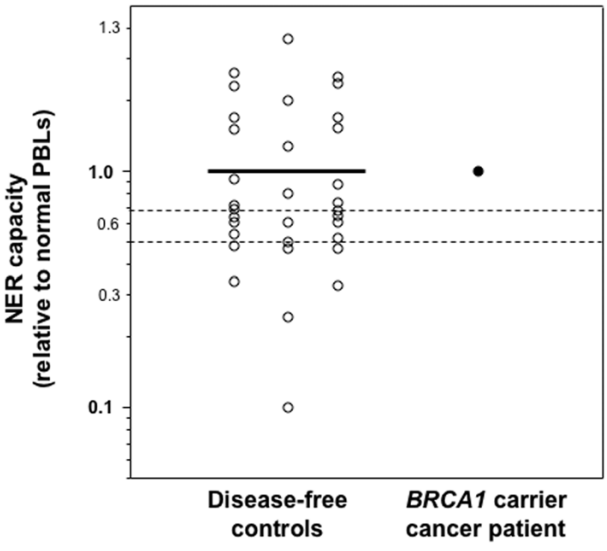

Figure 4
Comparison of the NER capacity of a PBL sample from our *BRCA1* mutation carrier patient with those of a population of disease-free controls. The dark horizontal line indicates the average for the normal population, while the dotted lines indicate upper limits for residual NER activity in patients with the hereditary NER deficiency disease XP (0.50) and the cut-off established in our breast tissue study that identified tumors with high sensitivity and specificity (0.70).

significant odds ratio of 37.4 [31]. A trend towards age dependence had been noted in the analysis of the UDS data of the normal controls (P = 0.059) [30]; addition of the patient sample supports this trend, but it still fails to reach significance (P = 0.056).

The functional NER assay was then applied to the contemporaneous disease-free breast reduction control sample, one sample each from the ipsilateral and contralateral breasts of the patient, and to a sample from the contralateral breast of an apparently sporadic breast cancer patient. The NER of the BRE non-diseased control was 1.82 times the average of our normal data set for this tissue and within the range of normal. The NER capacity of the ipsilateral breast epithelial sample was 1.05 times the average of our population of BRE controls, clearly exhibiting no overt DNA repair deficiency (Figure 5). The contralateral sample was very similar, with an NER capacity of 1.17 times BRE normal. Although the NER values of these two samples from the same patient are similar, they are not close enough to distinguish themselves as coming from the same individual (P = 0.16). The NER capacity of the contralateral sample from the sporadic breast cancer patient was 1.62 times the average of the BRE controls, also in the normal range.

Our earlier analysis of NER in our normal population revealed no effects of age or cell proliferation (as represented by the SPI). All of these additional patient samples are consistent with those results.

Discussion

At least two types of breast tumors are not accurately detected by traditional screening mammography: "interval" tumors that arise quickly between screenings, and tumors whose density is not sufficient to distinguish them from the surrounding normal tissue. The latter situation is more likely to occur in women with dense normal breast tissue, which, in turn, is more typical of younger women. Thus, mammographically undetectable tumors may have a number of characteristics, such as fast growth, low density, early onset and/or occurrence in dense breasts that might distinguish them from mammographically detectable tumors in terms of molecular etiology and clinical parameters of prognosis and response. The present patient had an early onset breast tumor, but had both hereditary susceptibility due to her *BRCA1* mutation and dense breasts, so her presentation is not unusual in this context. It is possible that breast tumors detected by complementary screening methods in the future will demonstrate unique clinical and molecular features, when it becomes feasible to perform such screening in the general population.

Since the *BRCA1* gene product is known to play a role in DNA double strand break repair [8,9], it has been suggested that decreased repair capacity is the basis of the breast cancer predisposition observed in mutation carriers [32-35]. Such a cellular phenotype has been difficult to demonstrate, however [36-39]. An alternate possibility is that the mutation affects the growth or differentiation of breast epithelial cells in a manner consistent with cancer susceptibility. It has been suggested that dense breast tissue is indicative of generalized hyperproliferation that might promote oncogenesis [29]. Our findings show that all 8 samples, derived from both the involved and the uninvolved breasts of a hereditary breast cancer patient develop normal epithelial architecture in vitro, implying that the epithelial/stromal (paracrine) interactions necessary for the development of this complex architecture are intact and normal in *BRCA1* heterozygotes despite their greater risk of breast cancer. The SPI results also indicate that this non-diseased epithelial tissue falls into the typical range of normal for BRE control cultures and is demonstrating typical growth in our HME tissue engineering system.

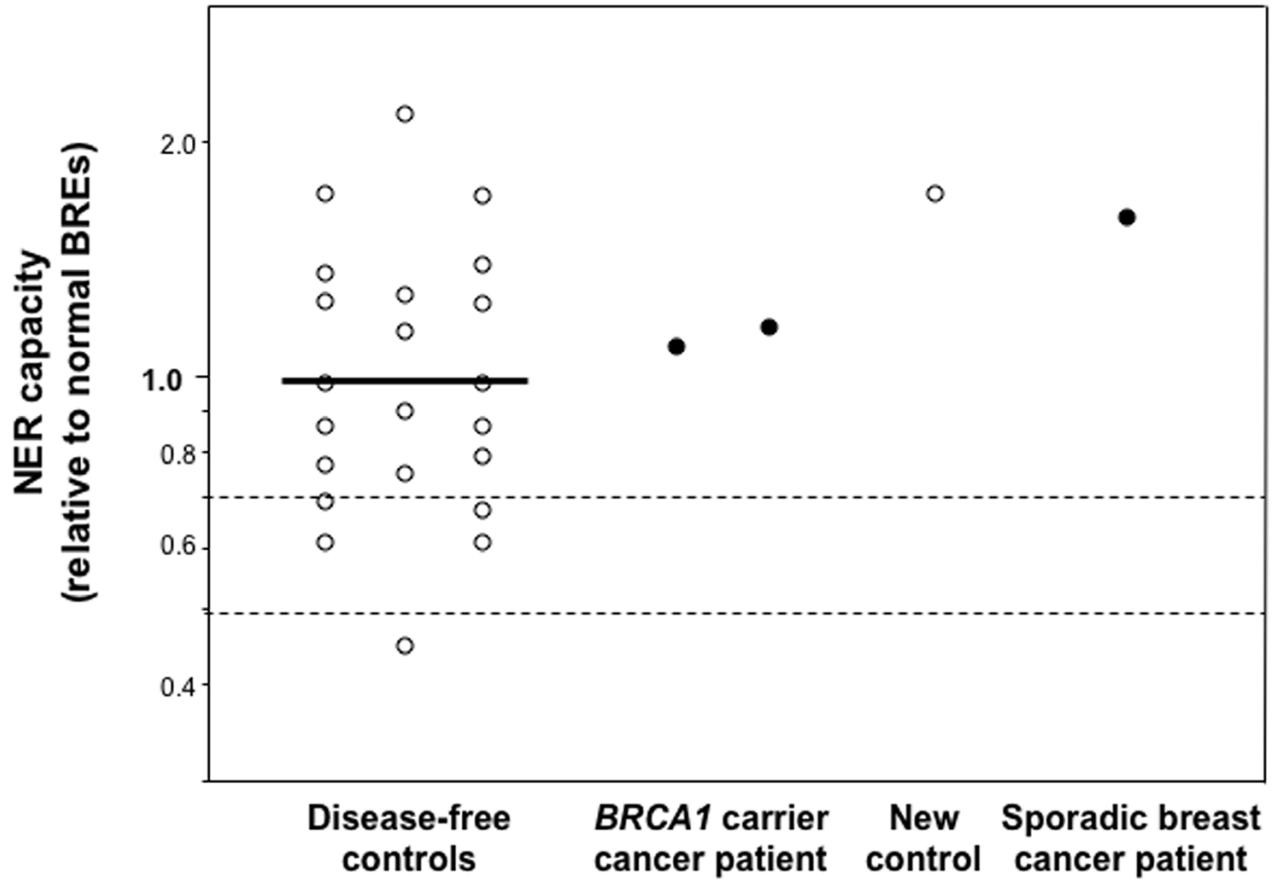

Figure 5
Comparison of the NER capacities of two samples of normal breast epithelium from our *BRCA1* mutation carrier patient with those of a population of disease-free controls who underwent breast reduction mammoplasty. The dark horizontal line indicates the average for the normal population of breast reduction epithelium (BRE), while the dotted lines indicate upper limits for residual NER activity in patients with the hereditary NER deficiency disease XP (0.50) and the cut-off established in our breast tissue study that identified tumors with high sensitivity and specificity (0.70). The patient sample on the left was derived from the ipsilateral (left) breast, while the sample on the right was from the contralateral (right) breast.

NER deficiency is most often associated with XP, sensitivity to UV-induced DNA damage and skin cancer [18-21]. The NER deficiency of XP patients is manifested in other tissues, however, as shown by their high spontaneous frequency of mutation in blood lymphocytes [40] and the occurrence of other types of tumors [41]. The observation that sporadic breast cancer patients have low levels of NER in peripheral lymphocytes suggests that sporadic breast cancer is associated with constitutively low levels of NER [14-16]. Our results from a single patient demonstrate, however, that while overexpression of *BRCA1* may enhance NER [22], haploinsufficiency for this gene does not necessarily result in detectable NER deficiency. Since it is clear that genomic instability is a necessary prerequisite for the completion of the complex multi-step carcinogenic pathway(s) involved in breast cancer, a fundamental difference in the mechanisms of genomic instability arising in hereditary and sporadic breast tumors would be likely to translate into fundamentally different patterns of molecular pathogenesis that could impact on clinical management.

The relative NER capacities of tumor and normal tissue may have important practical implications. If breast tumors from hereditary patients exhibit NER deficiency similar to that observed in sporadic patients, while their

normal tissues exhibit normal levels of this type of DNA repair, then the tumors would be hypersensitive to a range of chemotherapeutic drugs, including alkylating agents (cyclosphosphamide), cross-linking agents (cis-platinum) and bulky DNA adducting agents (melphalan). Individualization of chemotherapy based on some aspect of NER expression is being pursued in colon [42], testicular [43,44] and ovarian cancer [45].

Conclusion

This patient and her tumor represent the vanguard of a new population of early stage breast cancer patients that will be increasingly diagnosed as new screening technologies complementary to mammography are validated and become practicable. We have shown that low power MRI can detect a stage I tumor in dense breast tissue; the same technology can also impact upon interval tumors by staggering the procedure with mammography rather than applying them coincidently. Although we did not observe obvious differences in the growth rate or differentiation potential of the dense breast tissue from this patient, we cannot rule out the possibility that some or all of the tumors detectable only by complementary screening procedures will differ from the present clinical experience in important ways. Our live-cell analysis takes a step toward defining cellular characteristics that may be useful for cancer risk assessment, but we are only beginning to investigate the possibilities of the system. It may be that different growth conditions, or induction with genotoxic or estrogenic agents, will allow for the greater differentiation of breast tissue and tumor behaviours. This technique also allows for the application of functional assays to patient samples, as exemplified in this report by the UDS assay for NER capacity. Those UDS results, although from a single patient, demonstrate definitively that the constitutively low NER capacities reported in several sporadic breast populations do not arise as a pleiomorphic effect of *BRCA1* haploinsufficency. Thus, the basis of genetic instability, a fundamental element in breast carcinogenesis, may differ between sporadic and hereditary breast tumors. This results in different susceptibilities to inducing agents, mutations in different sets of oncogenes and tumor suppressor genes, and, ultimately, tumors of different molecular etiology that express different clinically relevant phenotypes.

Methods

Patients and controls

The patient was a 35.7 year old woman with strong family history of breast cancer recruited into a clinical trial of MRI screening for young woman at high risk for breast cancer with dense breast tissue [3]. Gadolinium enhancement images revealed a small 1 cm lesion in the upper-outer quadrant of the left breast, identified pathologically as an infiltrating ductal carcinoma. The patient underwent a modified radical mastectomy of the left breast and chose to also undergo a contralateral prophylactic total mastectomy. Blood and tissue were obtained for analysis with consent under Magee-Womens Hospital (of the University of Pittsburgh Medical Center) IRB # MWH-94-108.

Data from this hereditary breast cancer patient were compared to that from two additional patients as well as previously published controls. The first new control patient was a 20 year old women undergoing breast reduction mammoplasty. The second contemporaneous control patient was a 36 year old woman undergoing cosmetic surgery on her contralateral breast two years after successful lumpectomy to remove an apparently sporadic stage IIA breast tumor (2.5 cm, negative for estrogen and progesterone receptors, 13 lymph nodes negative). She had undergone standard radiotherapy and chemotherapy with adriamycin and cyclophosphamide. Histopathological analysis confirmed that the breast tissue from both of these control patients was free of cancer and within the acceptable histological range of normal.

Patient tissue culture and analysis

Fresh tissues from the patient were obtained within 5 hours of surgery. After pathological evaluation, excess tissue not needed for diagnosis was placed into DMEM containing 10% fetal calf serum and 3x antibiotic antimycotic (Sigma, St. Louis, MO) at 4°C. This tissue was then processed as described in Latimer *et al*. [30] and placed into culture on a diluted form of matrigel (1:1 with DMEM) in the novel MWRIα medium [7].

Eight samples of the principal patient's tissue were obtained for culture after bilateral mastectomy surgery. We were not able to obtain a sample of her tumor, because it was utilized entirely for clinical diagnosis. We were able to obtain 4 pieces of histologically normal non-tumor adjacent tissue at increasing 1 cm intervals from the tumor margin from her left (ipsilateral) breast. In addition, we obtained 4 similar pieces of fresh tissue from her contralateral breast. All were placed into primary explant (HME) culture.

For analysis of cell growth and in vitro differentiation, explants were cultured and imaged every second day using a digital Hamamatsu Orca camera for 30–60 days. Images were analyzed on a Macintosh G4 computer using QED imaging software (Media Cybernetics, Inc., Silver Spring, MD).

Control tissue cultures

Breast reduction mammoplasty tissues were obtained from patients ages 20–70 at Magee-Womens Hospital under the above IRB. A neighboring piece of mammoplasty tissue (from the same 0.25 cm^2 sample) to that

placed into primary culture was fixed and processed in paraffin. These sections were examined by a pathologist to verify the histological features and normality of the tissue. Breast tissue was processed as previously described [30]. Tissue was rinsed three times in PBS containing antibiotics, disaggregated and placed into MWRIα medium [7] on a thin coat of matrigel. Peripheral blood lymphocytes (PBLs) were obtained with consent from normal healthy control subjects ages 20–50 working at Magee-Womens Hospital or students at the University of Pittsburgh. Foreskin fibroblast (FF) tissue was obtained as discarded tissue from newborn infants after circumcision and utilized between passages 7 and 10. These control populations have been previously described in greater detail [30,46]. Breast tissue samples from the two new control patients were processed in the same manner.

Analysis of S-phase indices

Primary cultures of mammary tissue, established 10–14 days, were labeled with ^{3}H-thymidine for a period of 2 hours followed by a chase with cold thymidine for 2 hours and then processed for autoradiography. After a 10–12 day exposure, slides were processed and analyzed by two independent, blinded scorers who evaluated the tissue samples for the percentage of cells in S phase (characterized by complete coverage of the nucleus with silver grains).

Unscheduled DNA synthesis

NER was measured by autoradiography of unscheduled DNA synthesis after UV damage (UDS) [47,48]. After a total of 10–14 days in culture, without passaging, cultures were irradiated with UV light at 254 nm at a mean fluence of 1.2 Joules/m^2 for 12 seconds in the absence of culture medium, for a total dose of 14 J/m^2. Each sample was represented by at least two chamber slides. One chamber of each 2-chamber slide was shielded from the UV dose to be used as an unirradiated control sample. Primary cultures had not reached confluence and were still actively growing at the time the UDS assay was performed. Control FF were plated subconfluently 2 days before the UDS assay to insure that they also were not in a quiescent state brought on by confluence. After UV exposure, all cultures were incubated in medium supplemented with 10 μCi ml [^{3}H]methyl-thymidine (~80 Ci mmol^{-1}) (PerkinElmer Life Sciences, Boston, MA) for 2 hours at 37°C. Labeling medium was then replaced with unlabeled chasing medium containing 10^{-3} M non-radioactive thymidine (Sigma) and incubated for a further 2 hours to clear radioactive label from the intracellular nucleotide pools. After incubation in the post-labeling medium, cells were fixed in 1X SSC, 33% acetic acid in ethanol, followed by 70% ethanol and finally rinsed in 4% perchloric acid over night at 4°C. All slides were dried and subsequently dipped in photographic emulsion (Kodak type NTB2) and exposed for 10 to 14 days in complete darkness at 4°C.

The length of exposure of emulsion was determined in each experiment by preparing FF "tester" slides. After 10–12 days these tester slides were developed and grain counting was performed. If the nuclei over the foreskin fibroblasts averaged 50 or more grains per nucleus, then the rest of the experimental slides were developed. If the grain count was below this level, the remaining slides were left to expose 1–3 days longer before being developed.

Grain counting

After photographic development of emulsion, all slides were stained with Giemsa, then examined at a total magnification of 1000X on a Zeiss Axioskop under oil emersion for grains located immediately over the nuclei of non-S phase cells [48]. Local background grain counts were evaluated in each microscopic field over an area the same size as a representative nucleus, and this total was subtracted from the grain count of each nucleus in that field. The average number of grains per nucleus was quantified for each side of the chamber slide, both unirradiated and irradiated. The final NER value for each slide was calculated by subtracting the unirradiated mean (grains per nucleus) from the irradiated mean (grains per nucleus), after the initial subtraction of local background in each field. NER was initially expressed as a percentage of the activity of concurrently analyzed FF. Four FF slides were scored per experiment, by an average of three counters. 200 nuclei were counted per slide, for a total of 800, with an average of 61.6 grains/nucleus. Six slides were evaluated for the patient's PBL sample, two by each of three counters. An average of 195 nuclei were scored per slide (for a total of almost 1200), with an average of 7.5 grains/nucleus. Four slides were counted for the contemporaneous breast reduction control, two each by two counters. There were an average of 200 nuclei per slide and 14.1 grains/nucleus. Six slides were scored from the patient's ipsilateral breast tissue sample, two by each of three independent counters, and five slides were counted from the contralateral sample, again by three independent counters. An average of just over 100 nuclei were evaluated per slide for each sample, for a total of almost 600 nuclei for the ipsilateral sample and over 500 for the contralateral sample. As the NER capacities indicate, these samples had very similar counts; about 35 grains/nucleus for the ipsilateral sample and 28 grains/nucleus for the contralateral sample. Finally, four slides were counted from the contralateral sample of a sporadic breast cancer patient, by three counters. There were an average of 200 nuclei per slide and 29.4 grains per nucleus.

Statistical analysis

To ensure accuracy and guard against transcription errors, raw grain counts from the UDS assay were processed independently in duplicate, once using StatView (version 5.0.1, SAS Institute, Inc., Cary, NC), and once using the Data Analysis Toolpack of the Excel 2001 spreadsheet program (Microsoft Corp., Redmond, WA). The final count from slides of the same cell type within the same experiment and developed the same day were averaged together and expressed as a percentage of concurrently analyzed FF. These results were then normalized by comparison to the average for the tissue type control population [48].

Competing interests

The authors declare that they have no competing interests.

Authors' contributions

JJL conceived of the study, executed it, and drafted the manuscript. WSR recruited and consented the patient, provided clinical samples and information. JMJ evaluated the UDS assay and analyzed the data. AKS performed the histopathological analysis of the tissue. VGV participated in the study design and data interpretation. SGG participated in the design and coordination of the study and helped to draft the manuscript.

Acknowledgements

This study was supported in part by NIH grant CA 71894, US Army BRCP grants DAMD17-00-1-0681, BC033717, BC991187, DAMD17-00-1-0409, grant BCTR0403329 from the Susan G. Komen Breast Cancer Foundation and grants from the Ruth Estrin Goldberg Foundation and the Pennsylvania Department of Health. We would like to thank our clinical collaborators on this project, Dr. Jules H. Sumkin for his cooperation with this study, and acknowledge the work of our clinical coordinator, Michelle B. Huerbin. We greatly appreciate the technical contributions of Melissa C. Paglia, Shail B. Mehta, Christina M. Cerceo, Crystal M. Kelly, Julie A. Conte, Janiene A. Patterson, Ayodola B. Anise and Lynn R. Janczukiewicz to this study.

References

1. Institute of Medicine: *Mammography and Beyond: Developing Technologies for the Early Detection of Breast Cancer* Washington DC: National Academy Press; 2001.
2. Mushlin AI, Kouides RW, Shapiro DE: **Estimating the accuracy of screening mammography: a meta-analysis.** *Am J Prev Med* 1998, **14:**143-153.
3. Rubinstein W, Vogel VG, Sumkin JH, Huerbin MB, Grant SG, Latimer JJ: **Prospective sreening study of 0.5 Tesla dedicated magnetic resonance imaging for the detection of breast cancer in young, high risk women.** *BMC Women's Health* .
4. Byng JW, Yaffe MJ, Jong RA, Shumak RS, Lockwood GA, Tritchler DL, Boyd NF: **Analysis of mammographic density and breast cancer risk from digitized mammograms.** *Radiographics* 1998, **18:**1587-1598.
5. Lambe M, Hsieh C-C, Tsaih SW, Ekbom A, Trichopoulos D, Adami HO: **Parity, age at first birth and the risk of carcinoma in situ of the breast.** *Int J Cancer* 1998, **77:**330-332.
6. Hancock SL, Tucker MA, Hoppe RT: **Breast cancer after treatment of Hodgkin's disease.** *J Natl Cancer Inst* 1993, **85:**25-31.
7. Latimer JJ: **Epithelial Cell Cultures Useful For *in Vitro* Testing.** *U.S. Patent 2000 #6,074,874* .
8. Jasin M: **Homologous repair of DNA damage and tumorigenesis: the BRCA connection.** *Oncogene* 2002, **21:**8981-8993.
9. Rosen EM, Fan S, Pestell RG, Goldberg ID: ***BRCA1* gene in breast cancer.** *J Cell Physiol* 2003, **196:**19-41.
10. Jaloszynski P, Kujawski M, Czub-Swierczek M, Markowska J, Szyfter K: **Bleomycin-induced DNA damage and its removal in lymphocytes of breast cancer patients studied by comet assay.** *Mutat Res* 1997, **85:**223-233.
11. Nascimento PA, da Silva MA, Oliveira EM, Suzuki MF, Okazaki K: **Evaluation of radioinduced damage and repair capacity in blood lymphocytes of breast cancer patients.** *Braz J Med Biol Res* 2001, **34:**165-176.
12. Colleu-Durel S, Guitton N, Nourgalieva K, Legue F, Leveque J, Danic B, Chenal C: **Genomic instability and breast cancer.** *Oncol Rep* 2001, **8:**1001-1005.
13. Smith TR, Miller MS, Lohman KK, Case LD, Hu JJ: **DNA damage and breast cancer risk.** *Carcinogenesis* 2003, **24:**883-889.
14. Kovacs E, Stucki D, Weber W, Muller H: **Impaired DNA-repair synthesis in lymphocytes of breast cancer patients.** *Eur J Cancer Clin Oncol* 1986, **22:**863-869.
15. Xiong P, Bondy ML, Li D, Shen H, Wang LE, Singletary SE, Spitz MR, Wei Q: **Sensitivity to benzo[a]pyrene diol-epoxide associated with risk of breast cancer in young women and modulation by glutathione S-transferase polymorphisms: a case-control study.** *Cancer Res* 2001, **61:**8465-8469.
16. Kennedy DO, Agrawal M, Shen J, Terry MB, Zhang FF, Senie RT, Motykiewicz G, Santella RM: **DNA repair capacity of lymphoblastoid cell lines from sisters discordant for breast cancer.** *J Natl Cancer Inst* 2005, **97:**127-132.
17. Latimer JJ, Kisin E, Zayas-Rivera B, Kelley J, Johnson R, Grant SG: **Increased somatic mutation and reduced DNA repair in breast cancer patients and their tumors [abstract].** *Proc Am Assoc Cancer Res* 1999, **40:**440.
18. Mullenders LHF, Berneberg M: **Photoimmunology and nucleotide excision repair: impact of transcription coupled and global genome excision repair.** *J Photochem Photobiol B* 2001, **56:**97-100.
19. Cleaver JE: **Defective repair replication of DNA in xeroderma pigmentosum.** *Nature* 1968, **218:**652-656.
20. Luddy RE, Sweren RJ: **Skin cancer.** In *Malignant Diseases of Infancy, Childhood and Adolescence* 2nd edition. Edited by: Altman AJ, Schwartz AD. Philadelphia: Saunders; 1983:552-559.
21. Thompson LH: **Nucleotide excision repair: its relation to human disease.** In *DNA Damage and Repair, Volume 2: DNA Repair in Higher Eukaryotes* Edited by: Nickoloff JA, Hoekstra MF. Totowa, NJ. Humana Press ; 1998:335-393.
22. Hartman A-R, Ford JM: **BRCA1 induces DNA damage recognition factors and enhances nucleotide excision repair.** *Nat Genet* 2002, **32:**180-184.
23. Takimoto R, MacLachlan TK, Dicker DT, Niitsu Y, Mori T, el-Deiry WS: **BRCA1 transcriptionally regulates damaged DNA binding protein (DDB2) in the DNA repair response following UV-irradiation.** *Cancer Biol Ther* 2002, **1:**177-186. comment 1:187–188
24. **Breast Cancer Information Core** [http://research.nhgri.nih.gov/bic/]
25. Gierach G, Vogel VG: **Epidemiology of breast cancer.** In *Advanced Therapy of Breast Disease* 2nd edition. Edited by: Singletary SE, Robb GL, Hortobagyi GN. Hamilton: BC Decker; 2004:58-74.
26. Russo IH, Koszalka M, Gimotty PA, Russo J: **Protective effect of chorionic gonadotropin on DMBA-induced mammary carcinogenesis.** *Br J Cancer* 1990, **62:**243-247.
27. Russo J, Mailo D, Hu YF, Balogh G, Sheriff F, Russo IH: **Breast differentiation and its implication in cancer prevention.** *Clin Cancer Res* 2005, **11:**931s-936s.
28. Latimer JJ, Kanbour-Shakir A, Giuliano K, Kisin E, Kelley J, Johnson R: **Live cell microscopy of long-lived primary human mammary epithelium cultures (HMEC) from breast reduction mammoplasties and breast tumors [abstract].** *Breast Cancer Res Treat* 1998, **50:**255.
29. Boyd NF, Lockwood GA, Martin LJ, Knight JA, Byng JW, Yaffe MJ, Tritchler DL: **Mammographic densities and breast cancer risk.** *Breast Dis* 1998, **10:**113-126.
30. Latimer JJ, Nazir T, Flowers LC, Forlenza MJ, Beaudry-Rodgers K, Kelly CM, Conte JA, Shestak K, Kanbour-Shakir A, Grant SG: **Unique tissue-specific level of DNA nucleotide excision repair in primary human mammary epithelial cultures.** *Exp Cell Res* 2003, **291:**111-121.

31. Kelly CM, Johnson JM, Wenger SL, Vogel V, Kelley J, Johnson R, Amortequi A, Mock L, Grant SG, Latimer JJ: **Analysis of functional DNA repair in primary cultures of the non-tumor adjacent breast identifies two classes of breast cancer patient [abstract].** *Proc Am Assoc Cancer Res* 2003, **44:**974-975.
32. Buchholz TA, Wu X, Hussain A, Tucker SL, Mills GB, Haffty B, Bergh S, Story M, Geara FB, Brock WA: **Evidence of haplotype insufficiency in human cells containing a germline mutation in *BRCA1* or *BRCA2*.** *Int J Cancer* 2002, **97:**557-561.
33. Mamon H, Dahlberg W, Little JB: **Hemizygous fibroblast cell strains established from patients with BRCA1 or BRCA2 mutations demonstrate an increased rate of spontaneous mutations and increased radiosensitivity.** *Int J Radiat Oncol Biol Phys* 2003, **57(Suppl 2):**S346-S347.
34. Rothfuss A, Schutz P, Bochum S, Volm T, Eberhardt E, Kreienberg R, Vogel W, Speit G: **Induced micronucleus frequencies in peripheral lymphocytes as a screening test for carriers of a BRCA1 mutation in breast cancer families.** *Cancer Res* 2000, **60:**390-394.
35. Das R, Grant SG: **Unusual pattern of age-related somatic mutation in cell lines derived from carriers of mutations in the *BRCA1* and 2 genes [abstract].** *Am J Hum Genet* 2002, **71(Suppl):**251.
36. Nieuwenhuis B, Van Assen-Bolt AJ, Van Waarde-Verhagen MA, Sijmons RH, Van der Hout AH, Bauch T, Streffer C, Kampinga HH: **BRCA1 and BRCA2 heterozygosity and repair of X-ray-induced DNA damage.** *Int J Radiat Biol* 2002, **78:**285-295.
37. Trenz K, Rothfuss A, Schutz P, Speit G: **Mutagen sensitivity of peripheral blood from women carrying a BRCA1 or BRCA2 mutation.** *Mutat Res* 2002, **500:**89-96.
38. Baeyens A, Thierens H, Claes K, Poppe B, de Ridder L, Vral A: **Chromosomal radiosensitivity in BRCA1 and BRCA2 mutation carriers.** *Int J Radiat Biol* 2004, **80:**745-756.
39. Trenz K, Schutz P, Speit G: **Radiosensitivity of lymphoblastoid cell lines with a heterozygous BRCA1 mutation is not detected by the comet assay and pulsed field gel electrophoresis.** *Mutagenesis* 2005, **20:**131-137. 2005, Mar 22; Epub ahead of print
40. Norris PG, Limb GA, Hamblin AS, Lehmann AR, Arlett CF, Cole J, Waugh AP, Hawk JL: **Immune function, mutant frequency, and cancer risk in the DNA repair defective genodermatoses xeroderma pigmentosum, Cockayne's syndrome, and trichothiodystrophy.** *J Invest Dermatol* 1990, **94:**94-100.
41. Kramer KH, Lee MM, Scotto J: **DNA repair protects against cutaneous and internal neoplasia: evidence from xeroderma pigmentosum.** *Carcinogenesis* 1984, **5:**511-514.
42. Arnould S, Hennebelle I, Canal P, Bugat R, Guichard S: **Cellular determinants of oxaliplatin sensitivity in colon cancer cell lines.** *Eur J Cancer* 2003, **39:**112-119.
43. Koberle B, Grimaldi KA, Sunters A, Hartley JA, Kelland LR, Masters JR: **DNA repair capacity and cisplatin sensitivity of human testis tumor cells.** *Int J Cancer* 1997, **70:**551-555.
44. Koberle B, Masters JR, Hartley JA, Wood RD: **Defective repair of cisplatin-induced DNA damage caused by reduced XPA protein in testicular germ cell tumours.** *Curr Biol* 1999, **9:**273-276.
45. Selvakumaran M, Pisarcik DA, Bao R, Yeung AT, Hamilton TC: **Enhanced cisplatin cytotoxicity by disturbing the nucleotide excision repair pathway in ovarian cancer cell lines.** *Cancer Res* 2003, **63:**1311-1316.
46. Forlenza MJ, Latimer JJ, Baum A: **The effects of stress on DNA repair capacity.** *Psychol Health* 2000, **15:**881-891.
47. Cleaver JE, Thomas GH: **Measurement of unscheduled synthesis by autoradiography.** In *DNA Repair: A Laboratory Manual of Research Procedures Volume I* Edited by: Friedberg EC, Hanawalt PC.. New York: Marcel Dekker. 1981:277-287
48. Kelly CM, Latimer JJ: **Unscheduled DNA synthesis: a functional assay for global genomic nucleotide excision repair.** *Meth Mol Biol* 2005, **291:**305-320.

Pre-publication history

The pre-publication history for this paper can be accessed here:

http://www.biomedcentral.com/1471-2350/6/26/prepub

12

DNA Double-Strand Break Damage and Repair Assessed by Pulsed-Field Gel Electrophoresis

Nina Joshi and Stephen G. Grant

Summary

This assay quantifies the amount of DNA double-strand break (DSB) damage in attached cell populations embedded in agarose and assayed for migratory DNA using pulsed-field gel electrophoresis (PFGE) with ethidium bromide staining. The assay can measure pre-existing damage, as well as induction of DSB by chemical (e.g., bleomycin), physical (e.g., X-irradiation), or biological (e.g., restriction enzymes) agents. By incubating the cells under physiological conditions prior to processing, the cells are allowed to repair DSB, primarily via the process of nonhomologous end joining. The amount of repair, corresponding to the repair capacity of the treated cells, is then quantified by determining the ratio of the fractions of activity released in these repaired lanes in comparison with the total amount of DNA fragmentation following determination of a optimal exposure for maximum initial fragmentation. Repair kinetics can also be analyzed through a time-course regimen.

Key Words: DNA double-strand breaks (DSB); double-strand break repair; nonhomologous end joining; pulsed-field gel electrophoresis; DNA fragmentation; genotoxicity; clastogenicity.

1. Introduction

Of all the forms of DNA damage, double-strand breaks (DSBs) induced from exogenous sources, such as ionizing radiation and chemical agents, or endogenous sources, such as oxidative stress, may be the most deleterious, for if they are unrepaired or misrepaired, they can lead to carcinogenic transformation or cell death.

DSBs (and some proportion of single-strand breaks, when they are clustered closely enough) result in high-molecular-weight DNA fragments that can be liberated from the cell and resolved by electrophoresis. This technique can be thought of as a bulk method for performing the comet assay *(see* **ref. *1***, and Chaps. 9–11*)*, although with several advantages over that assay: (1) thousands to millions of cells are analyzed, rather than hundreds; (2) a single measurement for the population is derived, rather

From: *Methods in Molecular Biology, vol. 291, Molecular Toxicology Protocols*
Edited by: P. Keohavong and S. G. Grant © Humana Press Inc., Totowa, NJ

than hundreds; and, (3) multiple samples, including controls, can be analyzed on the same gel. Application of pulsed-field gel electrophoresis (PFGE) also allows for a greater separation of DNA sizes, giving a better characterization of the nature of the underlying DNA damage.

Both the comet assay and the PFGE assay have been used extensively to study DNA repair, by observing the reduction in migrating DNA when cells are allowed a period of repair following genotoxic insult. These assays are therefore functional measures of DNA DSB repair ***(2,3)***.

From experiments using cell extracts from *Xenopus* eggs ***(4,5)***, Chinese hamster ovary cells ***(6)***, and human cells ***(7–9)*** to repair plasmids containing breaks (e.g., the prokaryotic *lacZ* gene ***[8]***), as well as the transfection of damaged plasmids into DNA repair-deficient/proficient cell lines, two distinct DSB pathways—homologous recombination (HR) and nonhomologous end joining (NHEJ)—have been identified. In HR, the major DSB repair pathway in yeast, a homologous chromosome, or more frequently, a sister chromatid, is used as a template to repair the damaged copy of the sequence in an error-free manner ***(10)***. In contrast, NHEJ, the most prevalent pathway for DSB repair in vertebrates ***(11)***, is independent of sequence homology ***(12)***. In this process, the two ends of the breakpoint are religated together after limited modulation at the termini. Thus, small inserted sequences, as well as deletions, are often introduced by this repair process, making NHEJ an inherently error-prone pathway.

Although these cell extract and transfection techniques have provided valuable information, results from the cell extract experiments are often inconsistent ***(13)***, and there is always the possibility that repair processes in plasmids do not reflect normal DSB repair in genomic DNA in intact cells ***(14)*** (*see* also Chap. 18). Thus, an in vitro assay has been developed that quantifies the amount of repaired genomic DNA DSBs in attached mammalian cells ***(15,16)***. Repair capacity is only measured under conditions of maximum damage, which are likely to differ between cell lines and cell types. Thus, an optimal dose for DSB damage is initially determined, and then, after applying this optimal dose, DSB repair can be examined over time by determining the ratio of remaining DNA fragmentation in comparison with the unrepaired control.

Cells with deficiencies in DNA protein kinase (DNA-PK; believed to regulate the accessibility of DNA ends and possibly recruit repair factors in the NHEJ pathway ***[16]***), as well as mouse fibroblasts deficient in Ku80 (another NHEJ-related protein involved in the protection and alignment DNA ends ***[17]***), have decreased repair capacity in this assay. Deficiencies in the *BRCA2* gene, associated with HR pathways through Fanconi's anemia genes ***(18,19)***, have not been detected using this assay ***(20)***. Whether patients with Fanconi's anemia, ataxia telangiectasia, Bloom's syndrome, Nijmegen breakage syndrome, Berlin breakage syndrome, and Werner's syndrome, cancer-prone syndromes attributed to deficiencies in DNA DSB repair, are associated with the NHEJ pathway is unknown. Characterization of these processes is critical to our understanding of human disease as well as cellular responses to genotoxic stress. A technique for analysis of the other type of mammalian DSB repair, HR, is given in Chapter 31 (a variant of the host cell reactivation assay described in Chap. 28).

Finally, there are two modifications that might allow the PFGE assay to analyze other types of DNA damage. Taking a cue from the comet assay, this assay could be extended to analysis of the majority of single-strand breaks by converting them to DSBs by alkaline treatment ***(21)***. By running cell samples processed under both neutral and basic pH side by side, the contribution of single-strand breaks can be observed as the quantitative difference in DNA migration. Next, by allowing a longer period between in vitro exposure and analysis, this assay could be used to quantitate the amount of "complex" or irreparable DNA damage associated with high-energy radiation ***(22)***.

2. Materials

2.1. Generation of Double-Strand Breaks

1. T-25 (25-cm) cell culture flasks (Fisher Scientific, Pittsburgh, PA).
2. Appropriate growth media for each cell type, with appropriate amount and type of serum.
3. Cell culture incubator (e.g., ThermoForma Series II Water Jacketed CO_2 Incubator, Forma Scientific, Marietta, OH).
4. Irradiation source (e.g., cesium source, model 143-45A, JL Shepard, San Francisco, CA; *see* **Note 1**).

2.2. Cell Sample (Agarose Plug) Preparation

1. Trypsin (or other means of harvesting cells; Invitrogen, Carlsbad, CA).
2. 15-mL Conical tubes (BD Falcon, BD Biosciences, Bedford, MA).
3. Appropriate cell culture medium (serum-free).
4. Hemocytometer (Fisher) or Coulter counter (Beckman Coulter, Fullerton, CA).
5. 1-, 5-, and 10-mL Pipets and pipet aid.
6. 20-, 200-, and 1000-µL Micropipetors (Rainin, Woburn, MA) and appropriate pipet tips (Fisher).
7. Benchtop centrifuge (e.g., Sorval RT 6000D, Kendro Lab Products, Asheville, NC).
8. 50–56°C shaking water bath.
9. 1% InCert agarose solution (BioWhittaker, Rockland, ME). Incubate at 50–56°C to prevent solidification.
10. 100-µL Plastic plug molds taped on the bottom (Bio-Rad, Hercules, CA).
11. Lysis solution: 10 m*M* Tris-HCl, pH 8.0, 50 m*M* NaCl, 0.5 *M* EDTA, 2% *N*-lauryl sarcosyl (all Sigma, St. Louis, MO), 0.1 mg/mL proteinase K (Invitrogen).
12. Wash buffer: 10 m*M* Tris-HCl, pH 8.0, 0.1 *M* EDTA.
13. RNase solution (Invitrogen): 10 m*M* Tris-HCl, pH 7.5, 0.1 *M* EDTA, 0.1 mg/mL RNase. Make 2.5 mL per sample fresh each time.

2.3. Pulsed-Field Gel Electrophoresis (PFGE)

Although a number of PFGE apparatus have been developed, clamped homogenous electric field (CHEF) and asymmetric field inversion gel electrophoresis (AFIGE) are most often used for DSB analysis (*see* **Note 2**).

1. CHEF: CHEF DRII apparatus (Bio-Rad) with refrigerated water bath and circulating pump.
   AFIGE: Horizontal gel electrophoresis system, model H4 (Invitrogen) with refrigerated water bath and circulating pump.

2. Seakem agarose (BioWhittaker).
3. 0.5X TBE: 45 m*M* Tris-HCl, pH 8.0, 45 m*M* boric acid, 1 m*M* EDTA. Prepare a 5X stock solution in large volumes (~500 mL); can be stored indefinitely at room temperature.
4. 10 mg/mL Ethidium bromide (made up in 10-mL lots, kept wrapped in aluminum foil in the refrigerator).
5. FluorImager (Bio-Rad)

3. Methods

3.1. Generation of Double-Strand Breaks (see Notes 1, 3, and 4)

1. Cells should be firmly attached, semiconfluent, and in log phase growth when exposed to ionizing radiation (IR). Thus, they should be plated at least 48 h prior to exposure and the T-25 flasks seeded with the appropriate number of cells to attain these conditions (*see* **Note 5**).
2. Cool cells on ice to 4°C prior to irradiation.
3. Expose cells in T-25 flasks to a source of ionizing radiation at doses ranging from 10 to 100 Gy (or at optimized dose, if this has been predetermined). Include one flask as an unexposed control to determine background DNA fragmentation levels.

3.2. Cell Sample (Agarose Plug) Preparation

1. Harvest cells, by trypsinization or other appropriate technique on ice in 15-mL conical tubes (*see* **Note 6**). This process may take 5–10 min. Centrifuge the cells for 5 min at 800*g*. Wash the cells once in serum-free medium.
2. Resuspend the cells in serum-free medium and count the cells, using a hemocytometer or Coulter counter. Aliquot the cells at a concentration of 1×10^6 or multiples of 1×10^6 (e.g., 2×10^6, 3×10^6) into 15-mL conical tubes and spin for 5 min at 800*g*.
3. Remove excess media with a pipet without disrupting the cell pellet. Add 30 µL of serum-free media to the 15-mL conical tubes for each 1×10^6 cells. Triturate the cell suspension to ensure that no clumps are present.
4. Mix the cell suspension with an equal volume of 1% agarose incubated at 50°C. The final concentration of agarose should be 0.5% with 1×10^6 cells per 60 µL of serum-free medium and agarose solution.
5. Pipet the 60 µL (or 60-µL aliquots) into the precooled 100 µL plastic plug molds, and incubate on ice for 5 min until the plugs solidify.
6. Extrude the solidified plugs from the molds into a 15-mL conical tube by removing the tape from the bottom of the molds and pipeting lysis buffer directly over the plug.
7. Add 2 mL lysis solution and incubate at 4°C for 45 min.
8. Transfer the plugs to 50°C for 16–18 h in a moderately shaking water bath.
9. Wash the plugs once with 2 mL washing buffer. Incubate in 2 mL of fresh washing buffer for 1 h at 37°C in a moderately shaking water bath.
10. Transfer the plugs to 2 mL RNase solution and incubate for 1 h at 37°C.
11. Plugs can then be stored in 5 m*M* EDTA buffer at 4°C indefinitely.

3.3. Preparation for Plug Gel Electrophoresis

1. Cast a 0.8% agarose gel in 0.5X TBE with the appropriate comb when using the Bio-Rad CHEF-DRIII or a 0.5% agarose gel when using AFIGE. Allow the gel to solidify for approx 1 h.

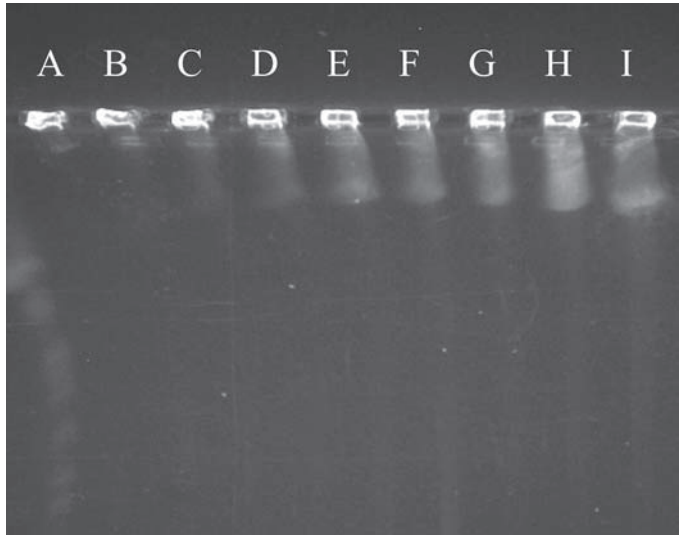

Fig. 1. DNA fragmentation following irradiation. lane A, unirradiated control; lane B, 5 Gy; lane C, 10 Gy; lane D, 20 Gy; lane E, 30 Gy; lane F, 40 Gy; lane G, 50 Gy; lane H, 60 Gy; lane I, 70 Gy. The dose yielding the maximum amount of DSB DNA damage is 60 Gy.

2. Remove the comb after solidification, and load the plugs into the wells. Seal the wells with agarose to ensure that the plugs are not released from the wells during electrophoresis.
3. Place the gel into a precooled (10°C) electrophoresis box with 0.5X TBE.
4. Electrophorese for 23 h at 200 V with 60-s pulses for the first 8 h, followed by 120-s pulses for 15 h with the Bio-Rad CHEF-DRIII ***(23)***. Using AFIGE, cycles of 1.25 V/cm for 900 s in the forward direction and 5 V/cm for 75 s in the reverse direction ***(23)*** should be used (*see* **Note 7**).
5. Stain the gel for 1 h with 0.5 µg/mL ethidium bromide (*see* **Note 8**).
6. Expose the gel to a FluorImager for analysis.
7. Quantitate the DSBs present by determining the ratio between the fraction of activity released from the plug (FAR) vs the total DNA in both the plug and in the lane: FAR = lane counts/(plug + lane) counts ***(23)***.
8. For quantification of damage, FAR should be compared with a standard control or curve. For quantification of repair, the amount of migratory DNA in the experimental lane may be subtracted directly from that in the control (no repair incubation), provided that the total amounts of DNA in both plugs/lanes are similar.
9. To examine repair capacity, first determine the optimal dose of radiation (the dose that provides the maximum fragmentation), and then plot dose vs FAR (**Figs. 1** and **2**).

3.4. Analysis of the Time-Course of DSB Repair

1. Prewarm medium supplemented with serum to 42°C (sufficient to replace media in all experimental flasks).
2. Cool cells on ice prior to irradiation and expose each flask to the optimal IR dose determined in **Subheading 3.3.**, **step 9**.

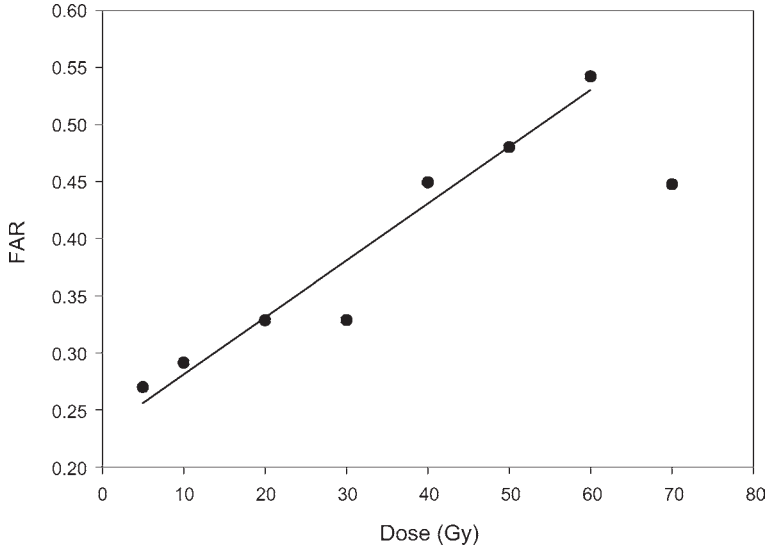

Fig. 2. Regression analysis of DNA fragmentation, quantified as the fraction of activity in the lane, vs dose to determine the optimal dose to be used to examine repair kinetics. A dose of 60 Gy provided optimal damage. FAR, fraction of activity released.

3. Replace medium in each flask with prewarmed medium (which rapidly restores the cultures to 37°C, at which temperature repair is activated):
   a. Return flasks to the incubator for various times to allow for repair (time points: 0, 10, 20, 30, 60, 120, 128, 240, and 360 min).
   b. After the predetermined repair incubation periods, remove the flasks, harvest the cells, and place on ice for 5–10 min.
   c. Process samples as in **Subheadings 3.2.** and **3.3.**

An example of the resulting gel is given in **Fig. 3**.

4. Notes

1. Direct DSB agents such as bleomycin, toposimerase II inhibitors, and carcinostatin, as well as enzymes that cleave DNA, such as *Bam*H1, *Pvu*11, *Hin*f1, and *Hae*III transfected into cells can be utilized as alternate sources of DBS damage ***(23,24)***.
2. PFGE separates larger DNA pieces than standard constant field electrophoresis by alternating the direction of the electric field at regular intervals, forcing the DNA to reorient itself constantly in new directions, resulting in far superior size separation. A number of PFGE apparatus have been developed, including orthogonal field agarose electrophoresis (OFAGE), transverse alternating field electrophoresis (TAFE), CHEF, and AFIGE ***(24)***. The choice depends on the type of equipment available, keeping in mind that CHEF and AFIGE have been most often used for DSB analysis. The AFIGE apparatus produces more uniform DNA fragments and should be used when the analysis does not require the precise size of DNA fragmentation ***(23,25)***. The CHEF gel apparatus should be used when size detection is important.

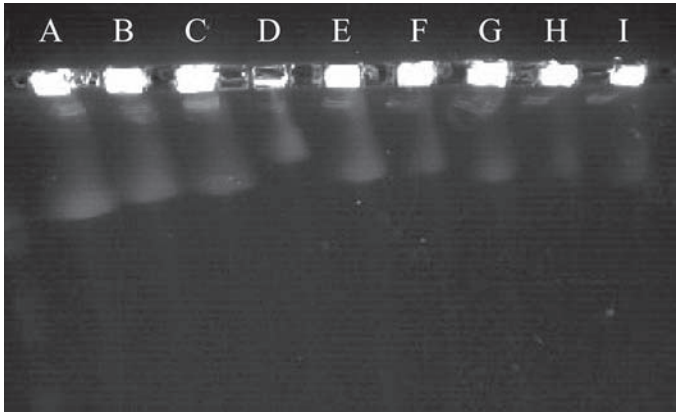

Fig. 3. DNA fragmentation resulting from repair of DSB damage induced by exposure of Ishikawa endometrial cancer cells to 60 Gy ionizing radiation (*see* **Figs. 1** and **2**) and repair for: lane A, 0 min; lane B, 10 min; lane C, 20 min; lane D, 30 min; lane E, 60 min; lane F, 120 min; lane G, 180 min; lane H, 240 min; lane I, 360 min.

3. If the intent of the assay is simply to quantify existing DNA damage, it may not be necessary to induce DSB. To allow for variability between gels, however, we recommend that, rather than using the absolute amount of migratory DNA as a measure of such damage, that experimental samples always be compared with known controls (such a comparison is inherent if the assay is used as a measure of repair, since migratory DNA from the cells allowed to undergo repair is considered relative to the same cells with no opportunity for repair). We have not yet established a control cell type with a stable level of "uninduced" DSB, so we recommend using radiated cells as controls. This also allows for exposures to different doses of radiation and/or for different incubation times for repair, as well as the establishment of a standard curve for the control cells.
4. If the intent of the assay is to measure repair capacity, an induction dose for maximum DNA DSB damage must first be determined by processing samples subjected to a range of IR dosages, as given in **Subheading 3.1.**, **step 3**., then optimizing the incubation time for repair according to the protocol given in **Subheading 3.4.**
   Using this maximum dose provides damage and a damage signal (migratory DNA) on PFGE that makes sure the entire repair capacity of the cells is engaged. This dose is always a lethal dose, however, and it would be useful to confirm results from such experiments at sublethal levels of exposure and DNA damage.
5. DNA from cells in S phase migrate three to four times more slowly than from cells in G_1 or G_2 phase ***(26)***. Thus, cells should be analyzed once they reach the plateau phase, increasing the number of cells in G_1/G_0 and decreasing the variability in fragmentation. This phenomenon occurs not only in this assay but also in other techniques that measure DNA fragmentation ***(24)***.
6. Cells and plugs used during this assay should remain on ice at all times to decrease repair except during the predetermined repair incubation period in **Subheading 3.4.**, **step 4**.
7. These electrophoresis conditions have been optimized for resolution of migratory DNA after a maximal induction of DSB (**Figs. 1** and **2**). Different conditions may need to be

developed for the lesser damage observed in unexposed cells or cells exposed to less efficient inducing agents than IR.

8. Cells and migratory DNA can also be detected using incorporation of radiolabeled thymidine (Sigma Aldrich, Maryland Heights, MO) and a Phosphoimager (STORM, Amersham Biosciences, Piscataway, NJ) or a scintillation counter (MicroBeta, Boston, MA) ***(16)***.

References

1 Singh, N. P., McCoy, M. T., Tice, R. R., and Schneider, E. L. (1988) A simple technique for quantification of low levels of DNA damage in individual cells. *Exp. Cell Res.* **175,** 184–191.

2 Speit, G. and Hartmann, A. (1995) The contribution of excision repair to the DNA-effects seen in the alkaline single cell gel test (comet assay). *Mutagenesis* **10,** 555–559.

3 DiBiase, S. J., Guan, J., Curran, W. J. Jr., and Iliakis, G. (1999) Repair of DNA double-strand breaks and radiosensitivity to killing in an isogenic group of p53 mutant cell lines. *Int. J. Radiat. Oncol. Biol. Phys.* **45,** 743–751.

4 Pfeiffer, P. and Vielmetter, W. (1988) Joining of nonhomologous DNA double strand breaks *in vitro*. *Nucleic Acids Res.* **16,** 907–924.

5 Lehman, C. W., Clemens, M., Worthylake, D. K., Trautman, J. K., and Carroll, D. (1993) Homologous and illegitimate recombination in developing Xenopus oocytes and eggs. *Mol. Cell Biol.* **13,** 6897–6906.

6 Feldmann, E., Schmiemann, V., Goeddecke, W., Reichenberger, S., and Pfeiffer, P. (2000) DNA double-strand break repair in cell-free extracts from Ku80-deficient cells: implications for Ku serving as an alignment factor in non-homologous DNA end joining. *Nucleic Acids Res.* **28,** 2585–2596.

7 North, P., Ganesh, A., and Tacker, J. (1990) The rejoining of double-strand breaks in DNA by human cell extracts. *Nucleic Acids Res.* **18,** 6205–6210.

8 Ganesh, A., North, P., and Tacker, J. (1993) Repair and misrepair of site-specific DNA double-strand breaks by human cell extracts. *Mutat. Res.* **299,** 251–259.

9 Boe, S. O., Sodroski, J., Helland, D. E., and Farnet, C. M. (1995) DNA end-joining in extracts from human cells. *Biochem. Biophys. Res. Commun.* **215,** 987–993.

10 Khanna, K. K. and Jackson, S. P. (2002) DNA double-strand breaks: signaling, repair and the cancer connection. *Nat. Genet.* **27,** 247–254.

11 Weaver, D. T. (1995) What to do at an end: DNA double-strand-break repair. *Trends Genet.* **10,** 388–392.

12 Valerie, K. and Povirk, L. F. (2003) Regulation and mechanisms of mammalian double-strand break repair. *Oncogene* **22,** 5792–5812.

13 Rathmell, W. K. and Chu, G. (1998) Mechanisms for DNA double-strand break repair in eukaryotes, in *DNA Damage and Repair*, vol. II: *DNA Repair in Higher Eukaryotes* (Nickoloff, J. A. and Hoekstra, M. F., eds.), Humana, Totowa, NJ, pp. 299–316.

14 Cheong, N., Perrault, A. R., and Iliakis, G. (1998) In vitro rejoining of DNA double-strand-breaks: a comparison of genomic DNA with plasmid DNA-based assays. *Int. J. Radiat. Biol.* **73,** 481–493.

15 Iliakis, G., Metzger, L., Denko, N., and Stamato, T. D. (1991) Detection of DNA double-strand breaks in synchronous cultures of CHO cells by means of asymmetric field inversion gel electrophoresis. *Int. J. Radiat. Biol.* **59,** 321–341.

16 DiBiase, S. J., Zeng, Z. C., Chen, R., Hyslop, T., Curran, W. J., and Iliakis, G. (2000) DNA-dependent protein kinase stimulates an independent active, nonhomologous, end-joining apparatus. *Cancer Res.* **60,** 1245–1253.

17 Nachsberger, P. R., Li, W. H., Guo, M., et al. (1999) Rejoining of DNA double strand breaks in Ku80-deficient mouse fibroblasts. *Radiat. Res.* **151,** 398–407.
18 Howlett, N. G., Taniguchi, T., Olson, S., et al. (2002) Biallelic inactivation of BRCA2 in Fanconi anemia. *Science* **297,** 606–609.
19. D'Andrea, A. D. and Grompe, M. (2003) The Fanconi anaemia/BRCA pathway. *Nat. Rev. Cancer* **3,** 23–34.
20 Xia, F., Taghian, D. G., Defrank, J. S., et al. (2001) Deficiency of human BRCA2 leads to impared homologous recombination but maintains normal non-homologous end joining. *Proc. Natl. Acad. Sci. USA* **98,** 8644–8649.
21 Olive, P. L. (1989) Cell proliferation as a requirement for development of contact effect in Chinese hamster V79 spheroids. *Radiat. Res.* **117,** 79–92.
22 Pastwa, E., Neumann, R. D., Mezhevaya, K., and Winters, T. A. (2003) Repair of radiation-induced DNA double-strand breaks is dependent upon radiation quality and the structural complexity of double-strand breaks. *Radiat. Res.* **159,** 251–261.
23 Kinashi, Y., Okayasu, R., Iliakis, G., Nagasawa, H., and Little, J. B. (1995) Induction of DNA double-strand breaks by restriction enzymes in X-ray-senstive mutant Chinese hamster ovary cells measured by pulse-gel electrophoresis. *Radiat. Res.* **141**, 153–159.
24 Olive, P. L. (1998) Molecular approaches for detection of DNA damage, in *DNA Damage and Repair,* vol. II: *DNA Repair in Higher Eukaryotes* (Nickoloff, J. A. and Hoekstra, M. F., eds.), Humana, Totowa, NJ, pp. 539–557.
25. Blocher, D. and Pohlit, W. (1982) DNA double strand breaks in Ehrlich ascites tumors cells at low doses of X-rays. II. Can cell death be attributed to double strand breaks? *Int. J. Radiat. Biol.* **42,** 329–338.
26. Loucas, B. D. and Geard, C. R. (1994) Kinetics of chromosome rejoining in normal human fibroblasts after exposure to low- and high-LET radiation. *Radiat. Res.* **138,** 352–360.